

MINISTRY OF EDUCATION, RESEARCH, YOUTH AND SPORT

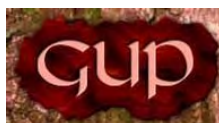


THE ANNALS OF “DUNAREA DE JOS” UNIVERSITY OF GALATI

**Fascicle IX
METALLURGY AND MATERIALS SCIENCE**

YEAR XXVIII (XXXIII),
March 2010, no. 1

ISSN 1453-083X



2010
GALATI UNIVERSITY PRESS

EDITING MANAGEMENT

RESPONSIBLE EDITOR: Prof.Dr.Eng. Viorel MINZU

ASSISTANT EDITORS: Prof.Dr.Fiz. Mirela PRAISLER
Prof.Dr.Eng. Teodor MUNTEANU
Prof.Dr. Ing. Iulian BÎRSAN
Prof.Dr.Ec. Daniela ȘARPE
Prof.Dr. Elena MEREUȚĂ

SECRETARY: Assoc.Prof.Dr.Eng. Ion ALEXANDRU

EDITING BOARD

Fascicle IX

METALLURGY AND MATERIALS SCIENCE

PRESIDENT OF HONOUR: Prof.Dr.Chim. Olga MITOȘERIU
EDITOR IN CHIEF: Prof.Dr.Eng. Nicolae CĂNĂNĂU
EDITORIAL SECRETARY: Prof.Dr.Eng. Marian BORDEI

MEMBERS:

Acad.Prof.Dr.Hab. Valeriu CANTSER–Coordinator of the Technical and Scientific Section of the Academy of Moldova Republic

Acad.Prof.Dr.Hab. Ion BOSTAN–Rector of Technical University of Moldova, member of the Academy of Moldova Republic

Prof.Dr.Rodrigo MARTINS–President of the Department of Materials Science, Faculty of Science and Technology,NOVA University of Lisbon,Portugal

Prof.Dr.Hab. Vasile MARINA–Head of the Materials Resistance Department, State Technical University of Moldova, Kishinau, Moldova Republic

Prof.Dr. Antonio de SAJA–Head of Department of Physics of Condensed Material, Faculty of Sciences, University of Valladolid, Spain

Prof.Dr. Strul MOISA–Chief Engineer Department of Materials Engineering, Ben Gurion University of the Negev, Israel

Prof.Dr. Alexander SAVAYDIS–Aristotle University of Thessaloniki, Dept. of Mechanical Engineering, Greece

Prof.Dr.Hab. Valeriu DULGHERU–Head of Department, Faculty of Engineering and Management in Machine Building, Technical University of Moldova

Prof.Dr. Ion SANDU –ARHEOINVEST Platform, Laboratory of Scientific Investigation and Cultural Heritage Conservation, „Al.I.Cuza” University of Iasi

Prof.Dr.Eng. Elena DRUGESCU
Prof.Dr.Eng. Anișoara CIOCAN
Prof.Dr.Eng. Maria VLAD
Prof.Dr.Eng. Petre Stelian NIȚĂ
Prof.Dr.Eng. Alexandru IVĂNESCU
Prof.Dr.Chim. Viorica MUȘAT
Prof.Dr.Eng. Florentina POTECAȘU
Assoc.Prof.Dr.Eng. Sanda LEVCOVICI



Table of Content

1.N. Cananau, D. Scarlat, G. Florea - Problems and Solutions Regarding the Centrifugal Casting of Wire Sheave for Heavy Cranes.....	5
2.Ioan Marginean, Bogdan-Alexandru Verdes, Sorin-Adrian Cocolas - Theoretical Study Regarding the Flow Conditions for Alloys through Thin Channels.....	10
3.Daniela Buruiana (Negoita), Gheorghe Florea, Alexandru Chiriac - The Process Involved in Making the Medals.....	16
4.Julieta Daniela Sabău (Chelaru), Vasile Filip Soporan, Ovidiu Nemeş – Time Analysis of King Matthias the I st Sculptural Group.....	20
5.Petrica Hagioglu, Constantin Gheorghies - Materials Used for Manufacturing Some Objects from 1600 before Christ – 500 after Christ Period.....	26
6.Elena Paraschiv, Victor Păunescu, Cristina Răducan - Sculpture, Extended Nature.....	33
7.Violeta Vasilache, Sonia Gutt, Ion Sandu, Gheorghe Gutt, Traian Vasilache - Electrodeposition and Characterization of Zinc-Cobalt Alloy Coatings.....	37
8.Elisabeta Vasilescu - Intercritical Thermomechanical Treatments Applied to the Steel Heavy Plates.....	41
9.Ovidiu Dima - Coating of the Lasting Moulds with Hard Alloys.....	46
10.Stefan Dragomir, Georgeta Dragomir, Marian Bordei - Performing System for Purifying Waste Water.....	51
11.Maria Vlad, Gelu Movileanu - Soil Pollution with Heavy Metals.....	56
12.Alexandru CHIRIAC, Gheorghe FLOREA, Ioan SARACIN, Olimpia PANDA - Sources of Emissions in the Sintering and Blast Furnace Plant.....	60
13.Viorel Munteanu - Modelling and Numerical Simulation of the Atmospheric Dispersion of Pollutants from an Integrated Iron and Steel Complex - Part I.....	63
14.Vasile Basliu, Ionut Constantin, Gina Genoveva Istrate, Ionel Petrea -Melting-Casting Plant Using Vibrating of Melts in order to Obtain Composite with Technological Utility.....	68

PROBLEMS AND SOLUTIONS REGARDING THE CENTRIFUGAL CASTING OF WIRE SHEAVE FOR HEAVY CRANES

N. CANANAU, D. SCARLAT, G. FLOREA

"Dunărea de Jos" University of Galati
email: ncananau@ugal.ro

ABSTRACT

The centrifugal casting of wire sheave is a technological method that ensures the important quality requirement, the continuity of the material in the active rolling zone of the sheave. However the centrifugal casting has some difficulties: the stability of the casting system, small productivity, gas permeability of the cast mould. The paper shows the problems induced by the centrifugal casting of these parts and the solutions for their solving.

KEYWORDS: centrifugal casting, wire sheave, productivity

1. Introduction

The wire sheaves for heavy cranes have, as characteristic, the relatively great diameter, compared to their thickness (Figure 1).

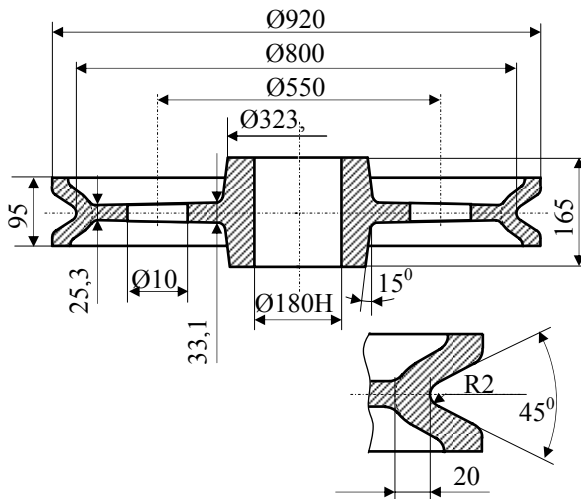


Fig. 1. Form and dimensions of the wire sheave

The wire sheave is obtained by casting from the alloyed steel according to the standard DIN 1683 GTB 18.5. The chemical composition of the steel for wire sheave is rendered in Table 1.

Table 1. Chemical composition of the steel, [%]

C	Mn	Si	P	S	Cr	Ni	Mo
0.25-0.35	0.4-0.9	0.2-0.45	max 0.03	max 0.03	1.3-1.6	1.3-1.6	0.2-0.3

The characteristics of the cast steel, after the heat treatment are rendered in Table 2.

The gravitational casting of these sheaves in the temporary casting mould presents some difficulties.

A quality requirement, which must be strictly met, is ensures of the material continuity in the rolling way zone of the wire sheave.

The presence of the gas gaps in this zone is strictly forbidden.

Table 2. Characteristics of the steel

Heat treatment	R _{p0.2}	R _m	A	Z	KCU	HB
u.m.	$\frac{N}{mm^2}$		%		$\frac{J}{cm^2}$	$\frac{daN}{mm^2}$
Q+T	640	780-980	10	20	39	232

To meet this requirement, the increasing of the mechanical work addition material practically is necessary.

This fact leads to the increasing of the material consumption and the greater costs of the mechanical working process, respectively, the greater general cost of the production process.

In the aim of the decreasing the work addition material and, at the same time, the ensure of the material continuity in the rolling way zone, taking into consideration that the dimensions of the wire sheave are adequate, the centrifugal casting, with

vertical rotation axe, is a possible technological process for making these parts.

The centrifugal casting presents some advantages:

- ensures of the continuity and a compact structure of the part in the important zone of the rolling way,
- the work addition material may be established at the minimum level,
- the dimensional precision, in the active zone, is better than at the gravitational casting.

2. Establishment of the revolution

The revolution of the casting mould at the centrifugal casting may be calculated with different calculus relations, recommended in the specialty literature. Thus, according to:

– [1] the revolution will be:

$$n = 300 \sqrt{\frac{k}{r}} \quad (1)$$

n is the revolution, in revolution per minute, r – the radius of the interior surface of continuous cast part, in cm, k – coefficient in function of the part material,

For the alloyed steel the values of the coefficient k is of 20 – 30, and for the radius r of 8 – 10 cm, the value of the revolution is

$$n = 474 - 581 \text{ rpm}$$

– [2] the revolution will be:

$$n = \sqrt{\frac{1800}{D_{int.f}}} \cdot k_g$$

$D_{int.f}$ is the interior diameter of the mould cavity, in meters, k_g – the coefficient which, for the centrifugal casting machine with the vertical turning axe has the value of 90 ... 100.

In case of the casting of part with 0.8 m, in diameter, we obtain:

$$n = 450 - 474 \text{ rpm}$$

3. Installation and structure of centrifugal casting mould

A new installation of centrifugal casting can require great initial expenses, which can't be supported, unlike the case of a high number of identical cast parts. Because the number of the wire sheaves is not great the investment for production of the centrifugal installation is not justified.

Therefore at the PROMEX Society in Braila for the organization of the experimental equipment was used a carousel lathe of 1100 mm of the revolution plate in diameter and the maximum revolution of 1000 rpm. The lathe was placed on a foundation, necessary for an adequate dynamic stability. Also it

was ensured an adequate protection system because the centrifugal casting installation may be dangerous.

The casting mould (Figure 2) consists of a metallic case, which ensures the setting of the segments from the mould compound.

The metallic case consists of the base plate 1, out of which is welded the cylindrical form 2. Inside the metallic case is placed the inferior casting mould 5 and the superior casting mould 6 pre-assembled with the hole form 8.

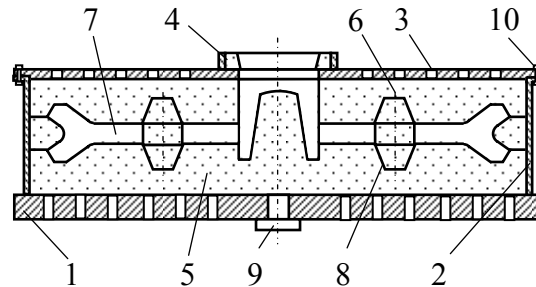


Fig. 2. Structure of casting mould:

- 1-base plate, 2-cylindrical form, 3-lid,
4-cast span, 5-inferior mould,
6-superior mould 7-mould cavity,
8-hole form, 9-centering shaft,
10-assembly elements.

The casting form is closed with the lid 3 through the assembly elements 10. In the center of the case on the plate of the carousel lathe is placed a centering shaft 9.

4. Conditions for parts casting

The Society PROMEX from Braila, Romania has electrical arch ovens of 3 and 5 tons and electrical induction ovens of 250 kg, for melting the carbon and alloyed steels. Thus, the melting capacity is better than the necessary material quantity for casting one part. Because of this more cast moulds are necessary for a charge of melted steel. This entails preparation of two, three cast moulds or small values for the time necessary for assembly of centrifugal casting mould, casting and exhausting of the mould with cast part.

The transport of the melted steel from the melting oven to the casting moulds is made with the crane and casting the ladle. The transport distance is of 35-40 meters. The casting ladle must have the adequate capacity, according to the necessary quantity for casting of the parts prepared in this aim. At the casting bay there are casting ladles, meant for casting of steel, of three and five tons. In the aim of security ensure of the worker at the time of the casting process was designed and worked a casting platform and protection screens in the proximity of the centrifugal casting machine (Figure3).

5. Results and discussions

In Figure 4 is shown an image of the centrifugal casting case, fixed and centered on the plate of the

carrousel lathe. In Figure 5 is shown a view of the cast part.



Fig. 3. Image of the casting platform.



Fig. 4. Image of the casting equipment.

The cast part presents a great quantity of iron oxides. The aspect of material leakage is caused, also, by the iron oxides, which are easily removed in the cleaning process.

The principal problems ascertained in the time of the casting process and in the view of quality of cast part are:

1. The relatively small productivity of the casting process,

2. Instability of the casting form in the time of the casting and solidification processes,
3. The presence of the open ducts at the superior surface of the part.

The reduced productivity is caused by the great duration of the preparing of the casting technological system: the assembly and centering of the metallic case on the turning plate of the carrousel plate and of the mould inside of case.



Fig. 5. Image of the cast part.

This problem may be solved by the rigid fixation of the metallic case and very good centering on the carousel plate. The assembly of the form by mould compound with the lid of the metallic case. In this aim there may work two or three lids prepared for assembly with the immediate case, when the cast part and the respective mould were extracted and the metallic case was cleaned with compressed air spurt. Thus, in a new mould will be shortly assembled in the metallic case.

The second problem imposes a very strong fastening and good centering of the metallic case on the plate of the carousel lathe and of the lid with the metallic case.

Well centering the mould into the metallic case, and the maintaining of centered position during the casting are very important.

If the axe of mould is, even very little, displaced in comparison with the revolution axe, in the casting process, the material, in the casting mould, leads to the increasing of the eccentric mass and, the great revolution can produce the vibration with the instability of the dynamic process.

That is why the maintaining of dynamic stability in time of casting and solidification is strictly imposed. In this aim supplementary centering elements are necessary.

The elements can be constituted by a system of centered columns, fixed in the base plate of the metallic case (three are sufficient). The mould has comprised corresponding guiding jacks. Eventually the lid may be provided with guiding holes. These systems will be made in the holes of the casting form (Figure 6).

At the circumferential surface of the cast part the continuity of the material was observed.

The cast part presents at the superior surface open ducts with the depth of 3 to 16 mm and 3 – 5 mm in diameter.

The cause of these holes is the small gas permeability of the casting mould.

The solution for solving this problem is ensure of the easy and extended capacity of the casting mould for evacuation of the gases form the cavity of the casting form.

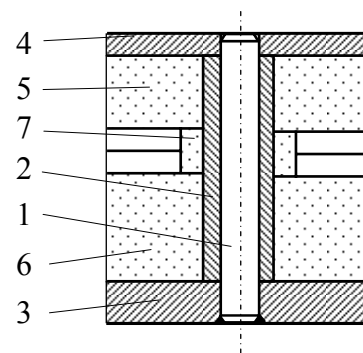


Fig. 6. System of complex centering:
1-guiding column, 2-guidning jack,
3-base plate of metallic case, 4-lid,
5-superior cast form, 6-inferior cast form,
7-form for holes.

In this aim canals must work at the contact surface of base plate and lid with the mould. Because the centrifugal casting process males at great revolution, circular and symmetrical canals are recommended. At the same time the canals system must communicate with the exterior through holes, sufficient many enough and with a symmetrical distribution.



6. Conclusions

The centrifugal casting is a good method for obtaining the parts with revolution form. In the case of the wire sheaves for heavy cranes, characterized with the diameter much greater than the thickness in the active zone, there are some special requirements.

These requirements refer to the dynamic stability in the technological process and to the quality of the cast part.

The experiment shows that the centrifugal casting process, of a wire sheave with the 800 mm in diameter, ensures the obtaining of the part, but some improvements are necessary, concerning the dynamic stability, productivity and gas permeability of the casting form.

The solutions proposed for improvement of this centrifugal casting system are:

- supplementary centering of the mould using the systems with guiding column and jacks,
- the use of two or three lids assembling the mould at the lid a priori of assembly with the base plate,
- working of net canals and holes for easy evacuation of the gases.

References

- [1]. **Gadea, S. a.o.** – *Manualul inginerului metalurg*, vol.2, Editura Tehnica Bucuresti, 1982.
- [2]. **Zubac, V.** – *Utilaje pentru turnatorie*, Editura didactica si pedagogica, Bucuresti, 1982.
- [3]. **Stefanescu, C.** *Indreptar pentru turnatori*, Editura tehnica, Bucuresti, 1972.
- [4]. **Stefanescu, D.M.** – *Stiinta si ingineria solidificarii pieselor turnate*, Editura AGIR, Bucuresti, 2007.
- [5]. **Fredriksson, H.** – *Metals Handbook Ninth Edition*, vol. 15, Casting, ASM International, Ohio, 1988.

THEORETICAL STUDY REGARDING THE FLOW CONDITIONS FOR ALLOYS THROUGH THIN CHANNELS

Ioan MARGINEAN, Bogdan-Alexandru VERDES, Sorin-Adrian COCOLAS

Politehnica University of Bucharest
email: marginean_ioan2002@yahoo.com

ABSTRACT

A common tool used to demonstrate the phenomenon of movement of liquids through thin channels is the capillary tube. When the lower end of the tube is placed vertically in a liquid (such as water), it forms a concave film. Surface tension pulls the liquid column up until there is a sufficient mass of liquid for gravitational forces to overcome intermolecular forces. The contact length (around the edge) between the top of the liquid column and the tube is proportional to the diameter of the tube, while the weight of the liquid column is proportional to the square of the tube's diameter, so a narrow tube will draw a liquid column higher than a wide tube. This paper wants to bring theoretical arguments to the possible flowing limits for alloys through thin channels.

KEYWORDS: thin channel, flow, limit conditions, capillarity, surface tension

1. Properties of metal melt

Metal melt properties can be grouped as follows:

- technological properties (fluidity or flow capacity, viscosity, density, surface tension);
- physical properties;
- thermodynamic properties.

Properties such as density, viscosity, surface tension, electrical conductivity are sensitive to structural features; they provide us with important information related to the melt structure.

1.1. Fluidity

Metal melt fluidity is one of the properties, which is related to the shape of the resulting product from solidification. Fluidity is defined as:

- flow capacity of the alloy-channels and cavity shape, expressed by the filling time, flow velocity, the length travelled in channels and filled cavities;
- filling capacity of the cavity shape, reproducing the finest details of configuration.

Factors influencing fluidity are:

- material properties shape;
- conductivity material form;
- diffusivity, heat storage capacity;
- cavity shape geometry, hydraulic pressure, external pressure applied to the alloy;
- viscosity, way of crystallization, purity alloy, casting temperature, specific heat, latent heat of

crystallization, solidification range, thermal conductivity, surface tension, which are intrinsic properties of the alloy;

- casting conditions.

The biggest influence on the fluidity has the solidification range of the alloy. When solidification range is higher, then flow is lower. Pure metals, eutectic alloys and chemical compounds have the biggest fluidity.

Alloy flows as long as it is in liquid phase and a period after solid phase occurred, see Fig 1.

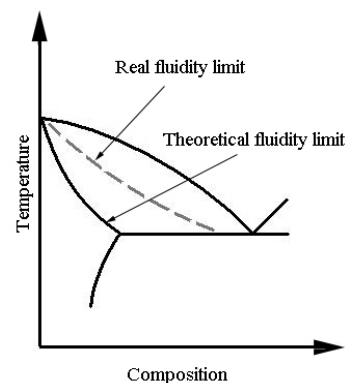


Fig. 1. Temperature range up to the alloy solidification runs.

Casting temperature affects fluidity of the alloy in the sense that higher temperatures mean higher



fluidity. When specific heat and density of the alloy it's higher, then the flow will be higher.

Thermal diffusivity of alloy ($a=\lambda/C_p\rho$) influences fluidity in the sense of her decreasing. Latent solidification heat (melting) affects the flow upwards.

Viscosity determines the flow velocity, which is defined by the dimensionless Reynolds criterion:

$$R_e = \frac{V \cdot d}{\nu} = \frac{V \cdot d \cdot \rho}{\eta} \quad (1)$$

where: ν is the linear flow velocity; d – hydraulic diameter; ν - cinematic viscosity, η - dynamic viscosity.

The influence of viscosity on fluidity resulting from the equation of laminar flow and alloy fluidity, being inversely proportional to the cinematic viscosity

$$(f = \frac{1}{\nu\rho}).$$

Surface tension influences fluidity by moistening or not moistening the alloy flowing channel. Alloys moistening the wall form have greater ability to fill the cavity mould (better fluidity).

The influence of material form is manifested by its ability to take heat from the liquid alloy and to liberate it.

When the ability to absorb heat transferred from the alloy is higher, then the flow decreases faster. If the coefficient of heat accumulation of the form is higher ($b_f = \sqrt{\lambda_f \cdot c_{p,f} \cdot \rho_f}$), then fluidity will be lower.

1.2. Density

At binary alloys consisting of components having similar physic-chemical properties the Vegard law can be applied:

$$\rho_{alloy} = \rho_1 \cdot x_1 + \rho_2 \cdot x_2 \quad (2)$$

where: ρ_1 and ρ_2 are the component densities 1 and 2, x_1 and x_2 atomic fractions of components 1 and 2.

In case of alloys components with differing physical - chemical properties, the Vegard law can not be used to determine alloy density because significant deviations occur.

Fraction between density and temperature of the metal is defined as the density temperature coefficient ($d\rho / dT$). For most elements, temperature coefficient of density increases linearly with the melting temperature.

Density of liquid metal is dependent on temperature, which is given by:

$$\rho_l = \rho_o + a \cdot t \quad (3)$$

where: ρ_o and a are constants that depend on the alloy nature, T - temperature in °C.

In case of transition metals with incomplete 3d layer, the density is given by:

$$\rho = \rho_{top} [1 - X'(T - T_{top})] \quad (4)$$

where ρ_{top} is the density of liquid metal at

absolute temperature of melting (T_{top}); X' -effective temperature coefficient of density.

This factor differs from the actual temperature coefficient of density in a relatively small heating over T_{top} , is given by:

$$X' = \frac{1}{\rho} \cdot \left(\frac{\partial \rho}{\partial T} \right)_p \quad (5)$$

1.3. Viscosity

Viscosity is the property of fluids to oppose deformation (movement) but which does not reduce their volume by developing unitary effort. This property is manifested only in fluids in motion and expresses the inner friction between fluid layers moving at different speeds.

The viscosity can be defined as follows: between the applied force (noted with ϵ) acting per unit area, which determines the relative displacement of two adjacent layers of fluid and the velocity gradient perpendicular to the applied force (dU / dZ) there is proportionality. Proportionality factor (η) is the coefficient of viscosity or dynamic viscosity.

$$\eta = \frac{\epsilon}{dU / dZ} \quad (6)$$

Relation (6) is the mathematical expression of Newton's law.

Stokes defined the relation between dynamic viscosity and density as the fluid cinematic viscosity:

$$\nu = \frac{\eta}{\rho} \quad (7)$$

Cinematic viscosity of metals and alloys at casting temperature is almost smaller than the temperature of water at room temperature, thus explaining their high fluidity. A relation is established semi-empirically by Andrade for dynamic viscosity of liquid metal at melting point:

$$\eta = \frac{B(M \cdot T_{top})^{\frac{1}{2}}}{V^{\frac{2}{3}}} \quad (8)$$

where: B is a constant, M - atomic mass, V - atomic volume.

Dynamic viscosity varies with temperature for liquid metals and alloys. This dependence is expressed by the relationship:



$$\eta = \eta_0 \cdot e^{-\frac{E_V}{RT}} \quad (9)$$

where: η_0 is the viscosity at reference temperature; E_V - activation energy of viscous flow.

Dynamic viscosity decreases with increasing of the temperature.

For binary liquid alloys, which are close to ideal alloys, alloy viscosity can be determined with relation:

$$\eta_{alloy} = \chi_1 \cdot \eta_1 + \chi_2 \cdot \eta_2 \quad (10)$$

where: χ_1 and χ_2 are molar fractions of components 1 and 2; η_1 and η_2 - viscosity components.

Viscosity is influenced by the existing impurities in metals and alloys.

1.4. Superficial tension

Surface tension is one of the properties of metal melt, which depends on two other properties, cohesion and adhesion. Atomic-scale phenomena can be regarded as if atoms or molecules within a substance are spaced sufficiently for each of them to be surrounded by a field of forces, which form a system equivalent to zero. Forces are forces of cohesion, named "Van der Waals" forces.

To separate atoms or molecules of the same type, some others must consume a mechanical work; it named mechanical work of cohesion.

The force that opposes atoms separation or molecules of that substance reported at length shall be known as surface tension (σ). At the melt surface occurs a flux of collectivized electrons, which tend quit the melt, but positive ions pull them back into the melt.

Metal melt surface is covered by a thin layer of liquid with negative loads, under which at a certain depth of atomic radius order, it is located a layer with compensating positive electrical loads. The two layers form a double layer with a thickness of interaction radius of an atom order. This double layer acts as an electrical condenser as a barrier, preventing, at least partially, the outgoing of electrons molten metal.

An atom in the melt, under the double layer, at a distance greater than the range of inter-atomic forces is surrounded by a field of forces, which together with its own forces form a system equivalent to zero. It has an effect of mutual annihilation of the forces of interaction between atoms, which allows free movement, as there is cohesion between them.

The surface tension varies with the degree of dispersion and the specific surface of dispersed phase. Under specific surface we understand the relation between the surface phase and its volume. When the dispersion exceeds a certain limit, the surface tension

starts to decrease, and when you reach the molecular dispersion of surface, the tension tends to zero.

A specific area can be obtained by dispersing phase or substance, or by inoculation in a liquid of very fine particles.

2. Obtaining ceramic-metal materials by impregnating

One method of obtaining ceramic-metal composites is to impregnate the porous ceramics with molten metal.

Although this process has been less studied and applied, it presents a higher interest. The process is based on the penetration principle of molten metal under the action of capillary forces.

The impregnation method finds many applications that can be infiltrated in the ceramic base mass of several types of molten metals and alloys.

The impregnation mechanism is governed by the relation of possible interaction between the solid phase with high melting point (ceramic shell) and liquid metal phase.

In this sense the following issues are highlighted:

- chemical reactivity, dissolving in metal of ceramic parts, with two consequences, the chemical transformation of metal and destruction of ceramic shell;

- moistening of ceramic material by molten metal.

For moistening, there are three possible cases:

Case 1: lack of solid surfaces moistening by liquid and lack of solubility of an element in the other;

Case 2: good moistening, but without solubility;

Case 3: good moistening and limited solubility of solid in liquid.

Case 1: contact angles and interfacial tensions are very high and the capillary action tends to reject the metal from blanks of ceramic shell. In this case it can be used an external force to force molten metal flow in capillary spaces or in some cases the problem can be solved by interfacial additives which tend to decrease moistening angle.

Case 2: solubility of the refractory metal oxide is practically zero, but the contact angle is very low (below 90°). In this case capillary forces are sufficient to induct metal penetration in ceramic structure.

Case 3: the diffusion phenomena and fluid flow creating a new act in accord with capillary forces. The liquid phase enters the capillaries, it tends to advance in areas where solid particles are in contact (intergranularly boundaries). At extremes, the ceramic shell can be disaggregated but solid liquid phase saturation at the domain limit solid solution before moistening, avoids excessive transport of material. Dissolved substance remains in solution or precipitates on existing solids particles or even precipitates separately

in the liquid phase of the solidified metal. This case is more complicated because in addition to capillary phenomena occur the diffusion of liquid or viscous creep processes. Thus, temperature and time become very important factors to control the impregnation process.

Classical methods of impregnation with molten metal are:

- total immersion - ceramic shell (matrix) is totally immersed in the metal bath;
- capillary-immersion - ceramic shell is suspended - partly immersed in the metal bath;
- through contact - ceramic shell is attached to solid objects falling gradually and melting by heating.

To obtain adequate impregnation are frequently applied external forces such as: supply by drop, compressing the fluid, centrifugal force or vacuum aspiration.

Composite material consisting of ceramic and metal is called cermet. A cermet is designed to have optimal properties of both components, such as high temperature resistance and hardness (like ceramic) and resistance to plastic deformation (taken from metal).

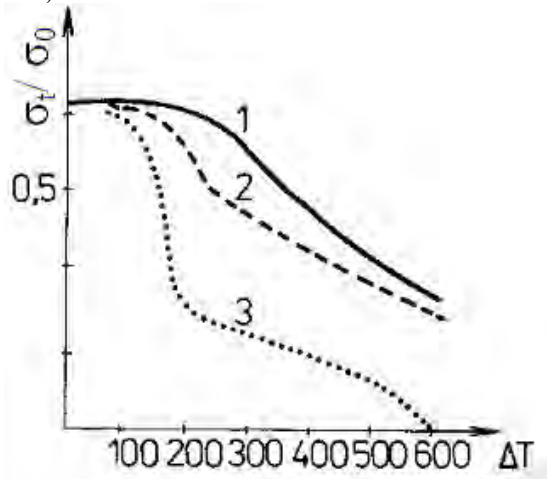


Fig. 2. Resistance variation at thermal shock for various cermet.

- 1 – cermet Al_2O_3-Cr , granulatory diameter of $Cr=1 \mu m$;
- 2 – cermet Al_2O_3-Cr , granulatory diameter of $Cr=25 \mu m$;
- 3 – Al_2O_3 .

Figure 2 shows the variation ratio of bending strength after thermal shock (σ_i) divided by the initial resistance to bending (σ_0) function by the value of thermal shock (ΔT).

3. Flow through porous media

Complete description of the process of isothermal flow through a porous medium can be done by considering a set of three equations:

- motion equation, which expresses the conservation of momentum;
- continuity equation, expressing mass conservation;
- state equation, providing a relation between state parameters $\rho = f(P, T)$.

Motion equation through porous media is known as Darcy's law, taking the form:

$$V_f = \frac{\rho g}{\eta} k_p \frac{h_1 - h_2}{L} \quad (11)$$

where: V_f - is the filtration velocity; ρ - fluid density; g - gravitational acceleration; k_p - permeability coefficient defined by relation $k_p = k \frac{\eta}{\rho g}$; k - hydraulic coefficient of conductivity or filtration coefficient; η - dynamic viscosity of the fluid; $\frac{h_1 - h_2}{L}$ - hydraulic gradient, L - cylindrical length of porous body.

If environment is homogeneously porous, k and k_p are constant.

Continuity equation in fluid flow through porous medium has the general form:

$$\frac{\partial m g}{\partial t} + \text{div}(\rho v_f) = 0 \quad (12)$$

4. Movement of liquid through porous medium

Highlighting fluid movement thru porous medium due to capillarity effect is highlighted by the introduction of a capillary tube in a liquid, which moistens the capillary wall (see Fig. 3).

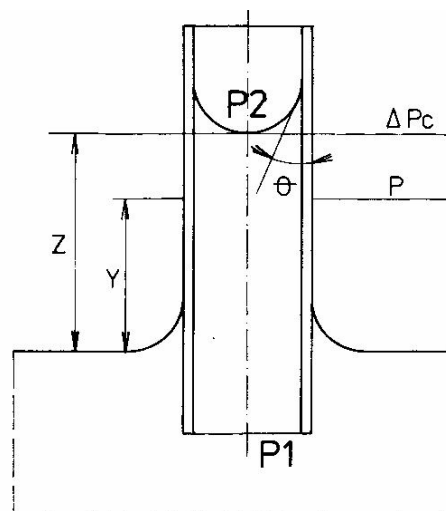


Fig. 3. Ascending of the moistening liquid in a capillary tube.

The ascendant movement of the liquid in the capillary is without external action until a given height (z). This is determined by lowering the free energy of the system to thermodynamic equilibrium, which causes a decrease in pressure between the free surface of liquid in the tank and the pressure from the free surface of liquid in the capillary.

Between liquid and its vapour there is an interface. Increasing the interface is consuming mechanical work.

If the movement of the liquid in the capillary tube is carried out isothermal ($dT = 0$):

$$dF = -P \cdot dV + \gamma \cdot dA \quad (13)$$

where γ is the surface tension.

Term $-P \cdot dV$ corresponds changing free energy between homogeneous phases participating in the case, and the term $\gamma \cdot dA$ represents free energy changes at system interface.

The change of the total system volume is given by the change in volume of each phase $dV = dV_1 - dV_2$. Given the state parameters of the two phases (P_1 and V_1 in the liquid phase and P_2 and V_2 in vapour phase), the term $-P \cdot dV$ of equation (13) becomes:

$$-P \cdot dV = -P_1 \cdot dV_1 - P_2 \cdot dV_2 \quad (14)$$

And so relation (13) becomes:

$$dF = -P_1 \cdot dV_1 - P_2 \cdot dV_2 + \gamma \cdot dA \quad (15)$$

If the process is isochoric, then:

$$dV = dV_1 + dV_2 = 0, \text{ so } dV_1 = -dV_2 \quad \text{and}$$

therefore:

$$dF = -P_1 \cdot dV_1 + P_2 \cdot dV_2 + \gamma \cdot dA \quad (16)$$

At equilibrium $dF = 0$ and results:

$$P_1 = P_2 + \gamma \cdot \frac{dA}{dV_1} \quad (17)$$

The difference between the two pressures, liquid pressure (P_1) and vapour pressure (P_2) is called capillary pressure.

Capillarity effect can be expressed as the maximum height of capillary rise of liquid (h_{\max}). Neglecting friction losses, maximum height results from the condition of equilibrium, i.e. at the end of ascent, the pressure difference will be equal to the hydrostatic pressure of capillary liquid column, i.e.:

$$\Delta P_c = \frac{2 \cdot \gamma \cdot \cos \theta}{r} = \rho_l \cdot g \cdot h_{\max} \quad (18)$$

From where:

$$h_{\max} = \frac{2 \cdot \gamma \cdot \cos \theta}{r \cdot \rho_l \cdot g} \quad (19)$$

ρ_l is the fluid density.

In a more general case is considered a fluid motion in an inclined cylindrical capillary (see Fig. 4).

Balance of forces will be given by:

$$\Delta P_c - \rho_l \cdot g \cdot z \cdot \sin \alpha - \Delta P_f = 0 \quad (20)$$

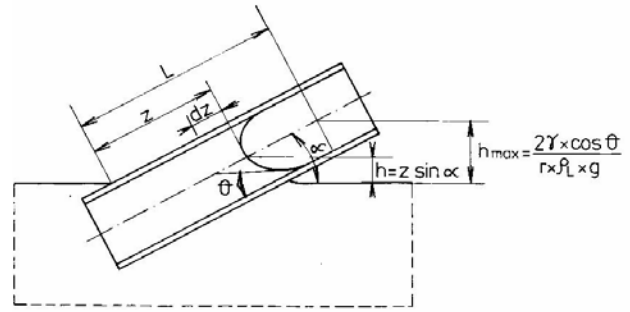


Fig. 4. Ascending of a liquid in an inclined cylindrical capillary

Where (ΔP_f) is a current value corresponding to the pressure drop length (z) and current velocity ($v = d_z/d_t$).

Pressure drop caused by friction can be expressed by Fanning-Darcy equation:

$$\Delta P_f = c_f \cdot \frac{z}{d} \cdot \frac{\rho_l \cdot v^2}{2} \quad (21)$$

Liquid ascending through capillary is possible only if the fluid pressure (P_1) occurs in the capillary. Pressure differences ($P_1 - \rho_l \cdot g \cdot y$) are equalizing in the liquid during transport. It results that in isolated cylindrical capillary liquid movement can be considered a process of equalization (balancing), such as thermal conductivity or diffusion. Under these conditions mass flow transport (M_m) can be expressed by the relation:

$$M_m = S \cdot \chi_c \cdot \frac{d(P - \rho_l \cdot g \cdot \gamma)}{dy} \cdot \rho_l \quad (22)$$

where: M_m is the mass flow of liquid through the capillary in kg/s; S - cross-sectional area of capillary in m^2 ; χ_c - liquid capillary conductivity coefficient in m^2/s .

Relation (22) shows that the height (y) Fig. 3, mass flow (M_m) is moved upwards as long as $P > \rho_l \cdot g \cdot y$.

Fluid pressure distribution is linear, so we can write:

$$\frac{P - \rho_l \cdot g \cdot \gamma}{y} = \frac{\Delta P_c - \rho_l \cdot g \cdot z}{z} = \frac{d(P - \rho_l \cdot g \cdot \gamma)}{dy} \quad (23)$$

And therefore the mass flow will be:

$$M_m = S \cdot \chi_c \cdot \frac{\Delta P_c - \rho_l \cdot g \cdot z}{z} \cdot \rho_l \quad (24)$$

We taking into account the definition of mass flow:

$$M_m = s \cdot \rho_l \cdot \frac{dz}{d\tau} \quad (25)$$

By equality of relations (24) and (25) follows:

$$\frac{dz}{d\tau} = \chi_c \cdot \frac{\Delta P_c - \rho_l \cdot g \cdot z}{z} \quad (26)$$

Comparing the above relations, we obtain the physical significance of capillary conductivity coefficient of the liquid:

$$\chi_c = \frac{r^2}{8\eta} \quad (27)$$

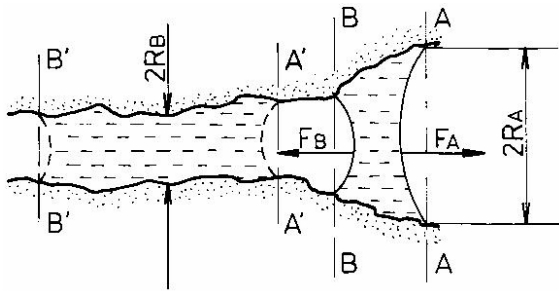


Fig. 5. Representation of a capillary pore with variable radius $r_A > r_B$.

Capillary conductivity coefficient is a physical quantity that depends on the radius of the capillary and on friction forces in the capillary fluid. Porous bodies do not always have cylindrical pores with the same radius (r), in most cases these pores have variable radius.

Considering a variable radius pore (see fig. 5), capillary depression created between the section (A) and section (B), makes the liquid move in position (A'B'). For section (A) and (B) have relations:

$$P_A = P_1 + \frac{2 \cdot \gamma \cdot \cos\theta}{r_A} < P_B = P_2 + \frac{2 \cdot \gamma \cdot \cos\theta}{r_B} \quad (28)$$

because $r_A > r_B$.

Pressures in the two sections can be expressed as the ratio between force and area, i.e.:

$$P_A = \frac{F_A}{S_A} = \frac{F_A}{\pi \cdot r_A^2} \quad (29)$$

$$P_B = \frac{F_B}{S_B} = \frac{F_B}{\pi \cdot r_B^2} \quad (30)$$

The F_A and F_B are the acting forces on the surfaces S_A and S_B , they are opposite forces. From equation (28) inequalities become:

$$P_A < P_B \text{ sau } \frac{F_A}{S_A} < \frac{F_B}{S_B} \quad (31)$$

But as $S_A = \pi \cdot r_A^2 > S_B = \pi \cdot r_B^2$, it results that $F_A > F_B$. Resulting forces $\Delta F = F_A - F_B$ cause fluid to move into position (A'B').

5. Conclusions

Theoretical investigations of binary liquid alloys show consistent changes in surface tension and viscosity with the increasing percentage of a component. Viscosity (η) and surface tension (σ) of system Ag-Sn and Sn-Zn decreases with increasing percentage of tin in its composition.

The capillary pressure acts to stabilize, but pressure convection acts otherwise. Stability criterion for a constant flow is based on a higher gradient of capillary pressure. This criterion defines a critical point. This critical point corresponds to maximum flow.

A constant flow is possible only in the sub critical zone (below the critical point).

Level value of a liquid by capillary flow is appreciable to a minimum values capillary radius (r) for example: a tube with a diameter of 2 m, water will ascend a little, approx. 0.014 mm. But at a diameter of 2 cm, the water would ascend for about 1.4 mm and for a 0.2 mm diameter, the water would ascend for 140 mm.

References

- [1]. Campbell, J.-Castings. Butterworld Heinemann, 2000.
- [2]. Beeley, P.- Foundry Technology. Butterworld Heinemann, 2001
- [3]. Dinsdale, A.T., Queded P.N.-The viscosity of aluminium and its alloys-a review of data and models. 1st Fe-Al Meeting, Boulder, 22.06.2003, p1-10.
- [4]. Tinklepaugh, James R.-Cermets. Reinhold Publishing Corporation, 1960.
- [5]. Batchelor, G.K.-An Introduction To Fluid Dynamics. Cambridge University Press, 1967.
- [6]. Ehrig, R., Nowak, U., Oeverdick, L. & Deuffhard, P.-Advanced extrapolation methods, for large scale differential algebraic problems. In High Performance Scientific and Engineering, Computing. Lecture Notes in Computational Science and Engineering, vol. 8 (ed. H.-J.Bungartz, F. Durst & C. Zenger), pp. 233-244. Springer., 1999.
- [7]. Rosendahl, U.-Uber die Grenzen des stationaren Flussigkeitstransportes in offenen Kapillarkanalen. Cuvillier Verlag Gottingen, 2007.
- [8]. Rosendahl, U. & Dreyer, M. E.-Design and performance of an experiment for the investigation of open capillary channel flows. Exps. Fluids 42, 683-696., 2007
- [9]. Rosendahl, U., Ohlhoff, A. & Dreyer, M. E.-Choked flows in open capillary channels: theory, experiment and computations. J. Fluid Mech. 518, 187-214, 2004.

THE PROCESS INVOLVED IN MAKING THE MEDALS

**Daniela BURUIANA (NEGOITA), Gheorghe FLOREA,
Alexandru CHIRIAC**

"Dunărea de Jos" University of Galati
email: dnegoita@ugal.ro

ABSTRACT

This paper presents a method that was experienced in the laboratory to manufacture a medal. There are three general techniques used to make medals: repoussé, striking and casting. Serigraphy technique is the most chosen for a relief type as it is the fastest and least expensive to produce. The final result is a unique work of art, with examples of the same medal exhibiting subtle variations in color and surface detail.

KEYWORDS: medals, serigraphy technique

1. Introduction

The medal as we know it today had its origins in the Italian Renaissance with the circular bronze commemorative portraits produced by Pisanello (c. 1395-1455) during the mid-fifteenth century. Medals are often viewed in a numismatic context because they share certain obvious characteristics with coins. Both are round, made of metal, and exhibit a portrait on the front (obverse) and an allegorical or narrative scene relating to that portrait on the back (reverse). Medals, however, have no intrinsic value.

They are produced for many purposes: to celebrate famous people, to mark important social or political events, or to memorialize personal milestones, such as births, marriages and deaths.

Until the seventeenth century, medals were often used as articles of personal adornment, attached to clothing or worn around the neck. As intimate sculpture in a double-sided relief format, medals have always been something to hold and turn into hand-personal objects for aesthetic and intellectual contemplation.



Fig.1. Designed by Pisanello 1447.



Fig.2. Aquila city commemorative medal.

The first great artist to create medals was the Italian painter Antonio Pisano, known as Pisanello, who modeled and cast a number of portrait medals of princes and scholars in the 1440s.

Many other artists followed his example, in Italy, the Low Countries, Germany and France. In the seventeenth century medals were extensively used to commemorate events and glorify rulers. In the eighteenth century prize medals became common. In the 19th century art medals became popular.

From its contributions in providing jobs and employee skills to delivering the dependable, high-quality and cost-effective components necessary to advance technology, metal casting has impacted virtually every improvement experienced by each passing generation.

2. Techniques for making medals

There are three general techniques used to make medals: repoussé, casting and serigraphy.

The repoussé method is a metalworking technique in which a malleable metal is ornamented or shaped by hammering from the reverse side. There are few techniques that offer such diversity of expression

while still being relatively economical. It is also known as embossing. A method of creating a relief design by hammering or pressing the reverse side of a metal surface; literal, meaning in French, "to push back".

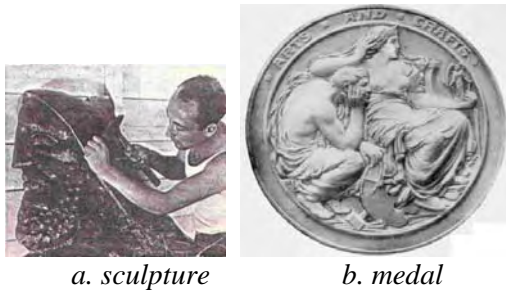


Fig.3. *Copper repoussé relief.*

The technique of repoussé is the one least frequently employed, although it was used quite widely in the Netherlands during the 17th century. Here the medal is made by hammering a thin shell of a metal blank into a hollow die on which the artist has made a design. The obverse and reverse of the medals, which are made separately, are then soldered together, the resulting medal being hollow. Embossing produces much the same effect but the process is reversed. Here the design is formed by pressing down the background, leaving the design in relief.

The repoussé and chasing techniques utilize the plasticity of metal, forming shapes by degrees. There is no loss of metal in the process, as it is stretched locally and the surface remains continuous.

The process is relatively slow, but a maximum of form is achieved, with one continuous surface of sheet metal of essentially the same thickness. Direct contact of the tools used is usually visible in the result, a condition not always apparent in other techniques,

where all evidence of the working method is eliminated.

3. Metal Casting and medals

Casting is considered to be the technique that has produced all of the great medals of the Renaissance period. In this case a model is engraved in relief, usually in wax on a slate disk. The wax model is then removed and molten metal is poured into the resulting matrix. A medallion with two sides would be made by the use of a casting jar, a two-part hollow frame.

Generally, chased medals are considered to be of lesser value as it is assumed that the artist wasn't satisfied with the product as originally made, although one may just as easily conclude that an artist's finishing touches on a work of art improve its quality. This final cast and chased medal may then be used as a model for further castings.

However, whenever a medal is recast in this way the resulting product often has somewhat less definition than the first cast and is always smaller in diameter since metallic objects shrink when cooled. Each time a medal has been recast from medals which have themselves been recast the resulting product not only has still less definition but is also of still smaller diameter. The whole thing starts with an idea, then that idea is translated into words and sketches, photographs and other reference material are also used as guides.

A graphic designer will then render the idea and finally a medal designer produces the final drawing of your medal.

Starting with an already rendered image cuts the design phase short, however the work of our medal designer who produces the final drawing is inevitable.

The model then will be cast in plaster and reduced to the proper size using a special reducing pantograph and will then be used to produce the pressing.



Fig.4. *Modeling technique:
a. mechanical, b. computers, c. manual*

If your medal has a special shape, then a cutting process is necessary. The cutting is a costly process, so unless you have clear reasons, it is recommended to choose a circular shape or standard sizes.

The press utilizes very high pressure to impress upon the blanks a negative motive of the die.

After fixing the top and bottom dies in the minting press, blanks are fed to the press and are stamped on both sides at once. If the medal is required to have a low relief then one strike is enough, however, proof or high relief medals may be struck two or more times.

Different procedures are used to produce different types of medals. The medals can be gold or silver plated. They can be chemically treated (artificially oxidized) to give them an antique appearance, surface polishing may be applied; even hand color-filling may be required.

4. Serigraphy technique

This option is the most chosen for a relief type as it is the fastest and the least expensive to produce.

A 2D black and white design is produced with computer graphics software (fig.4b) where black areas are read as extruded and white areas as embossed.

The final drawing can be used directly to produce the medals. It may need to be turned after collar and press process.

The surface may need to be smoothed as well. Finally, it is heat-treated to harden it. The exact optimum degree of hardness must be achieved in order to avoid cracking under strong pressure while striking.

Specifying the thickness of medal is presented in Figure 5.



Fig.5. Medal with double-sided.

This serigraphy technique is also known as screen-printing or silkscreen. It is a stencil technique that employs fabric stretched tight on a screen support frame. The loops have been blocked on the mesh so that ink does not pass through them. The ink covers everything except for the blocked-out sections and the image appears on the medals.

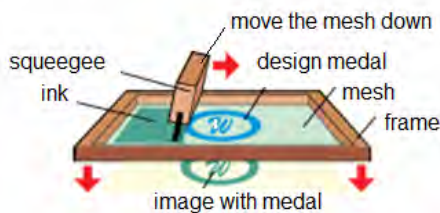


Fig.6. Serigraphy technique.

A screen is made of a piece of porous, finely woven fabric called mesh stretched over a frame of wood (Fig. 7).

Currently most meshes are made of materials such nylon and polyester.

Areas of the screen are blocked off with a non-permeable material to form a stencil, which is a negative of the image to be printed; that is, the open spaces are where the ink will appear.



Fig.7. Applying the ink to the screen.

The screen is placed atop a substrate such as fabric. Ink is placed on top of the screen, and a fill bar (also known as a flood bar) is used to fill the mesh openings with ink.

The process begins with the fill bar at the rear of the screen and behind a reservoir of ink. Moving the mesh down to prevent contact with the sub layer and



then using a slight amount of downward force pulls the fill bar to the front of the screen.

This effectively fills the mesh openings with ink and moves the ink reservoir to the front of the screen.

The ink that is in the mesh opening is pumped or squeezed by capillary action to the substrate in a controlled and prescribed amount, i.e. the wet ink deposit is proportional to the thickness of the mesh and or stencil.

Applying ink to mesh and the screen is lowered and the squeegee is pulled across the screen.

In order to avoid damage to the area that does not have printed image that is the inverse of the border and the next model are covered with the same paint. The medal on one of the sides is introduced in nitric acid. The achievement of care forms can lead to high-quality products.



Fig.8. University "Dunarea de Jos" medal

Proof finish beautifully highlights the relief structure. Multiple strikes may be needed to bring out all design details.

5. Conclusion

A medal can either be created using the repoussé or cast techniques developed in the classical world and perfected during the Italian Renaissance.

Casting requires the preparation of two original face models, the obverse and the reverse, in wax or plaster.

A graphic designer will then render the idea and finally draw the medals.

One last operation that could mark the clinching of the work, after polishing it, is the application of some paints and lacquers after the chemical attack.

References

- [1]. www.historicalartmedals.com;
- [2]. Hart, G. H. & G. Keeley, 1945. *Metal Work For Craftsmen*, London: Sir Isaac Pitman & Sons.
- [3]. Hodges, H., 1989. *Artifacts. An Introduction to Early Materials and Technology*, London: Duckworth
- [4]. Jones, D. M. (ed.) (2001). *Archaeometallurgy*, London: English Heritage Publications.
- [5]. Konkova, L. V. & G. G. Korol, (2003). South Siberian Imports in Eastern Europe in the 10th - the 13th centuries: *Traditions of Metalworking*, in *Archaeometallurgy in Europe*. Proceedings. Milan: Associazione Italiana di Metallurgia.

TIME ANALYSIS OF KING MATTHIAS THE IST SCULPTURAL GROUP

**Julieta Daniela SABĂU (CHELARU) ,
Vasile Filip SOPORAN, Ovidiu NEMEȘ**

Technical University of Cluj-Napoca
email: julieta_dana@yahoo.com

ABSTRACT

The paper presents a study on the degradation of the King Matthias I sculptural group caused by environment factors and influenced by the casting technology and by the assembling method. During this study, samples from inside the statue were used and analyzed through microscopy and X ray diffraction.

KEYWORDS: bronze casting, corrosion, microscopic analysis, cooper alloy, time bronze patina

1. Introduction

King Matthias the Ist sculptural group is one of the most representative sculptures in Cluj Napoca, Romania.

It consists of an equestrian representation of the king lying on a stone pedestal in front of which are represented in an attitude of worship holding flags Blasiu Magyar, an old army leader, Paul Chinezu, Ștefan Zapolya and the ruler of Transilvania, Stefan Bathory.

The whole statuary group presents remarkable plastic properties and the equestrian figure impresses through its monumental stillness [1].

The monument is the creation of Fadrusz Janos, a Slovakian artist, who was the disciple of Edmund Heller. He became famous soon after his first work, a cross exhibited in the Art Museum in Budapest in 1891. His most renowned work is King Matthias the Ist sculptural group, which received the first prize in the 1900 World Exhibition in Paris (Fig.1).

The statue was unveiled, in Cluj Napoca, in 1902.

The statues were made of bronze on a metal frame and according to the laboratory analysis, the composition of the alloy varies in different parts of the statue, there are variations in the percentage of tin, zinc, lead, but the content of copper exceeds 90 % of the alloy in most cases (Table 1) [2].



a)



b)



c)



d)

Fig. 1. King Matthias the 1st sculptural group: a), b), c) Images representing the mounting of the statuary group, d) The 1900 World Exhibition in Paris.

Table 1. The chemical composition of the alloy used in the casting of the King Matthias the 1st sculptural group

Chemical composition	Sn	Pb	Zn	Cu
	[%]			
Sample 1	7.17	0.08	0.36	remaining
Sample 2	8.00	0.52	1.30	remaining
Sample 3	7.72	0.41	0.21	remaining

The statue is 12 m high and 16 tones of alloy were used to create it. The thickness of the walls varies between 8 and 15 mm. The sculptural group is under

restoration and to establish the status of degradation the abdomen of the horse was opened to facilitate access to the fittings.



Fig. 2. Images depicting the inside of the sculpture.

The opportunity to enter inside the statue has allowed the study of the technology used during the casting process. Also, several samples were taken to examine the degradation of the copper used by old masters.

Each component part of the group is made of several pieces assembled together with steel screws (Fig. 2). The molding was made using the classic casting technology in sand and for more complex details the lost wax method was used.

2. Degradation factors

The degradation of the bronze used in great art works is a complex phenomenon which involves various electrochemical reactions triggered by several factors such as: environment pollutants, the composition of the alloy, the micro-structure of the

metallic material, humidity, the degree of surface processing, temperature and surface exposure time [3].

Studies have shown that the corrosion agents on a copper alloy surface are oxides, sulfides, carbonates, chlorides, sulfates of copper. Degradation caused by atmospheric corrosion depends on the chemical composition of the metallic material, on the pollutants and on the exposure time needed for the development of corrosion products [4].

Degradation appears mainly because of the interaction between water and corrosive substances on the surface of the materials. In the case of King Matthias the Ist sculptural group, the degradation occurred not only because of environmental exposure, but also because of the steel screws used for assembling the component parts, which caused galvanic corrosion (Fig. 3).



Fig. 3. Images representing the inside of the sculpture.

3. Materials. Working method

For the metallographic analysis, the samples were polished with alumina paste and washed with ammonia cupric chloride and with nitric acid to

determine their structure. The structure of the alloy used is homogenous, the crystals have polyhedral appearance with macles (Fig. 4), leading to high anticorrosive properties [5].

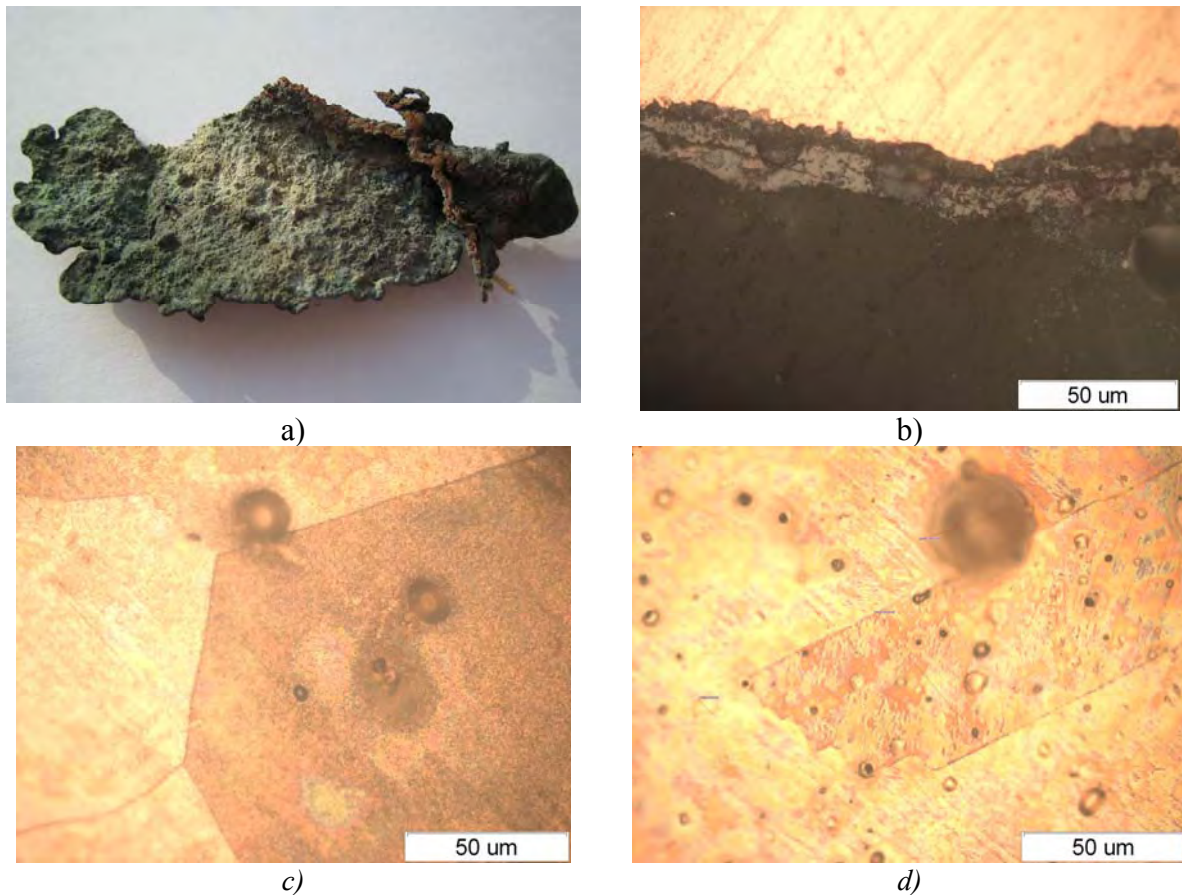


Fig. 4. Samples of the alloy used in the casting of King Matthias I sculptural group: a) raw sample; b) oxide layer; c) macroscopic structure; d) microscopic structure.

We can observe that in Figure 4b, the oxide layer is 10-50 μm thick. Research includes optical microscopy (OLIMPUS GS 51) and X ray diffraction (DRON-3 diffractometer). X ray diffraction examination (working conditions): DRON-3

diffraction device, Bragg - Brentano installation, acceleration voltage 25 kV, 20 mA electric intensity, detector voltage 600 V, slits 8,6,0.5,6 mm, wavelength $\lambda = 1.79026 \text{ \AA}$, Cobalt tube.

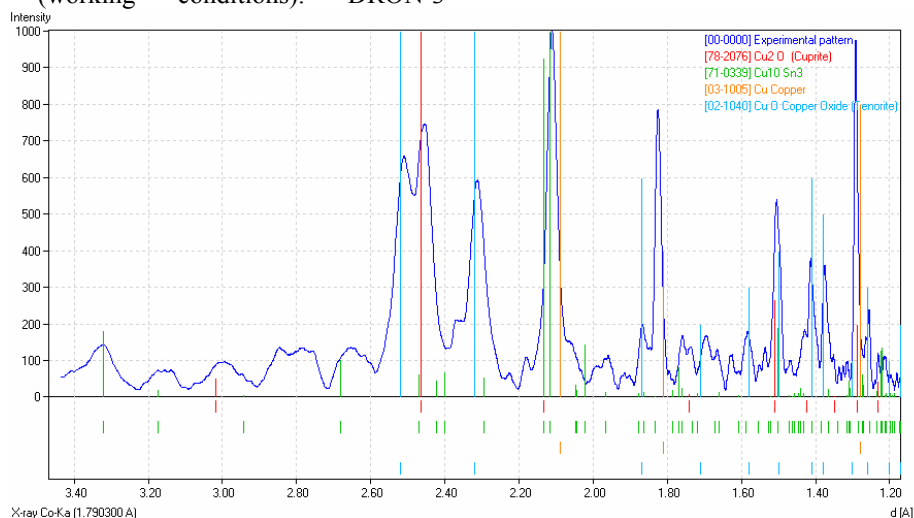


Fig. 5. X ray diffraction analysis of the oxide layer formed on the inner walls of the statue.

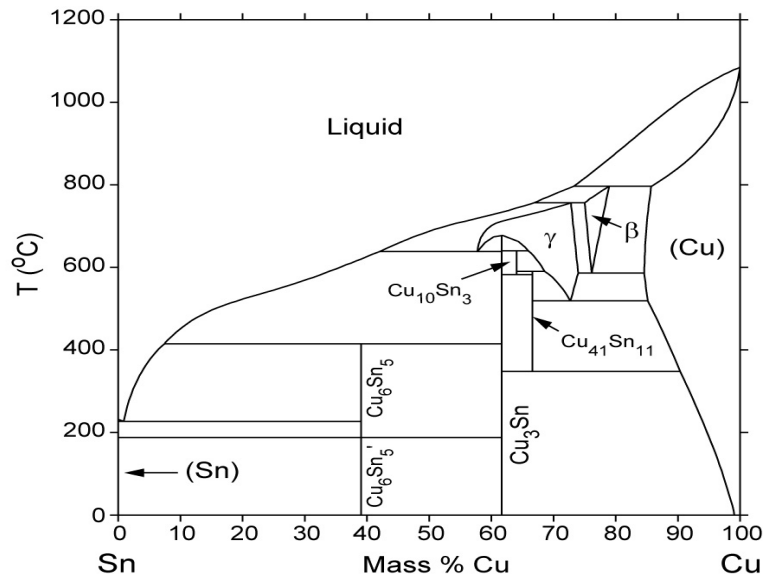


Fig. 6. Phase Diagram Cu-Sn [5].

Table 2. Calculated invariant equilibrium [6]

Reaction	Phase	Cu, %	Sn, %
$\gamma + \text{Cu}_3\text{Sn} \rightarrow \text{Cu}_{10}\text{Sn}_3$ 640.1 °C	γ	72.68	27.32
	Cu_3Sn	61.63	38.37
	$\text{Cu}_{10}\text{Sn}_3$	64.06	35.94

The main compounds identified after the X ray diffraction analysis in the bronze used for casting King Matthias I sculptural group are cuprit and

tenorit. These are the most common corrosion products and are usually found on metal surfaces.

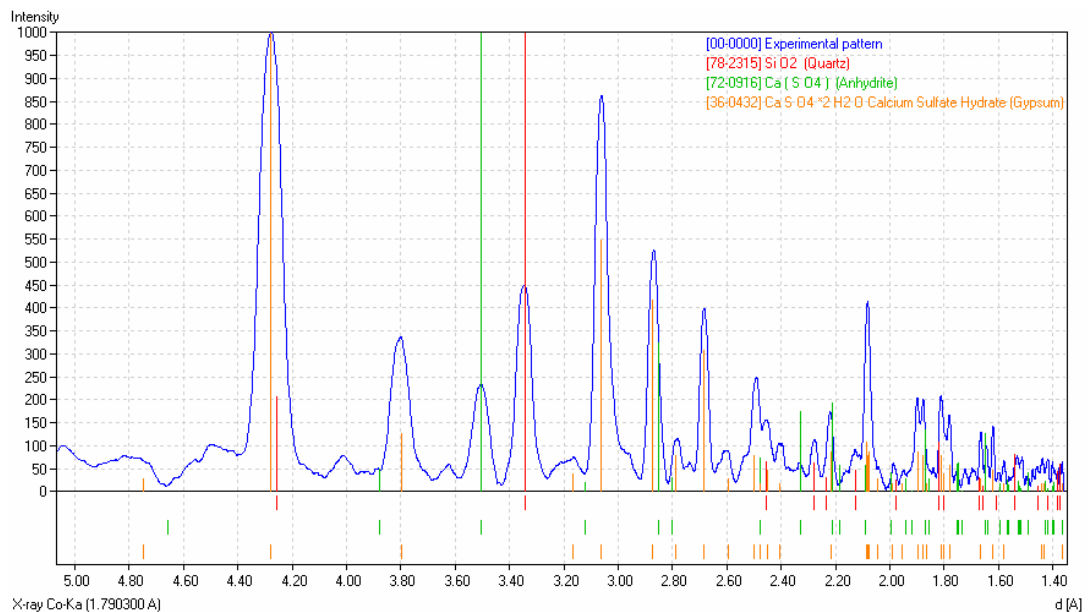


Fig. 7. X ray diffraction analysis of the sediments deposited on the inner walls of the statue.



Alongside copper oxides, copper was identified in small quantities, probably as a result of cuprit decomposition.

The samples also contain different phases in percentage values: salts, oxides of Mg, Fe, Al which could not be determined.

On the inner walls of the statue, large quantities of material sediments were found. After the X ray diffraction analysis, the sediment was identified as a residual mixture of compounds resulting from contamination: gypsum or calcium sulfate hydrate ($\text{CaSO}_4 \cdot 2\text{H}_2\text{O}$), sulphate calcium (CaSO_4) and quartz (SiO_2). Silicates may have resulted from the molding mixture or from the accumulation of airborne particles.

Hydrated calcium sulfate probably resulted from calcium carbonate reaction with sulfate ions.

4. Conclusions

The research has shown that degradation in the King Matthias the Ist sculptural group mainly occurred because of the casting technique used (on a metal frame) and of the assembly method (steel screws).

To a limited extent, degradation is caused by corrosive agents in the atmosphere, even though the

sculptural group has been exposed to environment factors for more than 100 years.

The research helped us understand the degradation mechanism of sculptures exposed to atmospheric elements and leads to determining a suitable conservation- restoration method for each monument.

Acknowledgments

The "PRODOC" POSDRU/6/1.5/S/5, ID 7676 project is thanked for financial support of this work.

References

- [1]. **Șt., Pascu, V., Marica** - *1850 Clujul istorico-artistic*, 1974
- [2]. **T., Kolozsi**, *Investigații preliminare consolidării și restaurării grupului statuar Matia Corvinul*, Transilvania Nostra, nr.7, 2008, pg. 2.
- [3]. **M., Buzatu, G.V., Ghica** - *Cercetări experimentale privind coroziunea metalelor metalice din monumentele de interes publi*, Revista de turnătorie, vol. 5,6, I, 2008, pg. 19.
- [4]. **I., Sandu** - *Deteriorarea și degradarea bunurilor de patrimoniu cultural*, vol I, Editura Universității Alexandru Ioan Cuza Iași.
- [5]. **V., Căndea, C. Popa** - *Inițiere în știința metalelor*, Editura Vega, București, 1995
- [6]. *** The National Institute of Standards and Technology is an agency of the U.S. Commerce Department Technology Administration.



MATERIALS USED FOR MANUFACTURING SOME OBJECTS FROM 1600 BEFORE CHRIST – 500 AFTER CHRIST PERIOD

Petrica HAGIOGLU, Constantin GHEORGHIES

“Dunarea de Jos“ University of Galati

email: petricah@yahoo.com

ABSTRACT

The appearance and the spreading of metallic objects produced a profound social change. The early metallurgy included two ages: The Bronze Age and The Iron Age. The late Bronze Age is considered to be the most important for biblical archeology, because it seems to correspond to the period when Moses lived and when the Hebrew people exited Egypt. According to archaeological testimonies, the first iron period coincides with the entrance in Palestine of two invader peoples. The Bible mentions six metals: gold, silver, copper, iron, steel and tin. Metals served to humans as the most important material for manufacturing weapons, manufacturing application, jewels, cult objects and, most importantly, for manufacturing tools.

KEYWORDS: metals, archeology, The Bible, history, metallurgy

1. Introduction

For more than 2000 years, bronze, a copper alloy, was to humans the most important material for weapons manufacturing for manufacturing application, jewels and, most importantly, for tools. It was widely used in all early cultures and it gave the name to a whole historic age, The Bronze Age.

All early civilizations considered bronze the most important material for a shorter or longer period during their history.

Bronze is an alloy, a mixture of many metals, usually copper and tin. It was used for the first time by the Egyptians, especially for tools and weapons manufacturing. In that time it was not easy to produce bronze. The main problem was obtaining tin. Possible mining regions were Iran and Cyprus. From 1600 B.C., when Egyptians had enough tin for themselves, bronze played an important role for them [1-3].

The Hindu manufacturers, on the other hand, had very productive stores and their bronze contained up to 15% tin. Until the middle of the second millennium B.C. the Chinese were masters in bronze molding. Bells and their full sounds were wonderful examples of their skill in metal processing.

The Greeks were masters in weapons and armor manufacturing. For example, their bronze helmets were already used in the Sumerian city of Uruk. In the Middle East it was used between 2200 and 800 BC.

Because gold is relatively soft it was used for precious vessels and jewels, but never for tools and weapons. Gold was coveted by leaders because it

symbolized power and authority. Thus Midas, the legendary Frisian king wished that all he touched become gold.

In Antiquity, gold was found especially in Egypt and Nubia, whose name means “land of gold”. In Greece, gold was found on islands and Thrace, and the Romans had mines in Spain and Dacia, currently Romania.

Gold objects made for burials in Ancient Egypt included coffins, altars and funerary masks. From 1000 B.C., iron helped the greatest empires into the classic Antiquity. The Greeks had been using it for weapons since the 6th century B.C., and in the Danube and The Alps regions, the Celts proved to be ingenious smiths by creating tough steel swords. The Romans produced their first weapons on the Elba Island, were the Etruscan smiths and their anvils.

The power of the Roman Empire relied especially on steel weapons and equipment. The Damask steel, made by mixing various types of iron and steel, was a model for the iron and steel processing art in late Antiquity.

Metals are mentioned in the Bible beginning with “The Book of Genesis 2, 10-14”. In the Bible six metals are mentioned: gold, silver, copper, iron, tin and lead. The Bible is a collection of books written under the influence of the Holy Spirit, over a period of approximately 1500 years: from Moses until The Apocalypse (1400 B.C.- 100 A.D.).

The early metallurgy includes the two ages: The Bronze Age and The Iron Age, and coincides with the events mentioned in the Bible. The Old Testament

shows the history of the Hebrew people and their life style in compliance with the Ten Commandments given by God to Moses. In addition to the dogmatic and moral guidelines, the Old Testament also contains rules of the social, politic and religious life, civil and religious laws.

The late bronze period (1550 – 1200 B.C.) is considered as the most important period for biblical archeology because it seems to coincide with the period of Moses and the exit from Egypt of the Hebrew people. The first period of iron (1200-190 B.C.), according to the archaeological data, coincides with the entrance in Palestine of two invading peoples. Thus, from the South and especially from the East, from Jordan (Joshua, I), the Hebrew entered, and from the North, more precisely, from The Aegean Islands, the Philistines came, who knew well how to process iron (II Samuel 13, 19-21), and they wanted to keep the secret, in order to maintain the technical superiority of their army, who wanted to conquer the same territories as the Hebrews.

2. Metallurgist in Antiquity, their conditions and life style

In the early Antiquity, the South – East of Canaan there was a very important center of copper metallurgy, from the Calcholithic until the Iron Age, at Pumon, currently Feyman, the most important center of metallurgy of Arabah. The sons of Cain (the Kenites), a small tribe mentioned in the Bible, were for a long time the copper metallurgists in Canaan. Jeremiah, in his book, confirms the Kenites believed in Yahweh (Jeremiah 35,19); all the data suggests that Yahweh was closely related to the metallurgist, from the discovery of copper and its processing [4 -6]. In the book of Zachariah an essential connection between Yahweh and copper is suggested, where the God of Israel is symbolized by two copper mountains (Zachariah 6, 1-6). Moreover, Ezekiel, in his prophesies describes the divine being as a man whose appearance was the same as copper (Ezekiel 40, 3). In Isaiah 54, 16, Yahweh is mentioned as the creator of both copper mining and of its processing.

3. Myths and legends of the people

The myths and legends of many ancient peoples expressed in various forms the faith in a savior. All peoples felt the need to be saved from evil. Mircea Eliade [7], in his comparative study, observed a close similarity in the faiths and the life style of metallurgist from all over the Antique world.

This uniqueness influenced their organization as a group that traveled long distances for material changes, for copper extraction and mining.

The Egyptian God of metallurgy, Petah, was considered to be the source of Ka. In Mesopotamia, the god of metallurgy was Enki, considered to be one of the main gods in the Akkadian pantheon [1]. As Ptah [8] in Egypt, he was celebrated in Sumerian hymns as being the most intelligent and also the loneliest god. In the tradition of metallurgy fighting against gods is common [7].

In Greece, the Cyclops, creatures symbolizing former metallurgists [9], were mentioned as the first beings who fought against Uranus, the main god of the Ancient Pantheon, and against all gods [5].

4. Metal objects from the Antique world

Metallurgy first developed in Anatolia, in today's Turkey. The mountains in the high regions of Anatolia were rich in copper and tin deposits. Copper was also extracted in Cyprus, Egypt, The Negev Desert, Iran and around the Persian Gulf. Copper was usually mixed with arsenic, but the constantly growing demand led to long distance commercial routes being established to and from Anatolia. Copper was transported by sea to the great kingdoms of Ancient Egypt and Mesopotamia.

In that period, it seemed that iron was used for ceremonial purposes only, as it was an extremely expensive metal, more expensive than gold. A systematic metallurgy of iron appeared for the first time in the Hittite Empire, in the 14th century B.C., and in India, starting in 1800 B.C. Between 1600 and 1200 B.C. iron was obtained by primitive casting, in the Hittite Empire (Anatolia and Caucasian Mountains). The disappearance of that empire allowed the information on iron metallurgy to circulate in the entire region, facilitating the evolution from The Bronze Age to The Iron Age [10 -15].

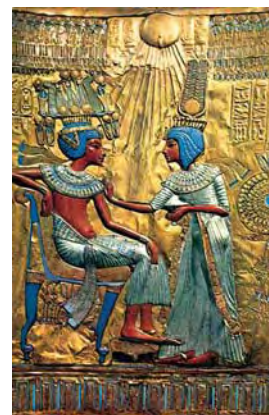


Fig. 1. The throne of Tutankhamen pharaoh (XIVth century b. Cr., the Museum of Cairo, Egypt).

The gold funerary objects in Ancient Egypt included coffins, altars and funerary masks. One example of gold used in burials is the treasure of the Egyptian Tutankhamen pharaoh, who reigned between 1333 and 1326 B.C.. Tutankhamen's chair, with its golden back, decorated with filigree can be observed in picture 1 and the pharaoh's funerary mask is presented in picture 2.



Fig. 2. *The Tutankhamen mask.*



Fig. 3. *Guns from Bronze Age, Romania.*

The European territory, rich in natural resources, is characterized by the presence of many treasures made of precious metals and stones [11-15].



Fig. 4. *The funerary diadem Kept in the Louver Museum.*

During the Hellenistic period (313 – 30 B.C.) the glitter and richness reached the highest levels. After

Alexander the Great defeated Darius the 3rd and conquered Babylon, Sosa and Panopolis, the great treasure of Persia was robbed and the riches were carried on 2000 mules and 3000 camels. The metals from this treasure were transformed by the Hellenic Kings into coins (the unique coin of Alexander the Great, made of gold – the stater). The only symbol of royal authority worn by all Hellenistic Kings was the diadem (Fig.4 – *the funerary diadem on display in the Louvre Museum*) adopted by Alexander from the Persian kings.



Fig.5. *Gold necklace.*

The Etruscans, the first inhabitants of Italic peninsula, were also interested in jewels. The Kings appeared in the ceremonies as supreme priests, wearing gold crowns, precious footwear, mantles richly embroidered and decorated with human faces, and they sat on a sumptuous thrones during trials and gatherings. During ceremonies dedicated to military victories, the King wore a scarlet toga, embroidered in gold, a golden crown, a sphere and a golden chain, and in the hand an ivory scepter with an eagle at its top.



Fig. 6. *Gold bracelets.*

In the 7th and 6th centuries B.C. jewels were formed by hammer, with filigree and granulations with abundant decorations. The decorative motives were applied on fibulas, earrings and necklaces, on bracelets and rings. Up to 20 miniatures were applied, representing heads of women, men, divinities and half – gods.

Dacia was also among the territories rich in natural resources. The manufacturers there processed iron, copper, silver and gold. Their workshops made necklaces, bracelets, rings and also armor elements. Apart from the specialized workshops, there were

nomad craftsmen who used to roam from city to city. Items from the 4th and 3rd century B.C. were discovered, which were made using the hammering technique to form stylized human and animal figures.

Among those jewelry items there were spiral bracelets, ornamental chains obtained by knitting threads and rings, bracelets with Hellenistic snake heads. The Geto-Dacian craftsmen also mastered the gold coating technique. The largest bracelet is an open cuff made of massive gold sheet, weighting 580 grams, decorated with 10 buttons fixed into holes.



Fig. 7. Muff opened gold bracelet – The treasure is stored in The National History Museum from Bucharest.

5. Metallic objects reminded in the Old and New Testament

During the exodus, the tent was a holy place for the Hebrew people (Exodus 33, 11). Its appearance and dimensions are mentioned in detail where Yahweh advises Moses to built it (Exodus 26) and where its building by the two skillful masters, Betaleel and Oboliah, is described (Exodus 36, 8-38). The most important objects are the altar of incensing, the candelabrum with seven arms (Menorah), the table for offerings, the Ark of the Covenant, the copper snake etc.



Fig 8. The Law Shrine (from the Capernaum synagogue IV-III century before Christ).

According to the description from Exodus (chapter 25, 10-22; 37, 1-9), the ark was a box made of acacia wood 1.25 m long, 0.75 m wide and 0.75m high. It was coated in gold and had rings fixed on it for transportation purposes. The lid of the ark was made of gold and had two cherubs with opened wings mounted on the sides. That lid was worshiped as “the throne of mercy”, where Yahweh would reveal himself to the people. Of all the descriptions and representations of the Lost Ark, we would like to mention the embossed representation found in the Capernaum synagogue (4th - 3rd century B.C.).

The contents of the Ark have been debated through the centuries. The general consensus is that the first tablets containing the Ten Commandments, which were broken by Moses, and the second tablets, which remained intact, were contained in the Ark.



Fig 9. The candelabra with seven arms – Menorah.

The New Testament mentions the following objects:

- the anchor (Acts 27, 29-30), a small coin - the smallest roman coin, rating a half of a condrat (Marcus 12, 12, Luke 21, 2)
- the cohort - the military unit of 1000 soldiers (Acts 10, 1: 21, 31, Mathew 27, 27, Marcus 15, 16, John 18, 3-12).
- the sword – defense weapon used especially in the old wars (Mathew 26,55: 47, 51: Marcus 14, 43: 47, 48: Luck 22, 52: John 18, 10).
- a vessel- recipient used at home or as cult object made of various materials, such as clay, wood, stone, copper, gold , silver etc. (Mathew 12, 29; Marcus 3, 26; Luck 17, 31).

In the New Testament, Judaism was not a closed world. Palestine was part of the Roman Empire and many Hebrews had connections with the pagan world, with the Hellenistic world, especially with those from Alexandria, in Egypt.



Fig 10. *The coins used in the New Testament.*

Long before coins were introduced, merchants traded in wares. Anything could be traded, from objects, metal, wood, food or livestock.

In the Old Testament the shekels and the talents served as coins. They were not coins but weights and remained as such at least until the 7th century. The traders weighted the silver or other metals and buyers carried their own weights in leather bags, for control (Deuteronomy 25, 13).

During the New Testament period there were three types of coins in Palestine: the official Roman coins, the coins of provinces, meaning the Greek coins and the local Hebrew coins, which were supposedly made in Cesarea. The contribution that Hebrews paid for the Temple was in Greek coins, those made at Tir - the drachmas, not in Roman coins. The coins were made of silver, gold and copper,, bronze or brass. The most usual coins mentioned in the New Testament are the Greek tetra-drachmas and the Roman dinars. Those were the coins paid to the workers. In the New Testament period, the financial system was well organized.

The Roman army was particularly well organized. Every military campaign was conducted by a general (dux) who was always an aristocrat. During the Republic, the generals were consuls or former consuls, or at least former praetors, to whom the Senate granted the title "imperium" or allowed them to conduct an army. During the empire, the supreme commander was the emperor, who named a general from his relatives or friends.

In the year 27 B.C., Augustus instituted new elite troops - the Praetorian Guards – with the exclusive mission to defend the emperor. At the beginning, they were nine cohorts, out of which three stayed in Rome and the others in the nearby cities.



Fig. 11. *The golden helmet- has fixed the imperial eagle.*

Later, the cohorts increased to twelve. The Praetorian uniform was similar to that of other legions, except for the helmet which was gold coated and had the imperial eagle on it.



Fig. 12. *Roman palladium.*

The shield had a rectangular shape, slightly curved, but also were oval shields. On the embossed center soldiers drew various motives, mostly personal symbols or those of the legion.

The sword was short with a metallic grip and a cross hilt guard (on the both margins of the blade), with simple or double edge, designed for close combat.

The javelin or pilum had a sharp tip followed by a thinner portion, designed to break on impact and leave the tip inside the victim.



Fig 13. *Roman soldiers endowed with fight equipment*

6. Had the metals importance diminished in the New Testament?

The Hebrew people were already formed. Metals were known, as well as cult objects, ceremonial and civil objects. The New Testament had another dimension. It presents the arrival of our Savior, Jesus Christ, His activity, the spreading of the Gospel, and it also presented the activity and the acts of the Holy Apostles with less focus on the social, political and economic life. The importance of metals in the New Testament did not diminish.

The Old Testament contains the history of humanity preparing for the savior and that savior comes in the New Testament. Both Testaments are parts of the same divine purpose: the savior of humanity, prepared in the Old Testament and described in the New Testament.

The Savior Jesus Christ is a unique figure in human history. Many studies were made about His

life and work, each in compliance with certain historical, philosophical, social, political and economical ideas. That is why He is presented at one time as a thinker, then as a philosopher, a moralist, an ideal dreamer, or a visionary.

Nevertheless, for the Christians, Jesus Christ is a divine human being, He is the Son of God, Whose mother is Holy Virgin Mary and Who lived as a historical person in the time of the emperors Augustus (31 B.C. -14 A.D.) and Tiberius (14 – 37 A.D.). The Gospel preached by Jesus Christ, is a moral and religious, message, not a social, political or economic one [11 -12].

Evan though Jesus preached to the Hebrew people, His teaching has a universal meaning. It is destined for the whole world.

Written by different authors, with different goals, each book and each author with a different personality, the books of the New Testament reflect the social customs and the realities of the distant periods when they were written.

7. Basilicas built by the emperor Constantine

In the first three centuries of the Christian era Christianity was forbidden and Christians were persecuted because of moral principles which defied the faith in many gods, and the cult for the Empire.



Fig. 14. The fish- Christins symbol.

Constantine the Great was the first emperor who understood that the persecutions amplified the internal disorder. Realizing that the new religion could become a powerful aid for the state, he gave full freedom to the new religion trough the Mediolanum Edict (Milan of today) from the year 133 A.D.. The faith spread all over the empire and across its borders, during Theodosius I the Great (379 - 395 A.D.) becoming the only religion allowed by the state [19-20].

7.1. The God' s Birth Basilica

The Church of the Nativity in the heart of Bethlehem marks one of Christianity's most sacred sites - the birthplace of Christ.

Situated on Manger Square 8 kilometres (5 miles) from Jerusalem, the church is built over a grotto where the Virgin Mary is said to have given birth to Jesus. The church's large fortress-like exterior stands as a testament to its turbulent history. For centuries, it was one of the most fought over holy places. It was seized and defended by a succession of armies - including Muslim and Crusader forces.

In 333 A.D. the Emperor Constantine completed the basilica, which attracts thousands of pilgrims from around the world every year. The original structure was completely destroyed in the early 6th century. It was rebuilt in its present form in 527-65 A.D. during the rule of Emperor Justinian. Over the years, the site has been expanded.

7.2. The church of the Holy Thumb



Fig.15. The church of the Holy Thumb (Jerusalem - exterior from the church).

The Church of the Holy Sepulchre (Latin: Sanctum Sepulchrum), also called the Church of the Resurrection (Greek: Ναός της Αναστάσεως, Naos tis Anastaseos; Arabic: كنيسة القيامة, Kanīsat al-Qiyāma) by Eastern Christians, is a Christian church within the walled Old City of Jerusalem.

The site is venerated by many Christians as Golgotha,[1] (the Hill of Calvary), where the New Testament says that Jesus was crucified,[2] and is said to also contain the place where Jesus was buried (the sepulchre). The church has been an important pilgrimage destination since at least the 4th century, as the purported site of the death and resurrection of Jesus. Today it also serves as the headquarters of the Greek Orthodox Patriarch of Jerusalem, while control of the building is shared between several Christian churches and secular entities in complicated arrangements essentially unchanged for centuries.

7. 3. The Holy Sophie church from Constantinople

The Holy Sophia church was built by the emperor Constantine the Great in the forth century, at Constantinople. There is nothing left from the first constructed church. Short time after its destruction,

the second church was built by his son, Constantine and by the emperor Theodosius the Great.



Fig 16 The Holy Peter basilica- general view.



Fig. 17. Gold coins(the solidus) during the Constantine the Great

7.4. The Holy Peter basilica from Rome

The Holy Peter basilica in Rome was built on the spot of the Caligula and Nero circus, where, according to the Christian tradition, Peter was crucified in 67 A.D.. The church was constructed between 319-329 by Constantine the emperor, to shelter the chain with which Saint Peter was tied when he was held prisoner in Jerusalem. The chains are kept under the main altar in the basilica. In the 15th century, the building was in ruins and Pope Julius the Second decided to build a new, higher basilica. The construction of the current building began on 18 April 1506 and ended in 1612, during the time of Pope Paul V. The basilica was sanctified on 18 November 1626 by Pope Urban the 8th. [20, 21].

8. Conclusions

The early metallurgy included two ages: the Bronze Age and the Iron Age. It coincided with the period in which the events related in the Bible happen.

In history, one of the most important elements for development was metal, including the New Testament period. Metals are presented in the Bible from the first Book. In the Old Testament they mention: gold,

silver, copper, iron, lead and tin.

The importance of metals in the New Testament did not diminish. Metals were used in all domains: social, political, economic, military and religious.

The Old Testament describes the history of the chosen people and their life in compliance with the Commandments given by God to Moses.

The New Testament has another dimension: the arrival of our Savior, Jesus Christ, His activity, the spreading of the Gospel, and it also presents the activity and the acts of the Holy Apostles.

The Hebrew people were already formed. They knew the metals, the cult objects and the civil and religious laws.

References

- [1]. Anzallang N., *Iahweh the Canaanite god of Metallurgy?* Journal for the Old Testament (Oxford 2009).
- [2]. Cettli, *Die Autoritat des Alter Testaments fur den Cristen*, 1906.
- [3]. Chauvin, *La mythologie greque Fayard*, Paris, 1992.
- [4]. Deunefeld L., *Le Massionisme*, Paris, 1929.
- [5]. Dodd C.H., *According the Scriptures*, London, 1952.
- [6]. Eliade M., *Forgerons et Alchimistes Flamariion*, Paris, 1977.
- [7]. Ghia Gh., *Atitudinea Mantuitorului fata de Legea Vechiului Testament*, Craiova, 1929.
- [8]. Grelot R., *Sens chrétien de l' Ancien Testament*, Paris, 1962.
- [9]. Koch (1995), *Civilizations of the Ancient Near East*, vol. III, ED. J.m. Sassom, Mac Millan, New York.
- [10]. Ksning E., *Die messianischem Weissegugen des A.T.*, Stutgard (3), 1925.
- [11]. Ramureanu I., *Istoria Bisericeasca Universala*, Edit., Institutului Biblic si de Misiune al Bisericii Ortodoxe Romane, Bucuresti, 2004.
- [12]. Screban N., *Vechiul Testament studiat duce la cel Nou*, 1876.
- [13]. Semen P., *Arheologia biblica in actualitate*, Ed. Mitropoliei Moldovei si Bucovinei, Iasi, 1997.
- [14]. Moisa S. „Some aspect regarding the ancient technology of metals in the biblical world of the Old Testament”, International Conference, Arctcast, Edit., Europlus, Galati, Romania, 2008.
- [15]. Bahat, D., (1986). "Este situată biserica Sfântului Mormânt pe locul înmormântării lui Iisus?", *Revista de arheologie Biblică* 12(3) (Mai/Iunie) 26-45.
- [16]. Biddle, M., (1999). *Mormântul lui Hristos*. Phoenix Mill: Sutton Publishing.
- [17]. Patrich, J., *Prima biserică a Sfântului Mormânt în lumina excavațiilor și restaurărilor*, Yosam Tsifir, Ed., Ancient Churches Revealed, Isreal Exploration Society, Jerusalem, 1993.
- [18]. Hagioglu P., Gheorghies C., *Metallic Materials used in manufacturing some cult objects*, International Scientific Conference, Advanced Materials and Technologies, UgalMat 2009, Galati, Romania.
- [19]. www. Arta SM.
- [20]. www. Judka.ro
- [21]. www. universus.ro
- [22]. www.wikipedia.org/wiki Mise
- [23]. ..wikipedia.org/.../Bazilica_Sfântul_Petru_din_Roma
- [24]. www.ercis.ro/actualitate/viata.asp?id.



SCULPTURE, EXTENDED NATURE

Elena PARASCHIV¹, Victor PĂUNESCU¹,
Cristina RĂDUCAN²

¹"Dacia" High School, Bucharest

²"Traian Vuia" High School, Bucharest

email: liliparaschiv_2009@yahoo.com

ABSTRACT

The paper portrays some aspects that show how nature is implemented into the graphic values domain by confronting the physical image of the artistic subject. The article presents some rules that have marked over time the representation of the human body in sculpture, based on the subtle game of proportion. There are also presented brief studies of works of art based on an analysis of framing surfaces the sides of which are in the golden section ratio.

KEYWORDS: sculpture, canon, proportion

1. Introduction

The models that are the bases of obtaining by casting the statues are all artistic creation, and the task of reproducing their exact form belongs to the foundry worker who creates those unique meaningful and sustainable pieces, exact copies of models in clay or plaster.

Taking into account that without shaping metal or alloy, taken by the rat, it would not be possible to obtain statues, thus the work of the two artists is very important. As the model is crucial, the artist has been always looking for the best, most expressive and not at least, the most well proportioned form.

Since ancient times, when statuary art appeared, artists have been seeking to represent objects such as nature represents objects not as anatomy does.

Excepting the relief located at a height, in which the deformations are specifically made to figure the real proportions, in all other cases, the harmonious arrangement of parts in volume and forms, was the constant preoccupation of artists.

2. The study of proportions

In classical Greece besides generalized processing bronze, human figure is represented in close correlation with the ideal proportions of the human body. When speaking of proportions, it is envisaged the dimensional relationship between its parts and between each part and the whole.

The study was based on the proportions of measurement systems that:

- took the whole as a unit (i.e. total body height) and then they split it into fractions: halves, quarters, sixths, eighths, etc.;

- took as a unit of measure one side of the human body, the so-called mode: head height, foot length, hand length, etc.

Realizing that the beauty of a figure lies primarily in scale, artists were concerned from the earliest times to find those ideal relationships between body sizes, that provide perfect beauty solution. Thus there were born, through the centuries, the canons or the systems of proportions. Each canon comprises a group of human body proportionality rules and suggests a certain aesthetic type. In all civilizations before the Greek one: Egypt, China, India, the canons rendering the human body were almost entirely conventional, its representation is the result of mechanical application of the canon. The first canon in its true sense, the Greek one, is linked to Policlet of Argor (450 - 400 BC), sculptor and theorist of art, in whose creation predominates figures of gods, heroes and winning athletes. He created the "canon" on the ideal proportions of the human body, on which he wrote a treatise.

His work "The Dorifor" (Fig. 1) illustrates this theory, but it is known only through Roman copies.

Policlet based his proportionality on human body parts, so on organic elements, rather than on conventional methods.

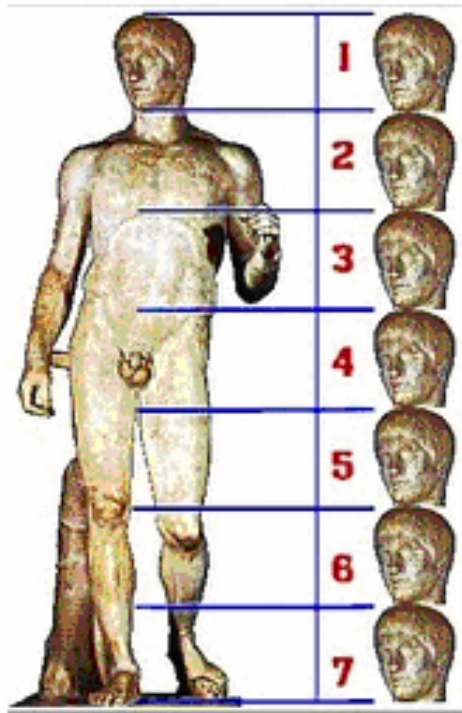


Fig. 1. The Dorifor man of 7 heads high.

Thus, the representation of the human body is not the result of the canon, but the result of studying the body.

The canon statue "The Dorifor", known as the "Seven-Headed Man" (due to the fact that his head height is equal to 1/7 of the total face height figure of the character) has remained, for a long time a model for artists after Policlet, having in addition to the works of that time a valuable attribute namely the movement. The Greek sculptor Lysip, who knew Policlet's work, has developed another proportionality in which the head as a module contains eight times the body height. Over time there have been some other canons: the Roman architect Vitruvius's (first century BC), of eight heads, the Durer's of 7, 8, 9 and 10 heads etc.; all having in common the arithmetic mode with whole numbers or with fractions. The multitude of variants shows that the proportions had not a generally valid form of expression. Only at the middle of the nineteenth - century, Adolf Zeising (1810 - 1876) discovered that there was a law of proportionality which predominated in nature and governed the proportions of the body of each individual, man or woman of any age, any race, in any moment of a lifetime, etc., i.e. a universal law and that law is the section of gold.

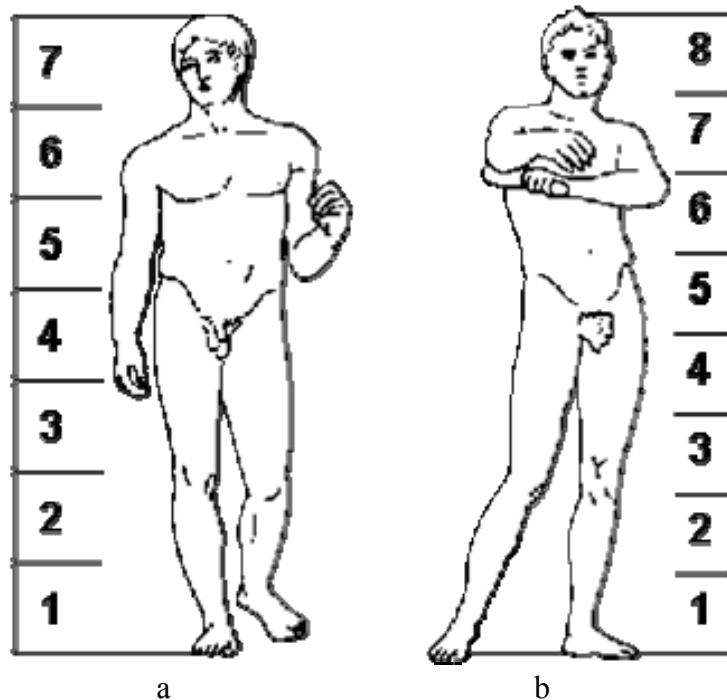


Fig. 2. The Greek canons: a-Policlet's canon; b-Lysip's canon.

On a straight line segment AB (with extreme points A and B) there is a single point (C) which divides it into two parts so that the ratio between the whole segment and the largest side is equal to the ratio between the largest (called a major part, marked

by M) and the smallest (sometimes called minor and marked by m) side ($AB / AC = AC / CB$) and vice versa. This way to divide a segment has several interesting properties, some of them rather strange,

that's why it was called the golden section (Fig. 3) marked by Φ (equal to the ratio $M / m = 1.618$).

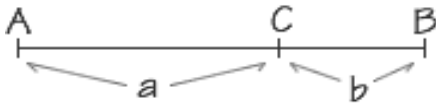


Fig. 3. Dividing a straight line segment, AB, into two parts by a third point C.

It was found that the navel divided the total human height by rules of the golden section (no matter the absolute value of total height), that each of the two segments of the total height thus obtained (down-navel and top-navel) is also divided by golden section; that each of the four segments thus obtained are divided again by the golden section, etc (Fig. 4).

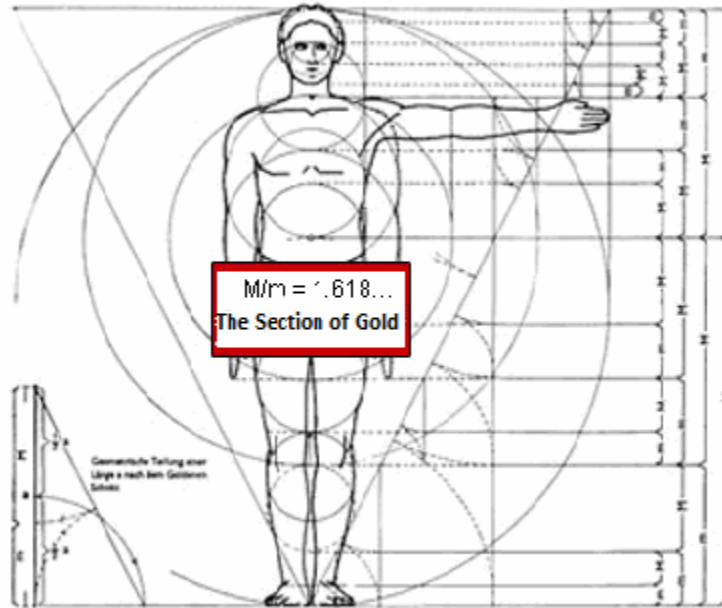


Fig. 4. The human body proportions after Zeising.

3. The proportions and the golden number

In the early twentieth century, Hambidge imagined a new theory of human body proportions based on an analysis of framing surfaces the sides of which are found in the ratio of the golden section or in related ratios.

The Golden section relations are found in the geometric figures, which are derived from regular pentagon, the pentagram and the star polygon and convex and star decagon.

Relationships between the sides of these geometric figures and the radius of the circle are dominated by the ratio Φ . The harmonic analysis of a nude by the square and the golden section is shown in Figure 5.

Based on a guided route by a double pentagon Lucie Wolfer - Sulzer made an analysis of a Kore in the Temple Erechteion (Fig. 6).

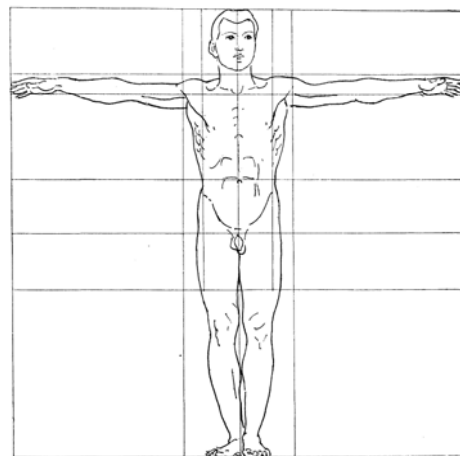


Fig. 5. The harmonic analysis of a male nude by square and golden section.

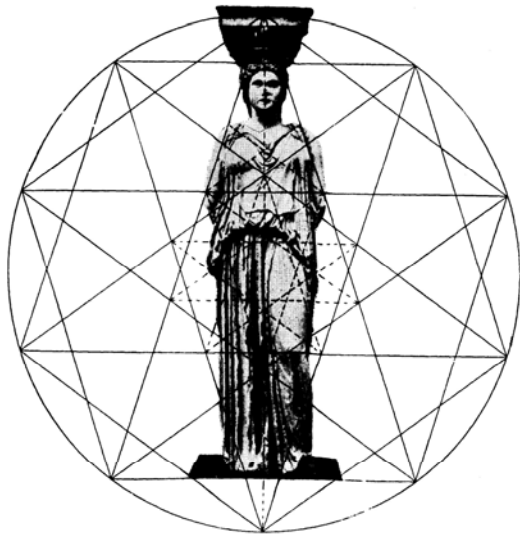


Fig. 6. *The analysis of a Kore in the temple Erechteion by double pentagon (of Lucie Wolfers-Sulzer Urbild Abbild und der Griechischen Form 1941).*

Using the same route of the double regular pentagon (called the pentagram) the architect Adrian Gheorghiu prepared analytical files on some of Brancusi's sculptures.

Figure 7 shows one of these analyses on the statue "Prayer", where he used the same route of the double regular pentagon, in which different sides, diagonals and axes cross each other making ratios and proportions or triangles and rectangles corresponding to the number $\Phi = 1.618 \dots$

The figure registers mainly into the inclined A'B'D triangle.

The parallel inclined diagonals AB, C'E', EC, A'B' points, separate or connect key elements of the composition: forehead, arms hook, line thighs, feet.

Note the oblique axis DD', the right hand wrapped at the intersection of the diagonals AC, BE, C'E' and the outer contour of the back on the directions D'B', A D C'A', so that the triangle ACD also enters the composition so the inclined attitude is emphasized.



Fig. 7. *The Prayer, 1907, The Art Museum of Romania.*

4. Conclusions

Geometry and space science are for graphic artists the arranging support of forms, the logical principle of organization of the graphic space.

Geometric unification, as shown, is the main means of arranging, but it never fails to exercise its domination over freedom of variation of the details that retain the viable initiative in motion in the orbits and paths between the monotony of scheme and the chaos of variation.

Art obeys the most general law of matter, the one that unifies order and deviation, rigour and exception, constraint and freedom, rule and repetition with creative imagination.

References

- [1]. G. Ghițescu, *The Constant of Art*, Meridiane Publishing, Bucharest, 1970
- [2]. H. Facillon, *The Art of Roman Sculptors*, Meridiane Publishing, Bucharest, 1989
- [3]. H. R. Radian, *The Book of Proportions*, Meridiane Publishing, Bucharest, 1981
- [4]. G. Ghițescu, *Artistic Anatomy*, vol II, Meridiane Publishing, Bucharest, 1965
- [5]. Gh.Florea, AL.Chiriac, I. Marginean, G.Croitoru, *The Art Foundry. The Design*, Europlus Publishing, Galati, 2009



ELECTRODEPOSITION AND CHARACTERIZATION OF ZINC-COBALT ALLOY COATINGS

Violeta VASILACHE¹, Sonia GUTT¹, Ion SANDU²,
Gheorghe GUTT¹, Traian VASILACHE³

¹Stefan cel Mare University Suceava,

²Al.I.Cuza University of Iasi, ARHEOINVEST Platform,
Laboratory of Scientific Investigation and Cultural Heritage Conservation,

³S.C. Daflog S.R.L. Medias,

email: violetav@usv.ro, gutts@usv.ro, g.gutt@usv.ro

ABSTRACT

Electrodeposited alloys are important in industry due to their properties which are superior to those of single metal layer. Zinc-cobalt alloys were co-deposited on gold substrate. Composition of the layers was established using SEM-EDX techniques. The influence of working parameters against stoichiometric composition of alloys was studied in order to find optimal conditions to achieve a desired final product. Some discussion about reaction mechanism was opened based on EIS diagrams. Application properties important for coating systems used in the automotive industry, such as friction behavior, adhesion, and corrosion behavior, were investigated on coatings with varying cobalt content. The corrosion resistance of the Zn-Co alloy layers was found to be better than the one of pure zinc coatings.

KEYWORDS: zinc-cobalt alloy, co-deposition, SEM-EDX technique, EIS

1. Introduction

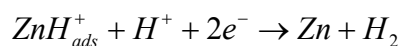
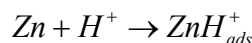
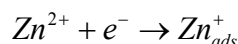
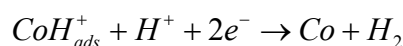
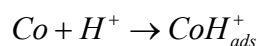
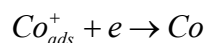
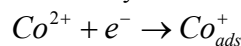
There is a growing interest in zinc coatings combined with elements of the iron-group metals (Fe, Ni and Co) on steel substrate thanks to results reported in the literature. These results show that the corrosion performance of these electrodeposits is superior to that of plain Zn coatings.

In machine building industry, zinc remains the principal metal for anti-corrosion applications, especially for protection of steel products. On top of the years, it has registered a significant increasing of electrodeposited alloys, because it was an important market demand for products with high quality coatings. In the front of the list, there are the automotive industry and the aerospace industry, also those applications for electrical components and for fixing devices.

In anticorrosion protection, cadmium is more used together with zinc. Because consumption of heavy metals has to be reduced year by year, until total elimination, there are researches meant to create new technologies and one of them is based on alloys electrochemically deposited, such as Zn-Ni, Zn-Co, Zn-Fe.

The electrochemical reactions which occur on cathode surface could be considered as having

evolution in two steps, according to Matloz. Zinc ions are deposited on their own substrate, on gold substrate used and on cobalt substrate. Also, cobalt ions are deposited on their own substrate, on gold substrate and on the zinc substrate. More, there have to be considered secondary reactions, those where Zn^{2+} ions combine with hydrogen to form ZnH^+ , as well as where Co^{2+} ions combine with hydrogen to form CoH^+ . Those intermediary species, formed in the adsorption process, will decompose finally in metallic Zn, and metallic Co respectively. The reactions mechanism may be written as follows [1, 2].



Co^{2+} and Zn^{2+} are dissolved as metallic ions,

hydrolyzed or not. Co^+_{ads} and Zn^+_{ads} which could or couldn't contain the hydroxyl group, are adsorbed univalent in intermediary reactions. Co and Zn form the metallic layers of cobalt and zinc respectively.

The kinetic of mass transfer is supposed to respect the Butler-Volmer equation:

$$i = i_0 \left\{ \exp \left[\frac{(1-\beta)F\eta}{RT} \right] - \exp \left[\frac{-\beta F\eta}{RT} \right] \right\} \quad (2)$$

where η is the over potential which measures the difference between the potential value when through interface is passed a current and the equilibrium potential; β is called coefficient of symmetry; F is the Faraday's constant, R - universal constant of gases, T - absolute temperature; i is effective cathode current density and i_0 is the exchange current density [3].

Under far away equilibrium conditions the anode reactions could be neglected.

2. Experimental details

The deposition of Zn-Co thin films was electrochemically performed at INCDFM-Bucharest-Magurele (National Institute of Researches and Development for Physics of Materials). To obtain layers with desired properties it was necessary to investigate the influence of deposition conditions (like discharging potential, bath composition, temperature and stirring of the electrolyte during the deposition process) against structure, morphology, composition, aspect and optical properties of the layers. We used the following compositions to prepare the electrolyte low acid for depositing of Zn-Co alloys: (the first solution) zinc chloride (ZnCl_2) 63 gL^{-1} , cobalt chloride ($\text{CoCl}_2 \cdot 6\text{H}_2\text{O}$) 15.32 gL^{-1} , potassium chloride 225 gL^{-1} , boric acid (H_3BO_3) $15\text{-}25 \text{ gL}$, pH 5-6, $t(^{\circ}\text{C})$ 21-38 $^{\circ}\text{C}$; (the second solution) zinc chloride (ZnCl_2) 63 gL^{-1} , cobalt chloride ($\text{CoCl}_2 \cdot 6\text{H}_2\text{O}$) 8.16

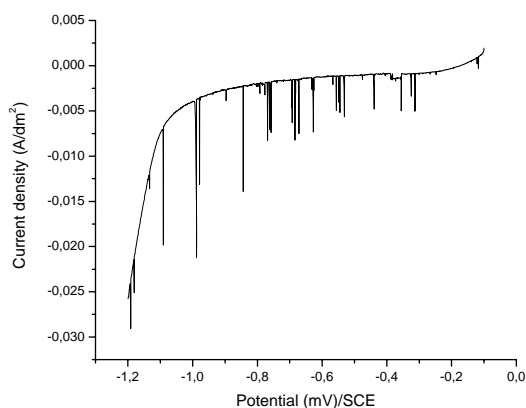


Fig.1. Polarization curve for described solution of electrolyte used for Zn-Co co-deposition recorded for the potential range from -100 mV to -1200 mV, 32 $^{\circ}\text{C}$ temperature, with magnetic stirring of the electrolyte.

gL^{-1} , potassium chloride 225 gL^{-1} , boric acid (H_3BO_3) $15\text{-}25 \text{ gL}$, pH 5-6, $t(^{\circ}\text{C})$ 21-38 $^{\circ}\text{C}$.

As working electrode we used a glass lamella having a gold thin layer deposited using sputtering method (using a Hummer 6 installation). The pH level was maintained between 5 and 6 naturally without addition of acids, because the salts were chlorides which after electrolytic dissociation have an acid character (except for KCl, salt of a strong acid and a strong base). The working temperature was between 21 $^{\circ}\text{C}$ and 38 $^{\circ}\text{C}$. A good adhesion was obtained using the next described method. The glass lamella was first polished, then gold plated in a sputtering installation. Also there were tried some samples with bright glass, but the result was negative because all the gold dissolved itself in solution. As reference electrode it was used the calomel electrode immersed directly in the electrolytic cell. Co-deposition of zinc-cobalt layers was performed using a potentiostat-galvanostat VoltaLab 40 and soft-ware VoltaMaster 4. Layers were analyzed with an EDX Shimadzu 720, at Stefan cel Mare University of Suceava and with a SEM VEGA II LSH, at Al.I.Cuza University of Iași. Other measurements were performed with a SEM Zeiss EVO 20 with EDX-Bruker detector, at INCDFM Bucharest-Magurele. To measure the structural and morphological properties, it was used an optic microscope Zeiss DSM 982 Gemini, at INCDFM.

3. Results and discussions

Figure 1 show the polarization curve for solution of electrolyte used for Zn-Co co-deposition recorded for the potential range between -100 mV and -1200 mV at 32 $^{\circ}\text{C}$, with a scanning velocity of 5 mV/s. Studying the behavior of solution, it was decided to perform deposition at -1000 mV, -1100 mV and -1200 mV.

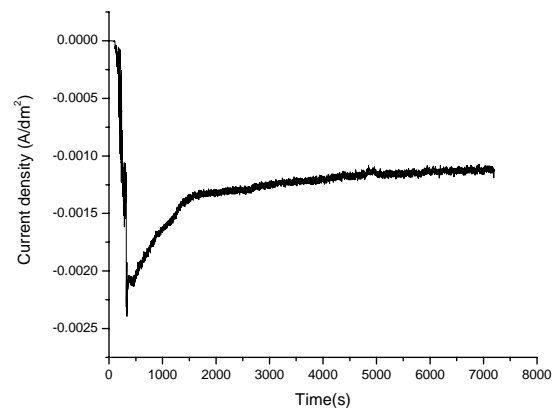


Fig.2. Crono-amperogramme recorded during Zn-Co alloy co-deposition at -1000 mV potential and 32 $^{\circ}\text{C}$, with magnetic stirring of the electrolyte.

Figure 2 presents the evolution of current density during electrodeposition process. As it could be seen, during the first 20 minutes of the process the decreasing rate of the current density is faster comparing with the decreasing rate recorded for the rest of the time.

The behavior is similar to those signed in other experiments and is close to the diminishing of ions concentration in solution. Figures 3 and 4 show

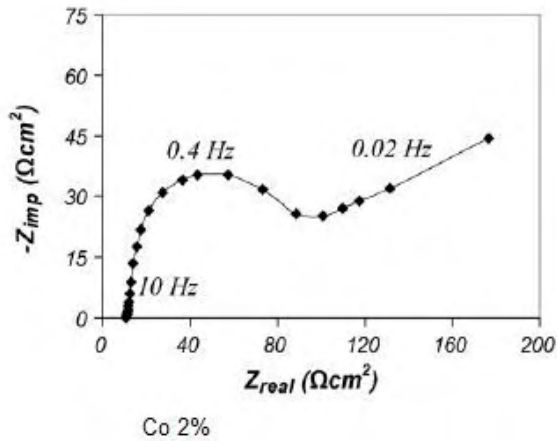


Fig.3. Nyquist impedance curve obtained for the second solution (low concentration of Co ions).

The capacitance of double layer (C_{dl}) could be calculated from the next relation:

$$Z(\omega) = \frac{1}{(i\omega C_{dl})^n} \quad (3)$$

where i is the complex exponent ($i=(-1)^{1/2}$), ω is the angular frequency ($\omega = 2\pi f$) and n is an exponent higher than 0.5 and smallest than 1.

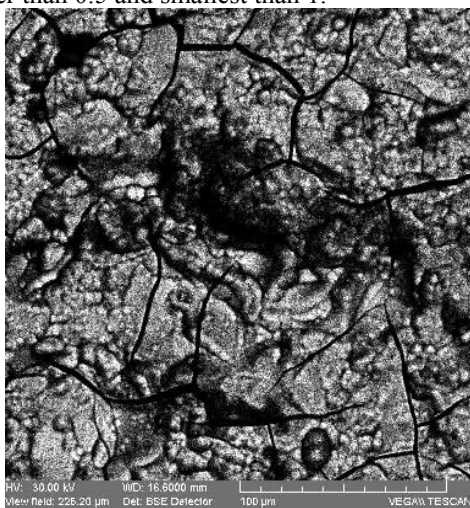


Fig.5. SEM image of a zinc-cobalt layer electrodeposited at -1000 mV and 24°C (first solution, 4% Co), with magnetic stirring of the electrolyte. Optical magnitude 1000X, VEGA TESCAN device.

Nyquist representation of Electrochemical Impedance Spectroscopy (EIS) diagrams obtained for those two solutions and it could be observed that there are not many differences between them. It is a single semicircle at high frequencies and the double radius (diameter) corresponds to the charge transfer resistance (R_{ct}). The resistance of the solution (R_s) is given by the distance between origin and the point where the semicircle begins.

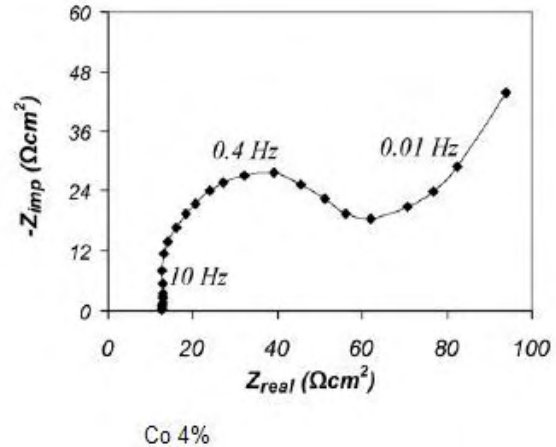


Fig.4. Nyquist impedance curve obtained for the first solution (higher concentration of Co ions).

We found for those two solutions the following values: $R_{s1}=15.5 \Omega\text{cm}^2$ and $R_{s2}=17.5 \Omega\text{cm}^2$, $R_{ct1}=61 \Omega\text{cm}^2$ and $R_{ct2}=103 \Omega\text{cm}^2$, $C_{dl1}=97 \mu\text{F}\text{cm}^{-2}$ and $C_{dl2}=84 \mu\text{F}\text{cm}^{-2}$.

The results confirm the fact there are not many differences regarding the influence of concentration of Co ions [4, 5, 6, 7].

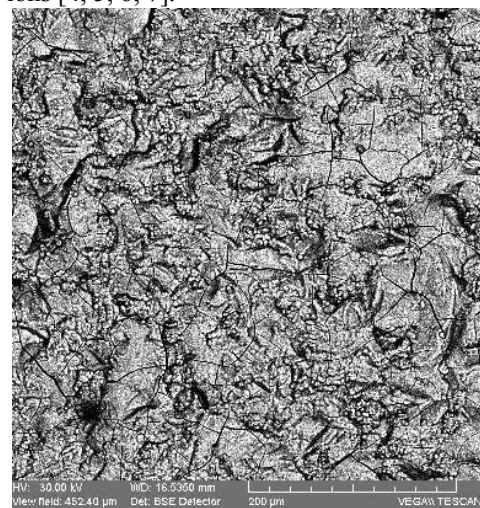


Fig.6. SEM image of a zinc-cobalt layer electrodeposited at -1000 mV and 32°C (first solution, 4% Co), with magnetic stirring of the electrolyte. Optic magnitude 1000X, VEGA TESCAN device.



Figures 5 and 6 show images of some samples of layers of Zn-Co electrodeposited using the first solution with a higher concentration of Co ions. Working at 32°C there was obtained a better aspect of the layer. Some micro-cracks could be observed, but these are not exactly a negative fact, because there are situations when cracks are desired for obtaining a superior protection against corrosion. At 38°C there were situations of dissolution of gold layer from lamella and exfoliation. Anyway, these experiments have to be reevaluated because there are only at the beginning in our collective themes.

4. Conclusions

The deposition of Zn-Co alloys has a future in technique and the researches will offer new solutions for development.

EIS diagrams prove that there are not many differences between the solutions where Co ions concentration differs in the range of low values. So, the mechanism of electrochemical reactions seems to be the same.

The analyses confirm that zinc-cobalt alloys were formed. Also it is confirmed that the percentage 58.710% Zn and 27.818% Co, Cl 5.676%, of those two metals in the deposited alloys depends on the working conditions.

The quality of the deposited layers could be controlled through the electrolyte concentration, discharge potential and working temperature.

References

[1]. **Bard, A. J.** - *Electrochemical Methods. Fundamentals and Applications*, John Wiley and Sons, New-York, 2001
[2]. **Brenner, A.** - *Electrodeposition of Alloys*, vols. I and II, Academic Press, New York, London, 1963.

[3]. **Di Bari, G.** - *Electrodeposition of Nickel, Modern Electroplating*, Fourth Edition, John Wiley and Sons, Inc. New-York, 2000
[4]. **Firoiu, C.** - *Technology of electrochemical processes*, E. D. P., Bucharest, 1983
[5]. **Grunwald, E., and co-workers** - *Treated of galvanic-technique*, House of Book of Science, Cluj- Napoca, 2005
[6]. **Paunovic, M., Schlesinger, M., Weil, R.** - *Fundamental Considerations, Modern Electroplating*, Fourth Edition, John Wiley and Sons, Inc. New-York, 2000
[7]. **Matlosz, M.** - *Competitive effects in the electrodeposition of iron-nickel alloys*, J. Electrochem. Soc., 140, nr.8, 1993, p. 2272-2279
[8]. **Valotton, P.M., Matlosz, M., Landolt, D.** - *Experimental investigation of the thermal effect in lead electrodeposition onto resistive substrates*, J. of Applied Electrochemistry, 1993, 23, nr.9, p. 927-932
[9]. **Vasilache, V.** - Thesis „Contributions to optimize the process of galvanic deposition of nickel and nickel alloys used in machine building”, Stefan cel Mare University of Suceava, 2008
[10]. **Roventi, G., Bellezze, T., Fratesi, R.** - *Electrochemical study on the inhibitory effect of the underpotential deposition of zinc on Zn-Co alloy electrodeposition*, Electrochimica Acta, 2006, 51, p. 2691-2697
[11]. **Lodhi, Z.F., et. co.** - *A combined composition and morphology study of electrodeposited Zn-Co and Zn-Co-Fe alloy coatings*, Surface and Coatings Technology, 2008, nr. 202, p 2755-2764
[12]. **Heydari, G., Heydarzedeheh Sohi, M.**, *Study of the corrosion behavior of zinc and Zn-Co alloy electrodeposits obtained from alkaline bath using direct current*, Materials Chemistry and Physics, 2009, 117, p. 414-421
[13]. **J. Mahieu1, K. De Wit1, B. C. De Cooman1 and A. De Boeck** - *The properties of electrodeposited Zn-Co coatings*, Journal of Materials Engineering and Performance, 2007, p.561-570
[14]. **Pedro De Lima-Neto; Adriana N. Correia; Regilany P. Colares; Walney S. Araujo** - *Corrosion study of electrodeposited Zn and Zn-Co coatings in chloride medium*, Journal of the Brazilian Chemical Society, 2007.
[15]. **Vasilache V., Gutt S., Gutt G., Vasilache T, Sandu I., Sandu G.I.** - *Determination of the Dimension of Crystalline Grains of Thin Layers of Zinc-Nickel Alloys Electrochemically Deposited*, Metalurgia International, vol.XIV(2009), nr.3, p.49-53
[16]. **Vasilache, V., Gutt, Gh., Vasilache - T.,** *Studies about electrochemical plating with Zinc-Nickel alloys-the influence of potential through stoichiometric composition*, Revista de Chimie, București, 2008, 59, nr.9, p. 878-885.



INTERCRITICAL THERMOMECHANICAL TREATMENTS APPLIED TO THE STEEL HEAVY PLATES

Elisabeta VASILESCU

„Dunarea de Jos” University of Galati, Romania,
email: elisabeta.vasilescu@yahoo.com

ABSTRACT

This paperwork shows the laboratory experiments made on X60 and X65 steels with several intercritical thermomechanical treatment applications. Two variants were used: "down-up" thermomechanical treatment with heating and rolling in the intercritical range and "up-down" thermomechanical treatment with preliminary complete austenitizing and rolling in the intercritical interval. High values of the strength characteristics and a good plasticity were obtained. A comparison was made with the obtained results of the classical thermal treatment application (normalizing).

KEYWORDS: intercritical thermomechanical, microalloyed steel

1. Introduction

The present world conjuncture regarding the plate products offers and costs imposed (to keep the markets) the making of the new technologies of the processing and thermal treatments that lead to the diminution of the energy consumption. The siderurgy is placed among the industrial branches with high level energy consumption therefore, the aim of this paper-work is to settle the reduction solutions of the energy consumption in the final stage of the plate-products thermally treated. [3]

The study of the national and international standards, that establishes the manufacturing conditions, mechanical and technological characteristics of the siderurgical products made of the hypoeutectoid steels, showed that there are cases when the thermal treatment characteristics are not precised. In these cases first of all, and when the treatment characteristics are not precised, the researches could be achieved to settle the reducing ways of the energy consumption by temperature decrease or final thermal treatment elimination.

It is supposed a nonconventional approach of the thermal treatment process by thorough studies regarding transformation mechanism and kinetics in the intercritical field of the structural steels and a better correlation to the previous stage - plastic deformation.

In the practice of the thermal treatments, the conservative positions are shown that impose the hypoeutectoid steels to be completely austenitized to achieve the normalizing annealing or quenching.

It has been considered for a long time that the

incomplete austenitizing to such steels leads to the fatigue strength worsening and to the increase of transition temperature at brittle fracture.

All national and foreign researches introduce the incomplete austenitizing for normalizing of the naval plates or some structural steels quenching and for normalizing of the welded joint thermal influence zones for some low Carbon Ni-Mo or Ni-Mo-V steels.

It was established that, by thermal treatment temperature reducing a certain values increase of the material strength and plasticity, and metal loss reduction due to oxidation during thermal treatment were gotten.

By a thorough study and systematisation of the results in this research field, a new orientation could be traced in the practice of the hypoeutectoid steels, the thermal treatment, which answers better to the purposes for which these siderurgical products are made.

The thermal treatment of the steels and cast-irons, based on the austenite getting and its subsequent transformation (annealing, quenching), is made traditionally, with complete austenitizing (for hypoeutectoid steels) or incomplete austenitizing (for eutectoid, hypereutectoid and ledeburite steels). [4]

From the austenitizing temperature point of view, the respective treatment of the hypoeutectoid steels could be considered as "overcritical" (above $A_{C1}-A_{C3}$ interval), and for the other steels as "intercritical" (in $A_{C1}-A_{Ccm}$ critic interval).

By heating, in the balance condition of a hypoeutectoid steel, in A_1-A_3 interval, its microstructure, pearlitic-ferrite initially, will become

austenite-ferrite.

Carbon concentration of the austenite and austenite ratio, as well, will depend on steel carbon content and heating temperature.

The highest possibilities of controllable variation of such characteristics, the steels with an extend A1-A3 range present, those with 0,10 - 0,30%C, respectively. [2]

Moreover, the fact should be specified that the studies balance situation could be achieved on the other ways such as: by steel heating in the austenite field (total austenitizing) and by show cooling up to a temperature placed within the A₃-A₁ interval (Fig. 1)

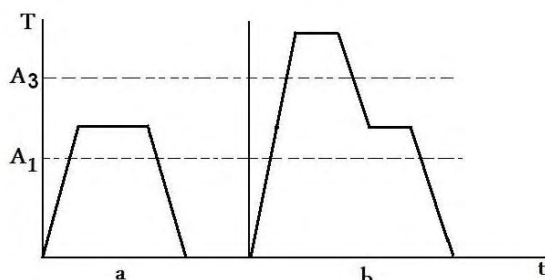


Fig. 1. Practical ways of an intercritical treatment for a hypoeutectoid steel

a) heating from the ambient temperature within the A₃-A₁ interval (down-up)

b) preliminary austenitizing and precooling within the A₃-A₁ interval (up-down)

This kind of the treatments were named intercritical thermal treatments and are used for thermal influenced zone recovery from electrosag welding of some Ni-Mo or Ni-Mo-V steels (with low carbon) and dual-phase steels, as well. The latest paper-works of specialty show that the intercritical thermal treatment could be used for some hypoeutectoid steel, as well, those with high Ni content, carbon-steel, and low alloyed steels for naval constructions. [1]

2. Laboratory experiments

Combining the thermal treatment with a plastic deformation in the intercritical field, an intercritical thermal mechanical treatment was achieved.

For experiments, X65 steel test pieces were used having the following characteristics (mentioned in Tables 1 and 2).

Table 1. Chemical characteristics of X65 steel

C	Mn	Si	V	Al	Ni	Mo	Ti	Nb
0.1	1.5	0.2	0.03	0.07	0.01	0.003	0.02	0.04

Table 2. The imposed mechanical characteristics steel grade

Steel grade	R _m , min [N/mm ²]	R _{p 0,2} min [N/m ²]	A min [%]	KV min [J]
X65	413	331	22	27

The intercritical thermo-mechanical treatment was used by the direct heating in the intercritical deformation field (down-up) and deformation in intercritical condition after a preliminary austenitizing (up-down) Fig. 2.

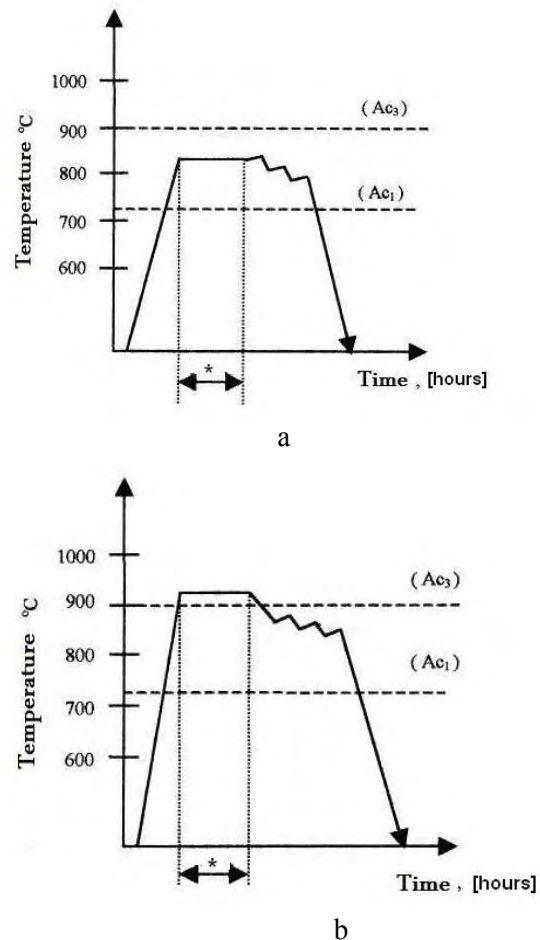


Fig.2. Intercritical thermomechanical treatments: a) down-up; b) up-down, *1/2 hour.

In the laboratory conditions, the thermomechanical treatment consisted of:

- heating in the austenitic or intercritical conditions;
- one passing rolling with a $\epsilon = 30\%$ and 20% reduction degree on the laboratory rolling mill having barrel diameter of $D = 129\text{mm}$;

- the rolling was achieved in the intercritical field (temperature of 850°C and 800°C) for both treatments: "down-up" and "up-down";
- the cooling after rolling was made in air

or water.

On the test specimen, thus obtained, the mechanical characteristics and structure were determined. The results are shown in Table 3.

Table 3. The experimental conditions of intercritical treatments

No exp	Experimental variants	Mechanical characteristics				
		ϵ %	Rm N/mm ²	Rp _{0,2} N/mm ²	A 5 %	HB
1	Heating to 920°C + cooling air(normalizing)	30	546	368	29	278
2	Heating to 920°C → cooling 850 °C → rolling → water	30	804	764	22	292
3	Heating to 920°C → cooling 850 °C → rolling → air	30	637	579	29	191
4	Heating to 920°C → cooling 800 °C → rolling → water	30	803	753	20	285
5	Heating to 920°C → cooling 800 °C → rolling → air	30	577	412	26	174
6	Heating to 850°C → rolling → water	20	834	685	26	292
7	Heating to 850°C → rolling → air	20	686	566	32	202
8	Heating to 800°C → rolling → water	30	1027	852	20	329
9	Heating to 800°C → rolling → air	30	651	498	20	215
10	Heating to 800°C → rolling → water	20	933	756	20	315
11	Heating to 800°C → rolling → air	20	651	498	20	215
12	Heating to 920°C → cooling 850 °C → rolling → water	20	880	696	20	301
13	Heating to 920°C → cooling 850 °C → rolling → air	20	636	526	26	148

3. Results and discussions

First experiment consisted in a classic normalizing treatment for results comparison (Table 1).

The group of second experiments consisted of "up-down" treatments where working conditions were different by the cooling way and deformation degree:

- austenitizing temperature T = 920°C;
- cooling at 850°C;
- rolling with $\epsilon_1 = 30\%$ and $\epsilon_2 = 20\%$;
- cooling water and air.

It is noticed that Rm and Rp_{0,2} mechanical characteristics values exceed the values provided by the norms (Table 2). In turn, the elongation is not framing, in all cases, in the values required by the norms.

Deformation degree did not influence appreciably the mechanical characteristics.

In case of such treatment, the best results are obtained in domains 3 and 5 with austenitizing temperature T = 920°C, cooling 850°C, rolling $\epsilon_1 = 30\%$ and air cooling. Water cooling brings about low elongation values. The structure is shown in Figs. 3a and 3b.

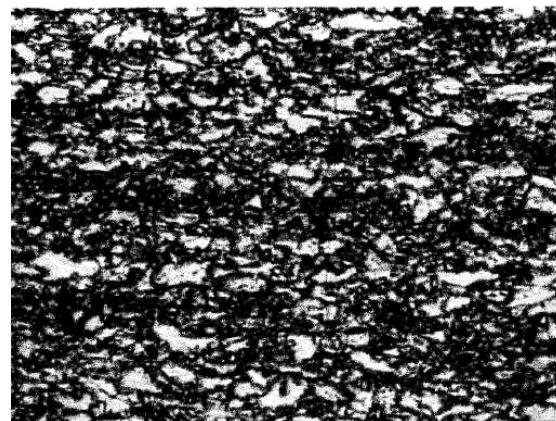
The third group of experiments consisted of "down-up" treatment thus:

- heating at 850°C and 800°C;
- rolling at these temperatures;
- air or water cooling;
- deformation degree $\epsilon_1 = 30\%$ and $\epsilon_2 = 20\%$.

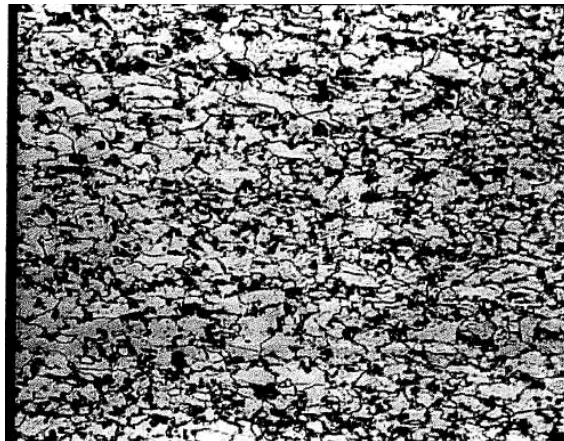
The best results were obtained in the domains 6 and 7 with heating at 850°C, rolling with $\epsilon_2 = 20\%$ and air / water cooling.

High values are obtained for both Rm and Rp_{0,2} and elongation as well (32% to the min 22% provided by norms).

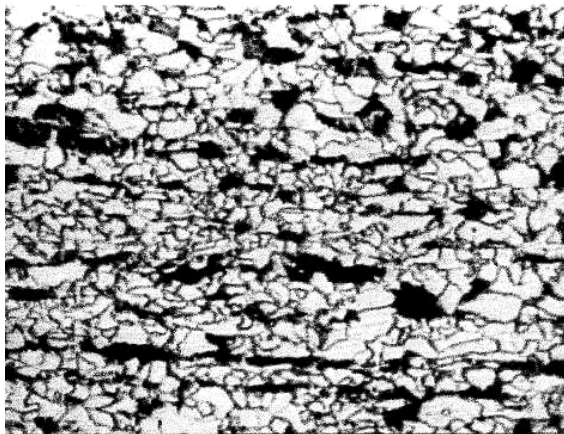
The structures are shown in Figs. 3c and 3d.



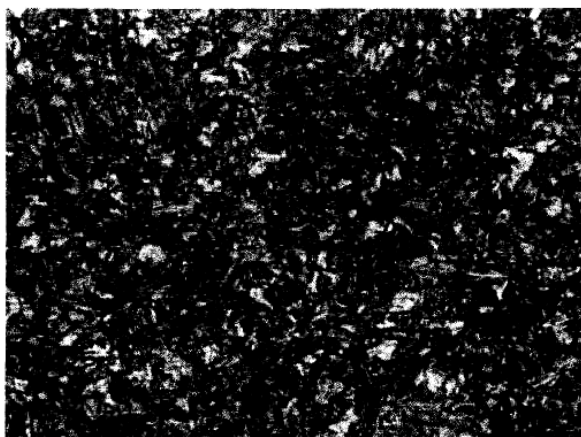
a)



b)



c)



d)

Fig.3. Specimen microstructure with intercritic thermomechanical treatment (x 500 magn., Nital etch 2%)

a) regime no.3; b) regime no.5;
c) regime no.6; d) regime no.7.

4. Conclusions

-all the experiment variants of the thermomechanical treatment lead to the increase of the mechanical characteristics values of the strength (R_m , $R_{p0.2}$) and some of them to the improvement of the plasticity characteristics (A_5 %);

-the experiment variants of the thermomechanical treatment with water cooling after deformation bring about high values for strength characteristics (over 2 times higher than in the "rolled" condition) but determine the elongation decrease even under 20% (smaller than in the "rolled" condition);

-the experiment variants of the thermomechanical treatment with air cooling after plastic deformation bring about mechanical characteristics improvement regarding both: strength and plasticity:

$R_m = 577-686 \text{ N/mm}^2$; $R_{p0.2} = 412-566 \text{ N/mm}^2$; $A_5 = 20-29$ %, frequently 26%. Studying the possibility of the thermomechanical treatment with air cooling after plastic deformation the following remarks are made:

-regarding the heating way: "up-down" or "down-up", the variants with preliminary austenitizing have the highest values of the plasticity characteristics $A_5 = 26-29\%$, when mechanical characteristics are kept at high values: ($R_m = 577-637 \text{ N/mm}^2$; $R_{p0.2} = 412-579 \text{ N/mm}^2$).

In the frame of these experiment variants it could be seen that the deformation degree, ϵ , in limits of 20-30% hasn't an important influence on the characteristics.

-the experiment variants of the thermomechanical treatment without preliminary austenitizing ("down-up") determine a decrease of the elongation from 26% to 20% even though the mechanical characteristics of strength are high, with the remark that the deformation degree from 20% to 30% does not influence meaning fully:

- regarding the plastic deformation temperature established between intercritical interval of the studied steel it could be noticed:

a) in the experiment variant with preliminary austenitizing and deformation at 850°C having deformation degree $\epsilon = 30\%$, a good assembly of mechanical characteristics is achieved ($R_m = 637 \text{ N/mm}^2$; $R_{p0.2} = 579 \text{ N/mm}^2$; $A_5 = 29\%$) in comparison to the temperature of 800°C ($R_m = 577 \text{ N/mm}^2$; $R_{p0.2} = 412 \text{ N/mm}^2$; $A_5 = 26\%$);

b) the experiment variant without preliminary austenitizing ("down-up"), also demonstrated that temperature of 850°C leads to the good results of the characteristics no matter to the deformation degree.



References

In conclusion, the experiment results show that X65 microalloyed steel is sensitive to the mechanical processing and the values of the mechanical characteristics are modified to the rolled condition or to the conventional thermal treatment but the optimum experiment variants that lead to the establishing of the technological conditions in keeping with the studied steel grade are characterized by the following parameters: *preliminary austenitizing at 920°C; plastic deformation temperature of 850°C; deformation degree of about 30%; air cooling after deformation.*

- [1]. **Doniga A., Vasilescu E.**, *Bazele tratamentelor termomecanice* E.D.P., Bucuresti 2004
- [2]. **Gadea S. si Petrescu M.**, *Metalurgie fizica si studiul metalelor* E.D.P., Bucuresti., 1983
- [3]. **Leger J.**, *Etudes des traitements intercritiques (A₁-A₃) des aciers hypoeutectoides* Mem. Scient. Met LXVII, nr. 5, 1971
- [4]. **Popescu N. s.a.**, *Tratamente termice neconventionale* Editura Tehnica, Bucuresti, 1990
- [5]. **Kula, E., Radcliffe, S.** Thermomechanical treatments of Steel, *Journal of Metals* no.10/1963
- [6]. **Komoda, A.** Effect of Austenite Grain Size and C content on the Substructure and Toughness of Tempered Martensite and Bainite, *Transaction ISIJ* no.5/1974
- [7]. **Tamura, I.** Some Fundamental Steps in Thermomechanical Processing of Steels, *Transaction ISIJ*, vol.27/1987
- [8]. **Elwazri, A. M.,s.a.** Methadynamic and Static recrystallisation of Hypereutectoid Steel, *ISIJ International*, vol.43/1982
- [9]. *Proc. Int.Conf.on the Thermomechanical Treatments of Steels*, Padua Italy, 2008.



COATING OF THE LASTING MOULDS WITH HARD ALLOYS

Ovidiu DIMA

"Dunărea de Jos" University of Galati
email: odima@ugal.ro

ABSTRACT

This paper presents the researches on the welded coating of lasting moulds used for casting at high melting temperatures. It shows that the coating through the flux welding with the addition of metal powders and graphite leads to a complex properties with a favorable resistance of abrasion and high temperature oxidation resistance compared to other methods analysed.

KEYWORDS: coating, refractoriness, abrasive wear, thermal stability.

1. Introduction

To obtain the lasting moulds with high durability it is recommended to use materials that ensure the following characteristics: wear resistance, high hardness, low adhesions, refractoriness, high temperature stability, thermal shock resistance, etc..

The main materials which are recommended for lasting moulds are: steels for hot working tools with V, W, Mo, Cr; special cast iron alloyed with Cu, Cr, etc.

2. Working method

For experimental researches we use the samples of hot working tools coated by welding with cladding welding flux and cladding welding flux and added powders.

2.1. Variant A: Cladding welding flux

The added material was WELDCLAD 3 tubular wire electrode which allows with necessary elements, to obtain the chemical composition prescribed in accordance with the working conditions. It results a plated layer with martensitic structure, high-alloy plated with chromium, which has a good thermal stability at the oxidation process. This material is structurally in harmony with the basic material, tools steel type 40VMoCr52.

Welding procedure parameters were:

- welding power source DC-direct polarity,
- universal Weldclad basic flow,
- tubular electrode diameter $d_e = 3.2$ mm and oscillation amplitude of 55mm,

- current intensity $I = 750-1000A$ for swing electrode $d_e = 3.2$ mm,
- current voltage $U = 26-34V$ to ensure rapid initiation and arc stability,
- preheating temperature $T_p = \text{min.} 320^\circ C$ and between layers $T_s = \text{max.} 450^\circ C$,
- speed advancing the wire electrode $V_e = 190-220$ m/min. ,
- 55mm oscillating amplitude of a layer welded wide 60mm,
- welding speed $V_s = 100-175$ mm/min.

2.2. Variant B: Cladding welding flux with added powders

The novelty consists in introducing and mixing a graphite quantity inside the ferroalloys powder. This quantity of graphite interacts, during the welding with the molten alloy bath, leading to the formation of martensite with a separation layer of complex carbides. To achieve this performance, it was studied the welding regime, to determine the favorable parameters. For these, it was established the set input wire electrode and the ferrous-alloys and graphite powder quantity.

Materials used for the research were:

- basic flow Fb20 STAS 10125-75.
- wire electrode S10Mn1 STAS 10123-75.
- ferro-alloys powder made by crushing and grinding and sieving using sieves with mesh size of 0.63 mm.

The grain size influences: the bath homogeneity, the dimensional uniformity trend, favouring the segregation trends.

The chemical composition of the clad layer used



for establishing the ferro-alloys powder composition (see Table 1). The high percentage of graphite leads to obtaining complex carbides. The presence of

vanadium in the composition prevents the growth trend of primary carbide crystals which adversely affect the abrasive wear resistance.

Table 1

Powders	FeCr	FeMn	FeSi	FeV	Ni	Graphite	Comments
%	70	6	9	1	4	10	Be welded with S10Mn1

The electric intensity is the most important factor of the welding process which depends on material quality and other technological factors. The experiences show the necessity of using a higher intensity, as in normal welding, considering the need to achieve a high temperature of molten metal bath to melt powders of ferro-alloys and melt mixing. Welding was done with wire S10Mn1, 2mm in diameter, the welding current intensity was $I = 480A$. Bath size and weld penetration size are suitable for inclusion and melting all the powder. It was studied the velocity regime (V_e) for the trolley wire electrode

and the velocity regime for the welding machine (V_s) studding the parameters behaviour in the following domains: $V_s = 21.5 \dots 63.5$ m / h and $V_e = 103 \dots 307$ m / h. It was found that keeping the ratio $V_e/V_s = 5$, the overheating basic material and the heat influence area are lower.

It was also found that participation in a ratio of between 1 and 1.5 the amount of ferro-alloys and wire led to superior results. Under these conditions the diffusion of the elements was more pronounced achieving uniform deposition tipped. The optimum working arrangements set is given in Table 2.

Table 2

Elements	V_e	V_s	Input eletrod wire	Input ferro-alloys and graphite powder	Input basic flow
U.M.	[m/h]		[g/100mm]		
	204	40.5	12.5	20.1	35

3. The analysis of welding coated samples

The analysis of samples coated by welding procedures consists in: the welding wire flux allied Weldclad 3 (Variant A), the flux welding wire S10Mn1 by adding alloying ferro-alloys and graphite deposit (Version B), and the arc welding discovered Sormait electrode currently used (Version C)

3.1 Chemical analysis of base material and coated material

The chemical composition of the materials was determined by spectral analysis of both materials, the

coated layer and the transition zone plated samples. The results of the determinations are presented in Table 3.

The steel base material corresponds to hot working tools with 0.38% carbon, 5.5% chromium, about 1.5% molybdenum, up to 1% and 0.5% Vanadium, Nickel.

Deposited material: for the Variant A, the composition is appropriate for a martensitic steel with 0.1% carbon, 12.5% chromium, 2% nickel, 1% molybdenum, while, for the Version B, the composition consists in the contribution of electrode wire and S10Mn1 graphite and ferroalloys powder (Table 1 and Table 2.).

Table 3

Sample	C	Mn	Si	Cu	Cr	Ni	V	Mo	Nb
	%								
Basic material	0.38	0.44	0.98	0.2	5.5	0.45	0.94	1.54	0.011
Layer Variant A	0.10	1.02	0.42	0.02	12.5	2.03	0.04	1.04	0.021
TA Variant A	0.18	0.79	0.21	0.03	6.4	1.42	0.09	0.42	0.095
Layer Variant B	2.61	1.11	1.80	0.05	20.58	1.37	0.15	0.12	0.012
TA Variant B	0.72	0.81	1.2	0.04	12.8	0.92	0.09	0.04	0.01
Layer Variant C	2.55	0.98	0.82	0.04	20.12	1.57	0.04	0.12	0.010

In the transition layer material (TA) because of the melted base material dilution, the chemical

composition differs widely, being characterised, in the following context: for the Variant A and Variant B,

decrease of the chromium and nickel concentrations and the increase of carbon concentration. To obtain the desired composition layers, relatively homogenous welding requires several overlapping layers.

For comparison it is also presented the composition layer deposited by arc welding SORMAIT discovered electrode (Variant C).

3.2. Hardness tests

The Hardness tests were done by Vickers HV₀₂ with small tasks. The results of hardness measurements and changes in the transition of basic material - coated layer, deposited by welding (Variant A, B and Variant C) are shown in Figure 1.

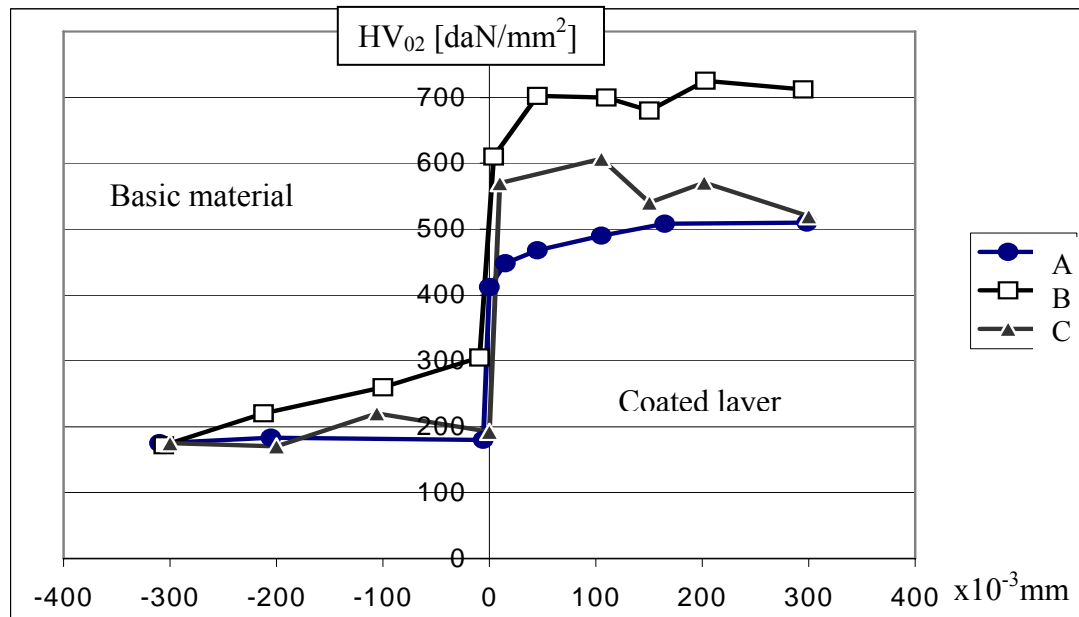


Fig. 1. The hardness variation in the transition-area of basic material BM - LAYER deposited by flux shielded arc welding (Variant A, B and Variant C).

In the case of the Variant A, the base material hardness is relatively constant 175daN/mm². Inside the fusion zone, the hardness variation is abrupt from 175 to over 400daN/mm².

The increase of the hardness on the depth of the plated layer increases relatively slowly but continuously, confirming the existence of the layer with diluted concentrations of the carbon and alloying elements. The next hardness layer remains relatively constant at about 510daN/mm².

In the case of welded clad with flux and additions of ferro-alloys and metal powders, Variant B, there is an increase of hardness in the material near the fusion zone caused by carbon diffusion and the rapid cooling. Fusion zone hardness increases rapidly at over 300daN/mm², still almost 600daN/mm² and attains the value over 700daN/mm² slightly oscillating because of carbides separations.

The increase is relatively steep and continuous compared to arc welding SORMAIT-discovered electrode Variant C, due to a more homogeneous layer; it will be highlighted and structure analysis, too.

3.3. Structure analysis

The structure analysis was done by optical microscopy. The base material used in the research, 40VMoCr52 steel grade, has a ferrite and pearlite structure with uniform polyhedral grains in a proportion of 50-50%. In the case of the Variant A the coating layer has a homogeneous martensitic structure with fine separation of ferrite delta. The transition zone with a width of few millimetre tenths has a characteristic structure with spinal ferrite results of overheating, followed by relatively fast cooling and the deposited material of martensitic heterogeneous structure and rough separation of delta ferrite. [11]

This structure leads to lower values and a slower increase in hardness.

If the welding flux has ferro-alloys in the addition (Variant B), the plated layer has a dendritic structure of martensite and carbides formed homogeneous needle-targeted form of heat propagation direction Figure 2. The transition zone in welding submerged powder flow presents a heterogeneous structure due to the formation of a diffusion layer of carbon and other elements into the basic material.

Note that the added powder was a large amount of graphite to form very complex carbides. The basic material is strongly carburized up to 0.7-0.8% C. Its structure is composed of one hundred to one hundred percent approximately, allied pearlite. Hardness in this area grows fast from 180daN/mm² to about 300daN/mm², Figure.3.

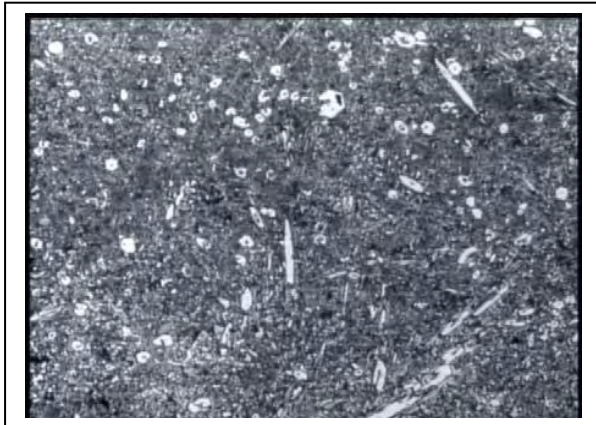


Fig. 2 Variant B layer structure made up of highly alloyed martensite and carbides dispersed fine needle, x200.

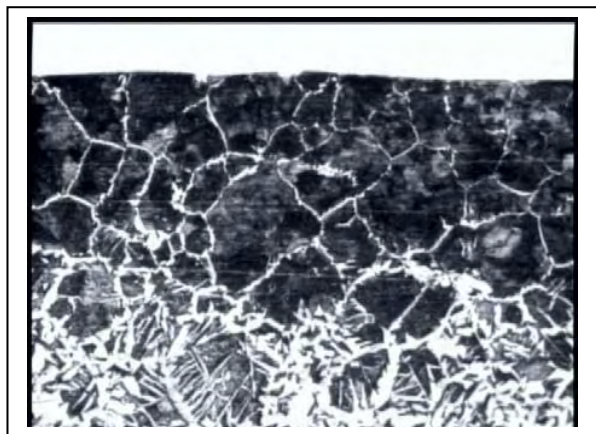


Fig. 3 Variant B, the transition area from basic material, x200.

Near the joint area, the layer deposited has a martensitic structure with finely dispersed carbide separation.

In the case of the plating arc welding with SORMAIT electrode, the layer structure consists of martensite with separation of coarse carbides (see Figure 4). Near the transition zone, the structure looks more uniform. As with Variant B, the transition is

highlighted in two sub co-driven diffusion of carbon and chromium. SORMAIT notes that electrodes have a concentration of over 2.5%C.



Fig. 4. Variant C, layer structure, martensite and coarse acicular carbide x200.

3.4. Determination of resistance to abrasive wears

The research physical model was a mechanical system composed of an abrasive disc in the revolution motion and plane sample.

The grinding wheel was covered with a determined grain abrasive paper.

Test system parameters were:

- sample area 0.5 cm²
- surface is abrasive paper with metallographic grit 800,
- grinding wheel speed of 25 rpm, grinding wheel diameter Dmin = 90mm, Dmax = 170mm,
- length of road travelled - 25 meters,
- number of turns - 56,
- the advance to a full rotation radius of 0.7mm/rev;
- burden of proof on press grinding wheel of 0.1 MPa.

The results of abrasive wear test are shown in Table 4 and Figure 5. How results from the abrasive mass loss at the samples covered with hard alloys, indifferent of the coating applied method, have an abrasive resistance much great of the base material.

The presence of dispersed carbides in martensite mass for allied Variant B and Variant C increased the resistance to abrasive wear, which is consistent with the values of hardness and degree of homogeneity of the structures.

Table 4

Samples type	Hardness		Mass loss abrasive wear			
	Vickers HV ₁₀	Rockwel	Sample1	Sample2	Sample3	Average
	[daN/mm ²]	[HRC]	[g]			
Cladding under flow Variant A	510	49	0.0041	0.0039	0.0043	0.0041
Basis material	180		0.0072	0.0069	0.0074	0.0072
Cladding under flow Variant B	720	60	0.0037	0.0035	0.0033	0.0035
Cladding by welding Sormait Variant C	540	51	0.0039	0.0036	0.0037	0.0037

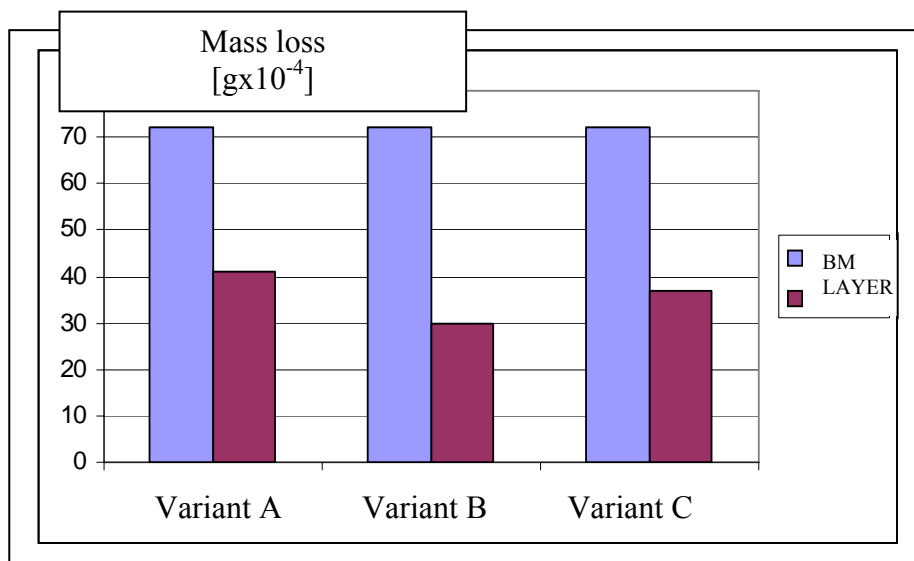


Fig. 5. The variation of the mass loss, during abrasive process, in the case of the welding clad layer for three variants examined.

4. Conclusions

These researches showed that the coating by arc welding is a method that allows the increasing of durability of the support material.

In the case of WELDCLAD 3 welding electrode in flow, because of the martensitic structure, the layer has a hardness increased up to approximately 50HRC. Alloying layer with over 12% with addition of Ni Cr Mo ensures the increase in refractoriness, the increase of the resistance to oxidation at high temperatures, high thermal stability, mechanical properties, hardness and the tenacity, ensuring reliability and resistance during the abrasive wear.

The welding flux with the addition of metal powders and graphite leads to formation of fine carbides dispersed in a mass of martensite, the structure having higher hardness, of 60HRC and consequently a higher wear resistance. For all the technological options discussed, preheating the work piece before welding ensures good weldability, avoiding cracks in the transition, the formation of welding flow transition areas with average

compositions which provide resistance to thermal cycles of repeated heating and cooling.

References

- [1]. L. Stoian - *Tehnologia materialelor*, Ed. Didactica si Pedagogica Buc. 1978
- [2]. I. Frantiu - *Materiale metalice placate* Ed. Tehnica Buc. 1969
- [3]. V. Miclosi, I. Lupescu - *Sudarea prin topire a otelurilor aliate*, Ed. Tehnica Buc. 1970
- [4]. S. Gadea, M. Petrescu - *Metalurgie fizica si studiul metalelor*, Ed. Didactica si Pedagogica Buc. 1981
- [5]. I. Chesa s.a. - *Alegerea si utilizarea otelurilor*, Ed. Tehnica Buc. 1984
- [6]. N. Cananau, O. Dima s.a. - *Tehnologia materialelor Indrumar de laborator*, Universitatea Dunarea de Jos Galati 1993
- [7]. I. Oprescu s.a. - *Utilaje metalurgice-* Ed. Didactica si Pedagogica Buc. 1977
- [8]. S. Levcovici. s.a. - *Ingineria suprafetelor-* Ed. Didactica si Pedagogica Buc. 2003
- [9]. N. Geru - *Metalurgie Fizica*, Ed. Didactica si Pedagogica Buc. 1981
- [10]. S. Gadea - *Manualul Inginerului, Metalurg-* Editura Tehnica Bucuresti 1983
- [11]. O. Dima - *Permanent forms for casting more sustainable cladding hard alloys*, Universitatea "Dunarea de Jos" Galati ARTCAST 2010.



PERFORMING SYSTEM FOR PURIFYING WASTE WATER

**Stefan DRAGOMIR, Georgeta DRAGOMIR,
Marian BORDEI**

"Dunărea de Jos" University of Galati
email: sdragomir@ugal.ro

ABSTRACT

Status of water pollution can be controlled and reduced. For this purpose it uses two types of processes, applied more or less consistently by the management and technical design. The first group of processes is characterized by a "preventive manner of driving" and includes all methods aiming at limiting discharge residue in water.

KEYWORDS: water pollution, purification, filtration performance

1. Introduction

Water is recognized worldwide as the main source to support life on Earth. In its natural state, water is found, mainly in three forms:

- liquid form, which is the predominant form;
- in solid form (ice, snow);
- in the form of vapor in the atmosphere and the clouds.

In nature, there is chemically pure water practically. Water will always contain, along with atoms of hydrogen and oxygen and, also, atoms of other substances, organic or inorganic, and even living organisms.

Depending on the substances contained and its concentration, there are two main types of water:

- water that can be consumed for drinking and cooking food,
- water which cannot be used for drinking or cooking because it contains hazardous chemicals dangerous for human beings, known as industrial water.

2. Water pollution

Maintaining water purity in the natural form means to maintain the content of salts and gases, and micro-organisms specific to a natural unspoiled waters. By means of water pollution, according to the

conclusions of the international Conference on this issue (Geneva 1961), "*changing the composition or status of water sources occurred as a result of human activity so that the waters become less appropriate for all or only some of the uses, that can gain its natural state.*" A city or an industrial complex, which has more channels to discharge wastewater and house residue, is a generator of multiple pollution. Pollutants in water under the form of suspensions (Figure 1) or other many components may fall into the following categories: organic substances; organic residues; non organic residues; radioactive substances; petroleum products; pathogenic microorganisms; hot water.

The volume of industrial waste water is generally 70% higher than the municipal waste water, and loading its harmfulness is much larger. Currently, the "range" of pollutants has diversified enormously, as a result of spectacular industrial growth in recent decades. Waste water, from the hostage complex has a special cleaning system, because of its large organic load.

Waste water from mining contains metals, inorganic pollutants, toxic products, dissolved or in suspension. In sectors where nuclear technology is developing, special precautions are necessary because of the effluent which contain radioactive substances can trigger "cascade pollution"; thermal energy released by hot water discharges cause pollution of rivers and lakes.

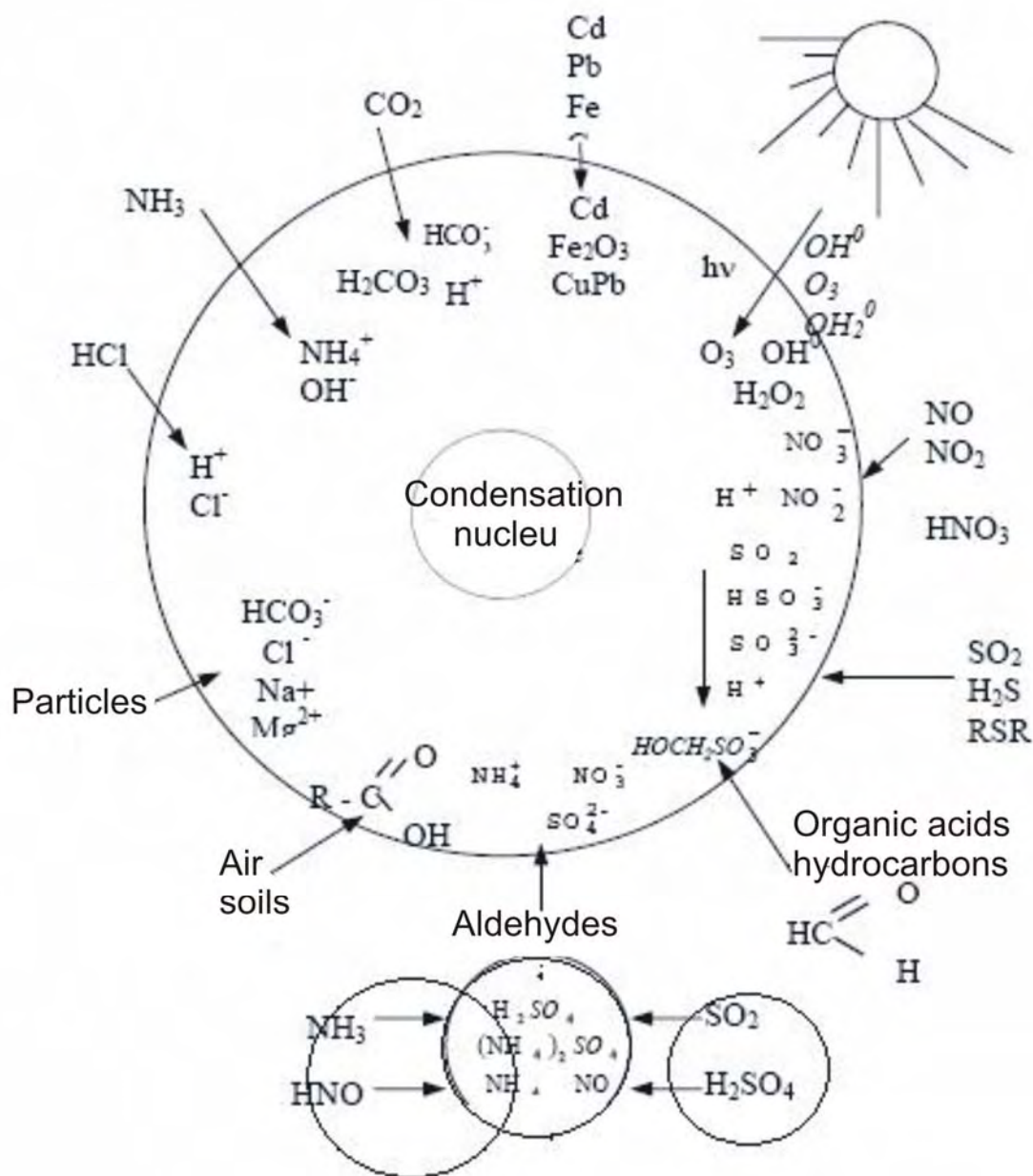


Fig.1. Influence of environmental pollution on a drop of water.

3. Water pollution data

The design stage of the industrial installations, transportation, utilities, etc., has adopted a concept which corresponds to a diametrically opposite orientation to the old one, characterized by the idea of "water washes everything".

Thus, the solid residue, especially substances of high toxicity, may be discharged or burnt. Also it is necessary to reduce water consumption of industry. Recirculation of water used as cooling agent and the

reintroduction of the system is used as a solvent, after appropriate correction quality. In the second group of procedures aimed at purification of water already used (polluted) by various methods of physicochemical filter and purifying wastewater can be used. A purifying by freezing (-20°C), to conserve the sample over a longer period of time (min. 30 days). In this case, the preservation by freezing can lead to loss of the elements to be analyzed by precipitation. In that case it must be a problem especially for phosphate and pesticides.



Table 1.

Indicators of quality	Analysis techniques	Limit detection	Other techniques
Organoleptic indicators			
- color	colorimetry	2.5mg/L pt. CO	colored discs
turbidity		0.1 NTU	Secchi disk
- smell	sensorial analysis		without smell
- taste	sensorial analysis		without taste
Indicators physic - chemical			
- pH		indicators	
specific electrodes			
- Pot.redox.rH		specific electrodes	
- conductivity (S cm ⁻¹)		measurement of conductometry	
- Cl ⁻	Volumetry (pp)	5.1 mgL ⁻¹	uncolor
- SO4 ²⁻	Gravimetrics (precipitation)		
- Silica	colorimetry	5.3 µgL ⁻¹	I.C.P.
- Ca ²⁺	Complexonometry	200 µgL ⁻¹	I.C.P.
A.A.			
- Mg ²⁺	A.A.		Colorimetry
- Na ⁺	Bright photometry	9.83 µgL ⁻¹	I.C;AA
- K ⁺	Bright photometry	49.7 µgL ⁻¹	
A.A.			
- Al ³⁺	Colorimetry		A.A.; I.C.P.
- Hardness	Complexonometry		Colorimetry
- Dry residue	Gravimetry (evaporation)		Conductivity
- T.A.		Alcalimetry	
- Dissolved oxygen (OD)		Volumetric specific electrodes	
- CO ₂ free	Measurement of acidity		Calculation of equilibrium calcium carbonic
Indicators of unwanted substances			
- MES	Gravimetric filtration or centrifugation		0.5 mgL ⁻¹
- NO3 ⁻	Colorimetry	1.2 mgL ⁻¹ NO 3-	Specific electrodes I.C. Absorbed.
- NO2 ⁻	Colorimetry		5 mgL ⁻¹ NO 2-
- NH4 ⁺	Colorimetry Alcalimetry	4.81 mgL ⁻¹ NH 4+	Specific electrodes
- NTK	Mineralization		0.5 mgL ⁻¹ N
- Oxidability KMnO ₄	Hot oxido- reduction	0.43 mgL ⁻¹ O ₂	Cold 4 h
- COT	Oxidation absorption IR		0.21 mgL ⁻¹
- H ₂ S	Distillation volumetric		Specific electrodes

The main modes of preservation of samples depending on the parameters were determined. Table 1 presents the main indicators of water quality, limits

of detection and the most commonly used methods of analyzing them. In this table are presented on a standardized national and European level other

instrumental methods used in laboratories equipped with analytical techniques such as: - ionic chromatography (IC) - spectrophotometry of plasma with inductive coupling (ICP) -- atomic absorption spectrophotometry (AA) - gas chromatography (CG) - liquid chromatography to high pressure (HPLC). In essence, the waste water must be subjected to a treatment which will remove pollutants loading up to a tolerable limit. Basically, purifying water includes a sequence of physical and chemical processes, biological and physicochemical necessary to remove various types of pollutants and the destruction of pathogens existing in the water. The filtering is done by retention (and disposal) of solid impurities, mainly, which are floating, or immersion in water source. By chemical treatment with certain substances neutralized, to obtain the elimination of some organic or inorganic substances whose presence made pure water. All through this process are disposed of living microorganisms and pathogens, an operation known as disinfection, which is usually made, by treatment with chlorine or nitrogen.

4. Water filtering system

A method often used for filtering water is the so called reverse osmosis. It enables people worldwide to transform possible contaminated water into water free of any substances. The RO (Reverse Osmosis – Fig. 3) can be seen today producing pure water from small private homes to space stations.

Reverse osmosis technology is seen virtually everywhere there is a need for pure water:

- drinking water;
- ice;
- production recovery of the water used in auto laundries;
- waste water
- biomedical applications
- applications Laboratory
- photo laboratory
- pharmaceutical industry
- industrial water recycling
- cosmetics industry
- feed
- greenhouse
- hemodialysis
- water heating used in the production of semiconductors
- battery electric industry

Reverse osmosis works on the following principle: a semi-permeable membrane similar to the cell membrane or intestinal capacity is selected. Water passes easily through the membrane due to the reduced size of the molecule while its other substances are passing very slowly or not at all. Water is present on both sides of the membrane presenting a

difference in concentration of dissolved substances. In normal osmosis – Fig. 2, water will tend to cross the membrane from the lower contaminant concentration solution to the higher concentrated contaminant solution, until both concentrations equalised the level inside of vessel. The pressure thus created is called osmotic pressure.

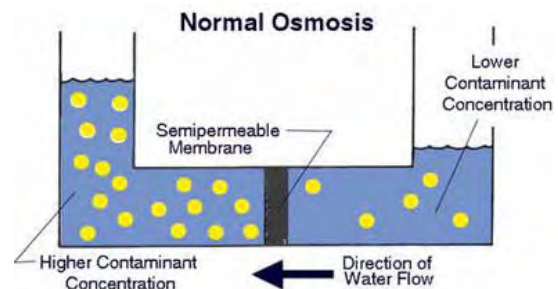


Fig.2. Process of normal osmosis.

The process of reverse osmosis forces water solution with a concentration greater than contaminants (water - source) to cross the semi-permeable membrane by low concentrated solution (processed water). High pressure source is used to reverse the natural osmotic process so that the semi-permeable membranes allow the movement of water while most contaminants rejected. The specific phenomenon that occurs is called "ion exclusion" on the surface membrane to form a film that allows "ion" passage of water molecules but not other substances.

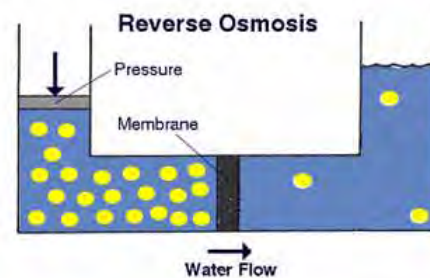


Fig.3. Process of reverse osmosis.

RO systems typically require a pre-filter with active carbon for the retention of chlorine which can destroy the membrane and a pre-filter sediment to retain materials suspended. Reverse osmosis is one of the most effective methods of treating water as regards very dangerous primary contaminants: arsenic, asbestos, atrazine (herbicides/pesticides), fluorides, lead, mercury, nitrates, nitrites and radium. The use appropriate Activated carbon filters suited (included in most RO systems) entails filtering water of volatile organic contamination (primary contaminants) and benzen, trichlorethylene, trihalometanii and radon. Some RO units are able to



remove the organic components of the water source such as Giardia harmful health and Criptosporidium. Water Quality Association (WQA) warns that RO membranes do not manage to remove all microorganisms. Specialists in water treatment must take into account firstly the quality of water source, the types of pollutants, climate consideration, and the territorial network configuration and do the project with specific design of integrating a cleaning system in all its complexity.

5. Conclusions

The study shows that for water treatment may be necessary to add chemicals to achieve the quality finally required.

We give some examples:

1. For potabilizing water, we add sodium hypochlorite and other disinfectants
2. To prevent lodging: add polyphosphates
3. To neutralize the pH: add acid or base
4. To remove sulphides, ammonia nitrogen, iron and manganese are added sodium hypochlorite, potassium permanganate, peroxide, etc.
5. To prevent corrosion, add sodium silicate solution.

Galati town, although it is one of the largest cities in Romania it does not have a station for waste water treatment. Also, the drainage system is incomplete and Galati tries to complete the restoration with the aid programs.

Another strong point is represented by the upgrading of the plant for treating drinking water for city residents and the construction of a sewage collector and a water purification stations for Galati city.

References

- [1]. **Leopa, A.** – *Sistem de recuperare a apelor uzate pentru colectivitati mici de locuitori* – Conferinta Națională "Cercetarea științifică în condițiile integrării europene" – AGIR Brăila, 28-29 mai 2004, Editura AGIR, ISBN 973 – 8466 – 50 – 4;
- [2]. ***Hotararea Guvernului nr. 621/ 2005 privind gestionarea ambalajelor și deșeurilor din ambalaje (*Monitorul Oficial nr. 639 din 20.07.2005*)
- [3]. ***Ordonanța de Urgență nr.196/2005 aprobată și modificată de Legea nr. 105/25.04.2006 privind Fondul de Mediu (*Monitorul Oficial nr. 393 din 8.05. 2006*)
- [4]. **Tăpălagă, I., Berce, P., Iancău, H.** - *Criogenia în construcția de mașini*, Editura Dacia, 1988, București;
- [5]. **Leopa, A.** – *Sistem de evacuare a reziduurilor menajere* – Conferinta Națională "Cercetarea științifică în condițiile integrării europene" – AGIR Brăila, 28-29 mai 2004, Editura AGIR, ISBN 973 – 8466 – 50 – 4.



SOIL POLLUTION WITH HEAVY METALS

Maria VLAD¹, Gelu MOVILEANU²

¹"Dunarea de Jos" University of Galati

²Environment Engineering and Biotechnology,
Faculty of "Valahia" University, Târgoviste

email: mvlad@ugal.ro

ABSTRACT

In this paper was studied soil pollution with heavy metals (copper, chrome, manganese, lead, zinc, cadmium, nickel) caused by the municipal waste from landfill. The level of soil pollution depends on rain regime which usually brings in soil the air pollutants but in the same time washes as the soil determining the pollutants transport through the emissary.

Mean value of the collected samples in four different points situated close to the landfill, were represented in the graphs and related to Maximum Admissible Concentration values. There were ascertained leads, zinc, nickel, cadmium, cation concentrations bigger than admissible values.

KEYWORDS: properties, soil, heavy metal, landfill

1. Introduction

The pollution of the soil produces a disorder of the balance of the constituent elements; it is difficult to fix the balance remake being very after elimination of the cause.

The depreciation factors of the soil could be the following:

- physical pollution;
- chemical pollution;
- radioactive or nuclear pollution;
- biological pollution.

The level of the soil contamination depends also on the pluvial regime which washes in generally the atmosphere, on the pollution agents which are deposited on the soil, but also in the same time wash the soil helping to circulate the pollution agents towards the emissaries.

The rains also favour deep contamination of the soil. The soil pollution depends also on its vegetation, as well as on the soil nature.

This is very important for the pursuing of the pesticides and artificial fertilisers persistency on the

agricultural lands or in the areas where there is a big amount of wastes, e.g. storage ditches.

The contaminants resulted from the municipality wastes could be: organic substances, heavy metals and their compounds, fats and oils, organic and inorganic substances, oils and auto pills (accumulators), other industrial wastes, etc.

2. Results and discussions

The medium values of the pH and conductivity variation of the soil samples, in four points (P1, P2, P3, P4) are presented in Figure 1. The pH value represents one of the most important values which characterize the quality of the soil.

In general, conductivity increases with the concentration on the ions, because in the concentrated solutions there are many ions which conduct the electric current.

Over a certain limit of the concentration, the conductivity decreases, the phenomenon being caused by the ions interactions that occur.

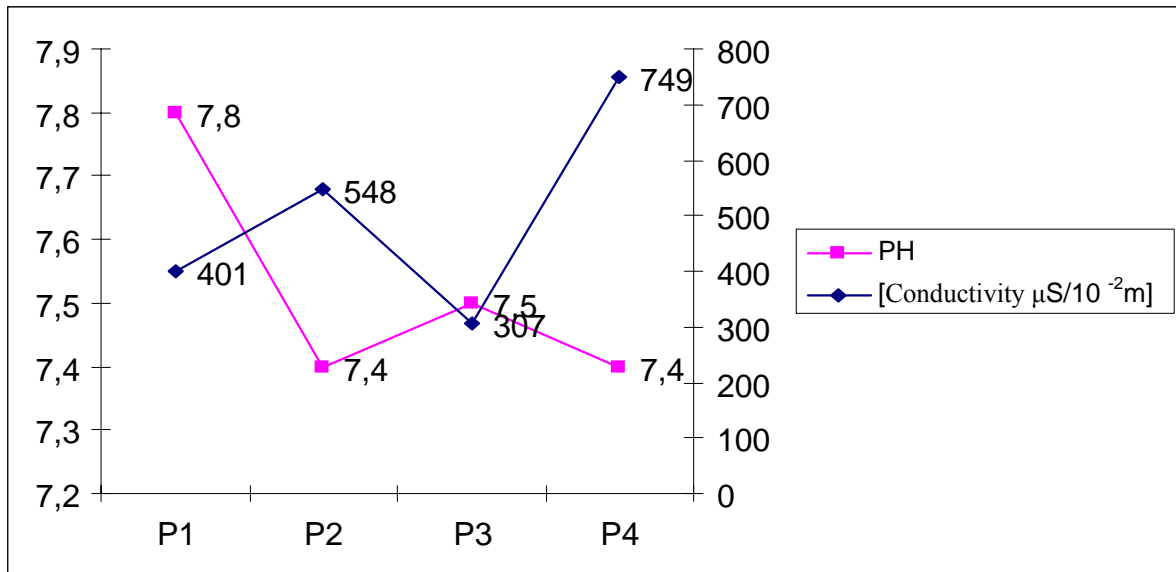


Fig.1. The conductivity and pH variation of the soil, in the points P1, P2, P3, P4.

It has been observed that the values of the pH vary between 7.4–7.8 but within the Maximum Admissible Concentration (MAC).

Conductivity varied between 307 $\mu\text{S}/10^{-2}\text{m}$, in P3 and 749 $\mu\text{S}/10^{-2}\text{m}$, in P4, so it was smaller than the MAC value (2500 $\mu\text{S}/10^{-2}\text{m}$).

Graphs from picture no 2 show that in soil the metals such as: Zn, Cr, Cu, are in amounts bigger than the nominal values, but they are nevertheless under the alert level which is 250 ppm for Cu, 300ppm for Cr and 700ppm for Zn.

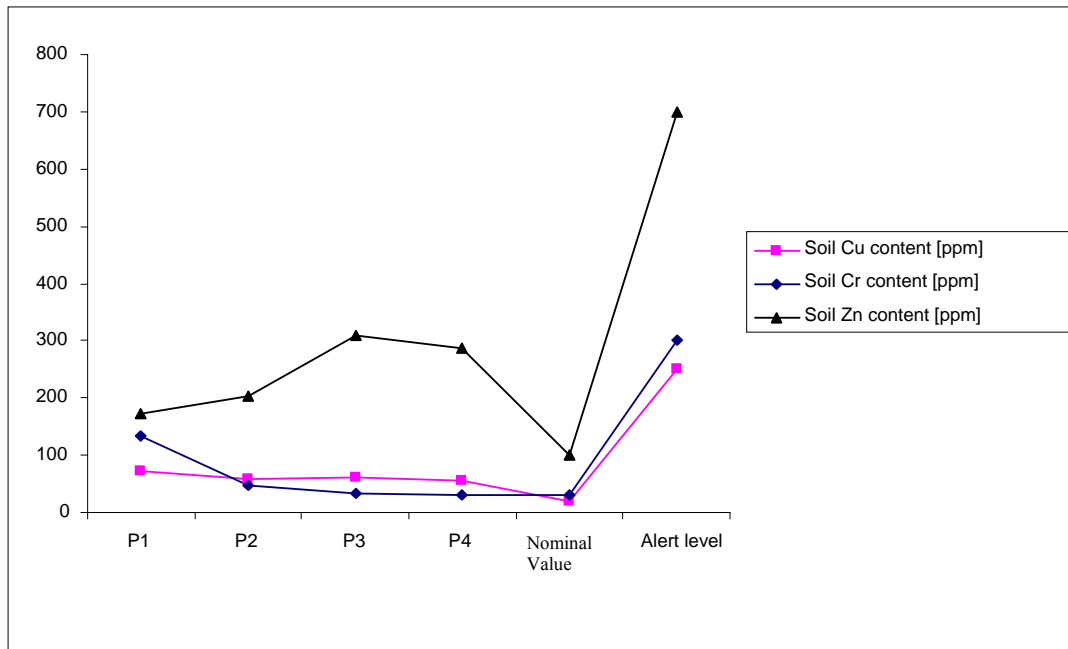


Fig.2. Copper, chrome and zinc content variation of the soil in the four points where were the samples taken.

The graph no 3 shows that in soil, the metals as Pb and Ni are found in amounts over the nominal value of 20ppm, but there are under the alert level

which is 200ppm for Ni and 250 ppm for Pb. The content variation of the oil products in the analysed soil samples - Fig 4.

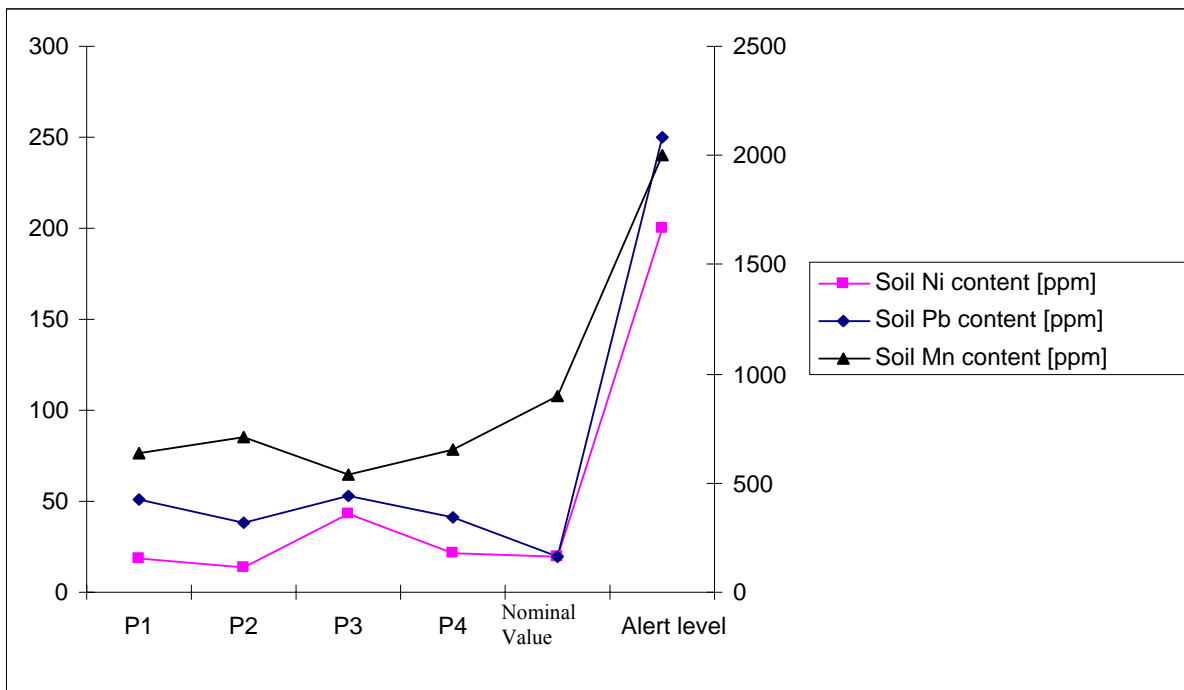


Fig3. Nickel, lead and manganese content variation of the soil in the four areas analysed.

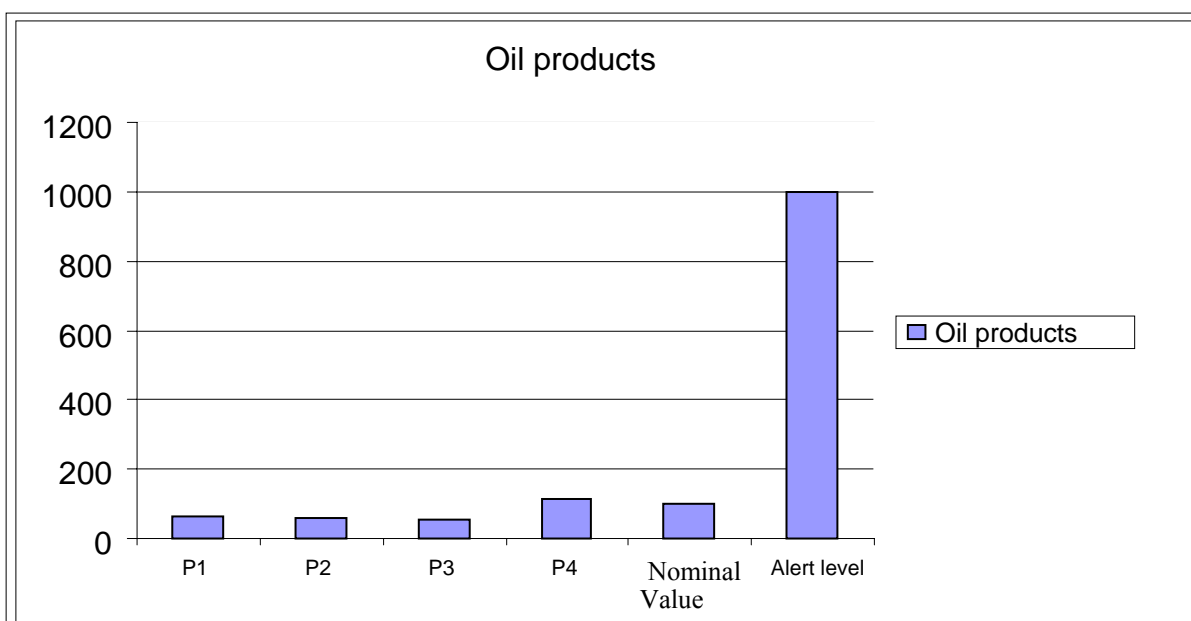


Fig. 4. The content variation of the oil products in soil, in P1, P2, P3, P4 points.

Following the analyses performed, it results that the pollution with the oil products, in generally, does not exceed the nominal value of 100ppm, but the existing amounts in the soil could generate certain inconveniences.

For example, the inadequate storages of the municipality wastes in the rubbish ditches are the

accidental deposits of the fuels/lubricants, construction materials, leached trickling from these ditches on the soils surface or in the interior layers; this imposes the appropriate hygiene of the polluted areas and the soil treatment through:

- Biological methods (biodegradation in situ, bulk biodegradation, decontamination in bioreactors).



- High temperature methods (decontamination using the combustion, decontamination using the thermal desorption).

- Physical and chemical methods (washing, flotation, extraction, oxidation, precipitation).

3. Conclusions

For the quantification of the pollution level of the soil, were compared the values obtained within the investigations made on the spot, followed by the laboratory analyses and the results were compared with the reference values provided by Minister Order no. 756/1997 for soils having less sensitive usages, as follows:

1. There were identified some exceeds compared to the admissible values for the heavy metals as: Ni, Zn, Pb, and Cr.

2. The contents situated above the admissible limits for Ni, show the possibility of soil pollution with galvanisation mud or any other metallic materials containing Ni resulting from construction materials, electronic components.

In conclusion, the parameters analysed exceed the Maximum Admissible Concentrations values.

3. The impact of landfill waste on the surface soil and inferior layer of earth, has pointed out that the leach ate can transport through the waste layers many organic and inorganic compounds and in the case of not respecting the legislation and normative of constructing ecological landfill, the soil from the surrounding landfill may be polluted.

References

[1]. Tjalfe G. POULSEN, *Solid waste management*, Aalborg University, Denmark, 2006.



SOURCES OF EMISSIONS IN THE SINTERING AND BLAST FURNACE PLANT

**Alexandru CHIRIAC, Gheorghe FLOREA,
Ioan SARACIN, Olimpia PANDA**

"Dunărea de Jos" University of Galati
email: sandu.chiriac@yahoo.com

ABSTRACT

The main technological operations for producing the sinter used for preparing the hot metal in the furnace are: preparation and transport of raw materials used for producing the sinter (transport, storage, crushing, sorting ore and coke); sintering the raw materials during the sintering tape preparation (cooling, smashing, sorting) and transport of the sinter.

KEYWORDS: blast furnace, sintering, pollutants emission

These operations are the sources of emission of pollutants into the atmosphere, and they appear like: dust, heavy metals in dust, CO emissions, CO₂, NO_x, SO₂, COV.

Table 1. Emission factors

Emission type	Value
	gram/tonne liquid steel
Dust	170-280 ²
Cd	0.002-0.04 ³
Cr	0.005-0.05 ³
Cu	0.007-0.16 ³
Hg	16-149.....
Mn	0.02-0.4 ³
Ni	0.002-0.04 ³
Pb	0.04-7 ³
Tl	0.005-0.03 ³
V	0.005-0.02
Zn	0.002-1.8 ³
HCl	17-65
HF	1.4-3.5
NO _x	440-710
SO ₂	900-1850
CO	13-43

The emission level of the pollutants in the sintering plant varies as: fine dust (after purifying in electro filters): 100-150mg/m³; Heavy metals from dust emissions. Gas emissions: SO₂: 400-1000mg/Nm³ for coke between 5 – 6mm; 800mg/Nm³ for 1mm coke; 500mg/Nm³ for 6 mm coke; NO_x: 200-310mg/Nm³ (values up to 700mg/Nm³ depending of the nitrogen composites in the fuel; Fluoride: 0.6-

1.5mg/Nm³; Hydrocarbons (methane, olefins, aliphatic compounds, phenols, aromatic compounds): 49-105mg C/Nm³ (for 11 determinations) and 20 – 90mg C/Nm³ (for 32 determinations); PCDD/F: 0.5 – 5ng I-TEQ/Nm³ (after purifying).

Gas emissions: Pb: ≤70mg/Nm³; Hg: 15-54µg/Nm³ (Electro filter purifying system + wet purifying) depending on the content of Hg in ore; Zn: 50mg/Nm³, before the purifying, lower values after treatment. The specific technological operations in the blast furnace hot metal production are: Preheating the air used for blowing through the openings of the furnace with the cowpers; preparation, dispensing, transport and load of raw materials in the furnace; Removal of the hot metal from the furnace and its pouring into hot metal ladle; Blast furnace slag processing to be converted into granulated slag.

These operations are the source of emission of pollutants into the atmosphere, as shown in the diagram in Table 2.

Table 2. Specific emission factors used for preparing hot metal

Pollutant type	Value
	gram / tone liquid steel
Dust	10-50
Mn	< 0.01-0.13
Ni	< 0.01-0.02
Pb	< 0.01-0.12
SO ₂	20-230
Nox	30-120
H ₂ S	0.2-20
CO	770-1750
CO ₂	280-500
PCDD/F	< 0.001-0.004



The emission level of pollutants in the hot metal making plant varies as follows:

- at the coppers: dust: < 10mg/Nm³; SO₂: 160-400mg/Nm³ (for increased gas furnace); NO_x: 70-400mg/Nm³; CO: up to 2500mg/Nm³ (internal combustors); 50mg/Nm³ for controlled burning (external combustors);

- at the hot metal casting sector; dust: < 10mg/Nm³;

- the burning blast furnace gas in coke ovens and coppers: dates are presented in Table 3.

The particulate matter is the main pollutant with negative effects on human health and ecosystems that

are released into the atmosphere by Arcelor Mittal S.A. The worst daily concentration can reach a maximum of 136µg/m³ in the South East Region of the plant and decreases to values of 30µg/m³ nearby Sendreni village, to 16µg/m³ values in the Vânători village and under 20µg/m³ in the Galati city.

Within the plant there are increases of the dust concentration, comparing with the daily concentration of 75µg/m³.

The average daily weight contamination of the atmosphere on the surface equipment in the Sintering and Blast Furnace Plant is 58.01%.

Table 3. The emission levels of pollutants in making hot metal

Pollutants	Emission levels	
	Before treatment	After treatment
Dust	3500 – 30 000 mg/Nm ³	1 – 10 mg/Nm ³
Hydrocarbons	67 – 250 mg/Nm ³	There is no information
Cyanides	0.26 – 1 mg/Nm ³	There is no information
Ammonia	10 – 40 mg/Nm ³	There is no information
HAP: - benzopyren - fluoranten	0.08 – 0.28 mg/Nm ³ 0.15 – 0.56 mg/Nm ³	There is no information
CO	20 – 28%	20 – 28%
CO ₂	17 – 25%	17 – 25%
H ₂	1 – 5%	1 – 5%
H ₂ S	There is no information	14 mg/Nm ³
Mn	There is no information	0.10 – 0.29 mg/Nm ³
Pb	There is no information	0.01 – 0.05 mg/Nm ³
Zn	There is no information	0.03 – 0.17 mg/Nm ³

The annual concentration in the worst situation reaches a maximum of 79.5 mg / m³ within the plant in a single point, and decreases to values of 15µg/m³ in the Sendreni village area and lower values of 3µg/m³ in the Vânători village and in Galati city.

The annual average concentration of 60µg/m³ is found in excess only within the plant.

These values are lower than those obtained by emission measurements made at points outside the plant, that show concentrations of particulate matter of 52µg/m³ in 2007 and 56µg/m³ in 2008.

The average annual weight contamination of the atmosphere on the surface equipment in the Sintering and Blast Furnace Plant is 77.25%.

The Sulfur dioxide (SO₂)

The hourly concentration in the worst situation reaches a maximum of 348µg/m³ within the plant, and decreases to values of 170µg/m³ in the Vanatori village and in Sendreni village and below 130µg/m³ in Galati city area. If we take into account the average annual concentration of 350µg/m³, we found that there are no exceeds neither within the plant nor in the plant neighboring areas.

The average hourly weight contamination of the atmosphere on the surface of the equipment in the Sintering and Blast Furnace Plant is 35.80%.

The daily concentration in the worst situation reaches a maximum of 103µg / m³ in the north west of the plant and decreases to values of 35µg/m³ in the Sendreni village and below 30µg / m³ in the Vânători village and in Galati city.

If we take into account the average daily concentration of 125µg/m³, provided by Order 592/2002 of MAPN, we found that there are no exceeds neither within the plant nor in the plant neighboring areas. The average daily weight contamination of the atmosphere on the surface of the equipment in the Sintering and Blast Furnace Plant is 32.36%. The annual concentration in the worst situation reaches a maximum of 34µg/m³ in the plant, and decreases to values of 6µg/m³ in the Sendreni village and below 2µg/m³ in the Vânători village and in Galati city.

The average annual weight contamination of the atmosphere on the surface of the equipment in the Sintering and Blast Furnace Plant is 27.18%.



The nitrogen dioxide (NO₂)

The hourly concentration in the worst situation reaches a maximum of 283 $\mu\text{g}/\text{m}^3$, within the plant, and decreases to values of 170 $\mu\text{g}/\text{m}^3$ in the Sendreni village and at 130 $\mu\text{g}/\text{m}^3$ in the Vanatori village and less than 120 $\mu\text{g}/\text{m}^3$ in Galati city. If we take into account the average daily concentration of 300 $\mu\text{g}/\text{m}^3$ we found that there are no exceeds neither within the plant nor in the plant neighboring areas. The average hourly weight contamination of the atmosphere on the surface of the equipment in the Sintering and Blast Furnace Plant is 11.67%. The annual concentration reaches a maximum of 16.7 mg/m^3 in the plant, and decreases to values of 2 $\mu\text{g}/\text{m}^3$ in the Sendreni village and lower values than 2 $\mu\text{g}/\text{m}^3$ in the Vanatori village and in Galati. If we take into account the average daily concentration of 60 $\mu\text{g}/\text{m}^3$ we found that there are no exceeds neither within the plant nor in the plant neighboring areas. The annual values obtained by modeling the dispersion of NO₂ emissions are comparable to those measured by DJSP Galati in 2007 and 2008 (average values of 4.3 and 4.0 mg/m^3). Regarding the average annual values of NO₂ indicator determined by IPM Galati at Filești Railway in 2008 (24.97 mg/m^3) the maximum annual value calculated using the dispersion program (16.7 mg/m^3) is lower, because in the values measured by IPM Galati we found also NO₂ emissions from urban traffic. The average annual weight contamination of the atmosphere on the surface of the equipment in the Sintering and Blast Furnace Plant is 25.98%.

The Carbon monoxide (CO)

The carbon monoxide appears in the technological processes that occur at Arcelor Mittal from incomplete combustion processes in heating ovens and heat treatment at the sintering process and coke batteries. The hourly concentration reaches a maximum of 0.5 mg/m^3 within the plant, and decreases to values of 0.26 mg/m^3 in the Sendreni village, at 0.24 mg/m^3 in the Vanatori village and lower than 0.2 mg/m^3 in Galati city. It appears that these values are lower than those provided by the law, but by simulating at the various levels from the ground, significant variations in the concentrations have been found, so that at heights over 20m the calculated values are approaching the limit values. Thus employees that are working at heights greater than 20 m are more exposed to CO poisoning than those working at ground level. The average hourly weight contamination of the atmosphere on the surface of the equipment in the Sintering and Blast Furnace Plant is 37.79%.

Conclusions

The specific emission levels of pollutants in the sintering and blast furnace plant reported in tones of

liquid steel are within the limits obtained by the EU countries, but towards the upper limit, which demonstrates the need for further concern for improving environmental performance through implementation of appropriate measures.

The prevention solutions - reduction and control / remedial analyzed and selected for testing / implementation in the Sintering and Blast Furnaces plant from Arcelor Mittal are grouped as follows:

- implemented solutions:
- tested solutions to implement:
- solutions that are not of interest at this stage:

The measurements of air pollutants took into consideration:

- characterization of a reference state in terms of environmental pollution and the contribution of manufacturing sinter sector and hot metal making at the pollution from Arcelor Mittal Galati platform, based on data reported in 2007

- the characterization of the current level of pollution of this sector compared to the previous stage.

The measurements results in October 2008 compared with the measurements from previous years at the controlled sources of the sintering machines and cowpers from furnaces in operation have shown the efficient measures assumed, they show the reducing of the contents of NO_x and CO from the sintering machines and the of maintaining same high values of CO at the furnaces cowpers 4 and 5. The contribution of the sinter manufacturing sector and hot metal making to pollution made by Arcelor Mittal Galati, expressed by weight average surface considered, on types of pollutants is:

Particulate matter: 58.01% (daily concentration) and 77.25% (annual concentration); SO₂: 35.80% (hourly concentration), 32.36% (daily concentration) and 27.18% (annual concentration); NO₂: 11.67% (hourly concentration), 25.98% (annual concentration); SO: 37.79% (hourly concentration).

This contribution is particularly important at the emission of particulate matter, when the gas emissions values are about one third of total emissions from the entire plant (for SO₂ and CO). However, the highly toxic pollutants were not monitored (VOC, PAH, benzopyrene, etc.) and therefore were not taken into consideration although they cause major environmental impact.

References

- [1]. Alloway, B.J. - *Chemical Principles of Environmental Pollution*, Blakie Acad. And Prof, Chapman and Hall, London 1997
- [2]. E.C-IPPC-BAT Reference Document of the Production of Iron and Steel, Serville (Spain) 1999.
- [3]. Kuhn, R.-*Analiza continua a gazelor la CAE*, In "Stahl und Eisen" 125, 2005 nr.4
- [4]. Avram N s.a -*Teoria proceselor de generare a poluantilor* - Ed.Printech, Bucuresti 2006



MODELLING AND NUMERICAL SIMULATION OF THE ATMOSPHERIC DISPERSION OF POLLUTANTS FROM AN INTEGRATED IRON AND STEEL COMPLEX - PART I

Viorel MUNTEANU

"Dunărea de Jos" University of Galați
email: viorel.munteanu@ugal.ro

ABSTRACT

The Iron and Steel Complex processes handle, store and undertake important amounts of raw materials (iron ores, coals, etc.) energy, fuels, waste waters, slags and other different types of wastes. These activities have an important environmental impact; therefore significant amounts of pollutants (gases, waste waters and wastes) are resulted.

In case of accidents involving emission of pollutants in the atmosphere, health authorities and local administrations often need to know what areas could be affected by dangerously high pollutant concentrations. The goal of the paper is to evaluate a ready-to-use and modelling system, including meteorological parameters and a dispersion model using FLUENT[®] 6.3, a flexible software and reliable to be used for such real-time evaluations, especially for trans-border regions.

KEYWORDS: pollutants dispersion, numerical modelling, chemical substances, air, water, soil

1. Introduction

The mathematical and numerical modelling of the pollutants dispersion in the terrestrial atmosphere has known along the time a continuous evolution. From the simplest mathematical models at the beginning of the 20th century (the Gaussian model, 1936), it reached over today the use of extremely complex models such as CFD type ("Computational Fluid Dynamics").

2. State of the art in air quality modelling

As described above, the aim of this work was to develop a model that has certain quality characteristics. This means that there currently exists no available method that suits this demand. In the following state of the art analysis, available methods are checked with regard to the required criteria.

2.1. Dispersion modelling

With dispersion models the dispersion of pollutants starting from one or more emission sources that might be point, line or area sources is calculated. Depending on the requirements, dispersion models are able to consider the topography, the development,

the velocity-, turbulence- and temperature-field, chemical and physical alterations and other parameters [1].

There are different possibilities to classify dispersion models:

- Mathematical and physical models [2]
- Mesoscale or microscale models [3]
- Models with a diagnostic or prognostic flow field pre-processor
- Simple models with homogenous terrain, models that consider the relief and land usage, models that consider the development [1]

Today's models are usually combined with a pre-processor, which calculates the flow field – the end result depends strongly on the beforehand-calculated flow field. For local scale considerations, CFD (computational fluid dynamics) models are first choice today [4, 5].

Generally it should be emphasized that the requirements for the input data are very high [6].

Their preparation and acquirement very usually is time consuming, as well as the final calculation run on the computer, which may take several days depending on the model and the regarded problem.

Table 1 gives a summary of the currently available dispersion models. The classification here follows the mathematical principle of the method.



2.2. Interpolation methods

In many countries, simple interpolation algorithms are officially applied, e.g. Kriging, Inverse Distance Weighting, Modified Shepard's Method and Radial Basis Function [7].

Input parameters are the geographical coordinates and the pollutant concentration values. The calculated concentrations at a certain site are a function of the distance to the measurement points [1]. According to the implemented approach, the number, direction and distance to the real concentration values can be considered.

With Kriging, it is moreover possible to include the spatial variation of the measured concentrations by using variograms [8].

One can differentiate between statistical and non-statistical approaches or "exact" (the input value is preserved in the output) and "inexact" methods. Single cases are normally not considered, the adjusted interpolation parameters are valid for all cases. Therefore, the result depends strongly on the geographical location of the measurement sites that should not be influenced by local emission sources [3].

Table 1. Classification and assessment of dispersion models

Model Type	Theoretical background	Advantages	Disadvantages
The Box model	The pollutants distribution is homogeneous, calculating thus the medium concentration of every pollutant in any point of the studied air volume.	It is used for a range of wind directions and speeds and a range of mixing heights.	- extremely limited; - the pollutant is uniformly distributed in the box across the area.
Gaussian models	- Gaussian plume model: analytical solution of the steady-state advection - diffusion equation [13]; - Gaussian puff model: analytical solution of the time varying advection diffusion - equation [14].	- short computing time; - easy to handle; - input data requirements are low.	- theoretical simplifications (homogeneous velocity and turbulence field); - not suitable for hourly values; - mainly suitable for homogeneous terrain.
Eulerian grid models (k-models)	- numerical solution of the advection diffusion using a finite difference technique.	- flexibility to process flow and turbulence inhomogeneities over time and space; - higher-order chemical transformation considered; - variable time scale.	- problems treating the advection (numerical diffusion, mass deficits, negative mass densities); - long computing time; - input data requirements are high.
Particle models (Lagrange)	- the model tracks point-like particles representing a trace species on their path; - the vector of the turbulent velocity is varied for each particle at each time step using a Markov process [2].	- natural phenomena involved in turbulent diffusion are largely reflected; - no numerical diffusion; - mass conserving; - delivers non-negative mass densities - consideration of complex geometry; - consideration of large areas; - physical and chemical alterations considered; - variable time scale.	- sampling error associated with the particle count; - long computing time; - input data requirements are high.

The utilization of these mathematical models in pollutants dispersion simulation especially in the urban areas became a real necessity, the number of this kind of studies growing from a year to another. Although the necessary hardware resources for high

scale simulation exceeds for the moment the possibilities of common user, this kind of simulations were and still are realized in research centres that own high capacity computers.

3. The geometric modelling of the studied geographic region

3.1. The virtual topographic description of the Galați – Cahul trans-border region

Every numeric simulation requires first the realization of a virtual, convenient mathematical

description of the physical space in which are realized the fluid flow and pollutants dispersion phenomenon. Because the dispersion process is a three dimensional one and for a correct reproduction of the altitude variation effects between different geographical areas analyzed, the virtual space in which the simulation is made has to be 3D-like.

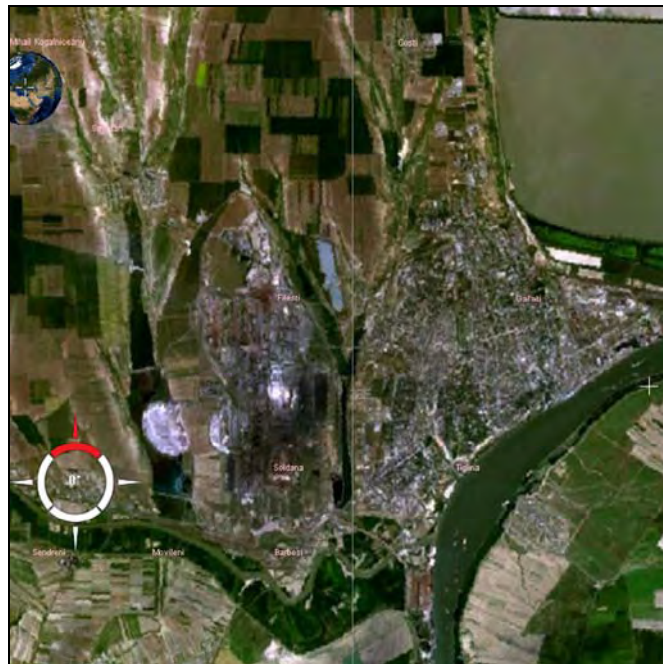


Fig. 1. Satellite view of geographic sector included in the numeric simulation.

For the area around Galați it was took into consideration an almost rectangular area with a side of 13 km. This area includes also the whole sector corresponding to the Arcelor Mittal iron and steel complex. Fig. 1 presents the geographic aria taken into consideration (approximately), seen from above. The geographic coordinates of the area are detailed in Tab. 2.

Tab. 2. Geographic coordinates of the analyzed sector

	Upper – left corner	Down – right corner
Lat.	45° 30' N	45° 22' N
Long.	27° 55' E	28° 05' E

The sector geometry, the basis of calculation domain, was taken from the NASA SRTM-90 database with specialized programs (with a precision of 3 seconds arch \approx 90 m) obtained by cartography with radar technology.

The SRTM models representation precision is remarkable considering the scale from which the data

were taken (approximately 80% from the solid surface of Earth is covered), the average marking error for the Romania territory being approximately 5 m.

3.2. The import, the rectifying and export of geometry using TGRID[®] 5.0 numerical processing program

The FLUENT[®] package pre-processing programs can not directly process the data contained in the SRTM models.

The information transfer must be realized in a compatible format, converting the original data in the STL format being the chosen modality. To avoid the subsequent errors, the local elevation information export resolution was imposed to be identical with the final numerical grid resolution.

Fig. 2 contains a graphic representation of the STL geometry imported in the TGRID[®]5.0 processing program.

It is seen that, in reality, the STL format is a geometry discrete, triangulated representation. It is obvious the fact that the representation precision is proportional with the clearly separation resolution.

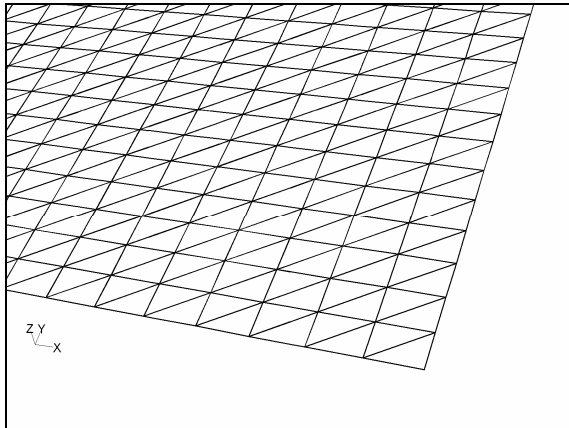


Fig. 2. The STL format geometry imported in TGRID[®]

For the scale in which the numerical simulations were made, it was considered sufficient a resolution of 50 m in the ground surface plane.

The resulting geometry from the direct data import in V TGRID[®] can not be used in the initial format, being necessary some rectifying operations:

a) „the welding” of triangles nodes situated in the same geographic place, with a specified tolerance (in STL geometrical format, the triangles are considered free, not connected to the neighbours);

b) the displacement of entire surface with a corner in the coordinates system origin (to minimize the rounding errors generated by the numbers of representation limits in the electronic calculus systems);

c) the scaling of surface dimensions from the geographic coordinate system used to protect the SRTM model to SI of units (arch degree → meters).

All these operations are very quickly realized with help from specific functions offered by the TGRID[®] program.

Finally, the rectified geometry is exported in a format that is compatible with GAMBIT[®] processing program (.msh), to be further processed.

4. Geometrical modelling and clear separation of the analyzes sector using GAMBIT[®] 2.4 processing program

4.1. The modelling of control volume geometry (the calculus domain)

As mentioned earlier, a series of three-dimensional flow effects prevents the correct

modelling of the dispersion phenomena in a limited 2D space in the sector near the ground.

Even if some types of presented mathematical models allow this kind of approximations, they are acceptable only if the dispersion is simulated over smooth geographic sectors, or if IT is previously known, precisely, the wind speeds distribution (the simulation being reduced to a simple equation solving that is modelling the dispersion).

Considering the following:

- there is a substantial inequality between absolute elevations of different analyzed surface points, which conduct to uneven distribution of wind speed and of atmospheric turbulence; this also determines an uneven dispersion of pollutants (the turbulent dispersion is faster then the molecular one);

- due to the ground surface interaction, in the lower atmospheric layers is formed a “limit layer” (boundary-layer flow), within which the wind speed varies very fast in height, according to an approximately logarithmic law;

- the height to which ground level interactions influence is felt (the thickness of boundary-layer flow) is about 500 – 700 m in the geographic areas as the analyzed ones,

- there was constructed a rectangular control volume, having as basis the analyzed surface and the absolute maximum height of approximately 1000 m (see Fig. 3).

4.2. Clear separation of the calculus domain and the numerical grid export

The control volume clear separation operation was realized using specific functions of GAMBIT[®] processing program.

This operation consists in distribution of the initial volume, of certain shapes, in smaller elementary cells. The final purpose is to obtain a three-dimensional network, used to make the mathematic model equation of the clear separation.

Due to the offered advantages:

- minimum number of cells for a given resolution;
- minimum deformation of the web for rectangular shaped domains cases;

- maximum precision for an imposed resolution (the numeric schemes are better adapted to structured networks);

it was chosen for realization of a structured type of clear separation network.

The detailed network parameters are given in Tab. 3.

Tab. 3. Clear separation network parameters

Network's resolution	X	261 nods ($\Delta x = 50$ m)
	Y	261 nods ($\Delta y = 50$ m)
	Z	51 nods (variable)
The distribution of nods	X	Homogeneous
	Y	Homogeneous
	Z	geometric, growth rate = 1.1
First cell layer height	$Z_0 = 0.6$ m	
Total number of cells	260 x 260 x 50 = 3,380,000	

In Fig. 3 is presented, as can be seen from the program's graphic interface, the clear separation grill of ground surface and that of calculus domain lateral borders. The following can be seen:

- the ground surface geometry was clearly separated again with quadrilateral elements (these has as a matter of fact the same resolution as the STL type initial clear separation);
- the grid nods are distributed on height according to a geometric law, being more frequent in the ground vicinity (the height of the first cells layer is 0.6 m), for two reasons:
 - speeds distribution and turbulence parameters (turbulent kinetic energy, especially) in the atmospheric limit layer are strongly dependent on altitude, the gradients being maximum on the ground vicinity;
 - the part with the most interest of the pollutants dispersion process is produced in the immediate vicinity of the ground.

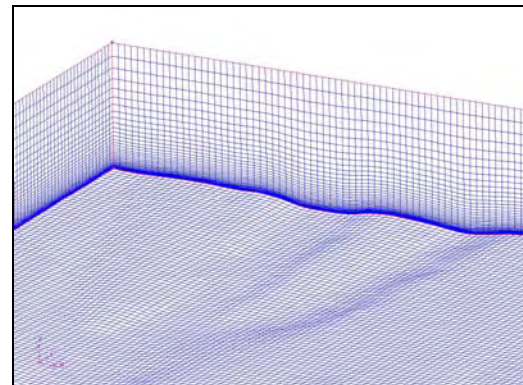


Fig. 3. Clear separation of ground surface and the lateral borders of the calculus domain.

To the calculus domain borders (exterior surfaces) were arrogated limit conditions specific to the FLUENT[®] program. These are synthesized in Tab. 4.

Tab. 4. Limit conditions

Area	Name	Condition type at the limit
Inferior surface	Ground	WALL
Superior surface	Exterior	SYMMETRY
Lateral surfaces	North	VELOCITY INLET, SYMMETRY, OUTLET (based on the simulated condition)
	South	Idem
	West	Idem
	East	Idem
Additional surfaces	Coke-oven plant	MASS FLOW INLET
	Blast furnace	Idem

The numeric grid was exported in the compatible format (.mh) with the FLUENT[®] numerical simulation and modelling program.

References

[1]. Nagel T., Flassak T., Bächlin W., Lohmeyer A. - *Optimierung des Luftmessnetzes von Baden-Württemberg*, Teil A Verfahren für Flächenhafte Immissionsdarstellung und Immissionsbezogene Klassifizierung., UMEG, Karlsruhe, 2002.
[2]. VDI-Guideline 3945 Pt. 3: *Environmental meteorology. Atmospheric dispersion models. Particle model*, Berlin, 1996.
[3]. Schädler G., Lohmeyer A., Bächlin W., Van Wees T. - *Vergleich und Bewertung derzeit verfügbarer mikrokaliger Ausbreitungsmodelle*. Forschungszentrum Karlsruhe, Berichte Umweltforschung Baden-Württemberg, Karlsruhe, 1996.

[4]. Moussiopoulos N. - *Recent advances in urban air pollution research*, Proceedings of the 8th International Conference on Environmental Science and Technology in 2003, University of the Aegean and Global Nest, Myrina, Lemnos island, Greece.
[5]. Louka P., Moussiopoulos N. - *Optimisation of CFD modeling methods for traffic pollution in streets within TRAPOS research network*, Proceedings of the 4th International Exhibition and Conference on Environmental Technology in 2003, Athens, Greece.
[6]. Bahmann W., Schmonsees N., Oestereicher R. - *TA Luft 2002*, in: Neue Anforderungen an meteorologische Daten für Ausbreitungsrechnungen. Immissionsschutz, 8. Jahrgang, Heft Nr. 1, Berlin, Bielefeld, München, 2003.
[7]. Hout D., et al. - *Guidance on Assessment under the EU Air Quality Directives*, in: European Environment Agency, draft, Copenhagen, 2000.



MELTING-CASTING PLANT USING VIBRATING OF MELTS IN ORDER TO OBTAIN COMPOSITE WITH TECHNOLOGICAL UTILITY

Vasile BASLIU, Ionut CONSTANTIN,
Gina Genoveva ISTRATE, Ionel PETREA

"Dunarea de Jos" University of Galati
email: vbasliu@ugal.ro

ABSTRACT

This paper presents the obtaining of composite materials with technological utility through vibration technology. In order to obtain these composites, and plant was designed and manufactured. In order to show the possibilities of these technologies, a number of composite samples were produced.

KEYWORDS: vibration, ferroalloy, composite of technological utility, FeTi32

1. Introduction

The research objective was to find a method for the valorization of granular ferroalloy (FeTi32). Current ISO 5445/1995 standards require a grain with the lower limit of 3.5 mm used in the development of deoxidation steel stage.

Factors that affect the obtaining of a complex deoxidant, reinforced with particles, can be divided into: - metallurgical factors
- technological factors.

Metallurgical factors are the following: solid fraction, temperature, size, morphology, distribution of solid particles and liquid matrix alloy, chemical composition.

Technological factors are: frequency [Hz], amplitude [mm], acceleration [m/s^2], temperature alloy castings, [$^{\circ}C$], time of vibration [min].

Following this process, because of continuous brawniene movement, additional material will be found in the mass of composite.

Benefits:

- reproducible results;
- low additional material segregation;
- wide range of working arrangements;

Disadvantages:

- very slow adjustment of the electric motor;
- the probability of accidental splashing vibrating mass.

- careful handling when pouring liquid metal;
- possibility of accidental splashing of vibrating mass.

The special part of these particular technical solutions adopted, consists in the fact that the

complex deoxidant with technological role has incorporated diverse proportion of complementary material (FeTi32) which is controlled, known and reproducible.

2. Experimental conditions

Mechanical mixing using a vibrating plant

Getting the composite through this method involves melting the aluminum alloy in the presence of particles followed by an intense agitation of the crucible through vibration.

Through vibration, for the majority of alloys, a series of beneficial effects can be obtained, such as:

- finishing the structure and, hence, improvement of properties;
- increasing the solidified alloy compactness by reducing the porosity;
- reducing the chemical, gravitational and segregation processes;
- advanced degassing of the composite material.

While melting alloys in temporary shapes, the solidification starts from the cool walls of the mould, as a result of a heat exchange between the cast alloy and the casting mould.

The solidification of casting alloys in temporary forms starting next cold walls of the form, as a result of heat exchange between molten alloy and mold. At first it forms a solid crust consists of equiaxed crystals that develop over time a zone of columnar crystals. If after melting aluminum alloy particulate form is subject to a process of mechanical vibration, the vibration causes the turbulent motion of the liquid alloy which leads to fragmentation of the columnar

crystals and their involvement in mass formation of liquid alloy, which will be partially re-melted or totally, the process is a function of temperature in the liquid alloy non-solidified and broken crystal fragment size. This has the effect of germination process intensification and intensification of broken crystals and re-melting. Heat involved in the mass of liquid alloy.

Favorable effect compaction vibration can be explained by the fact that mechanical oscillations create local pressures leading to increased penetration

rate of the alloy in the area biphasic capillary channels.

Agitation melt under the vibration action has the effect of decreasing the viscosity of liquid, whether to create favorable conditions for lifting the gas separation surface (on rising speed increases with decreasing viscosity Stokes law). At the same time introduces additional material FeTi32.

The operating principle is explained by the kinematics scheme, presented in Fig. 1.

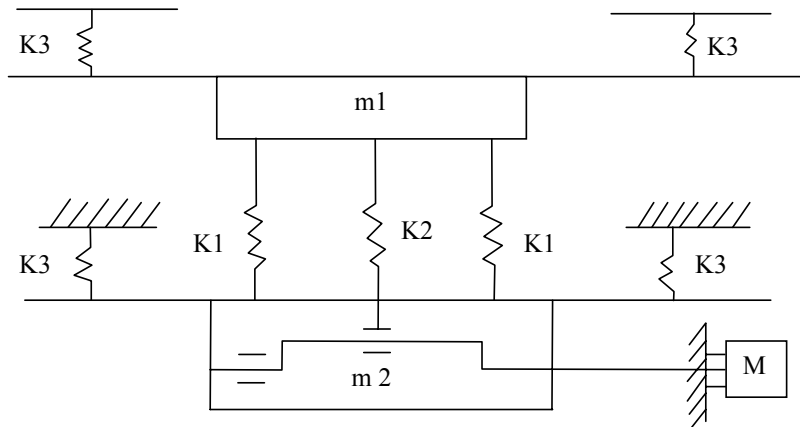


Fig. 1. Kinematic scheme of the plant: m_1 - the weight of the workpiece table and checked; m_2 - reactive load weight (counterweight) K_1 - stiff springs work, K_2 - spring stiffness; K_3 - stiff springs to maintain (control), M - electromotor.

The stand functioning is based on the resonance phenomenon of two mass in vibration m_1 and m_2 ; each of them is suspended by the maintenance springs with K_3 stiffness; the mass are tied together with the working springs K_1 .

The stiffness of the K_1 working springs can be variable, depending on the position of adjusting nuts.

$$Q = \frac{A \cdot f^2}{25} \quad (1)$$

Where: A - amplitude [mm] F - frequency [Hz] a - acceleration [m/s^2].

Table 1. Working regime for vibration mass

Working regime		
Frequency, F , [Hz]	Amplitude, A , [mm]	Acceleration, a , [m/s^2]
25	2.2	55
28	2.2	69
30	1.6	57.6
35	1.2	58.8
40	1.0	64
50	0.7	70



Fig. 2. Plant consists of three heating and vibrating stand for a crucible: 1- vertical furnace with forced bars, 2 - vibrating table, 3 - crucible.

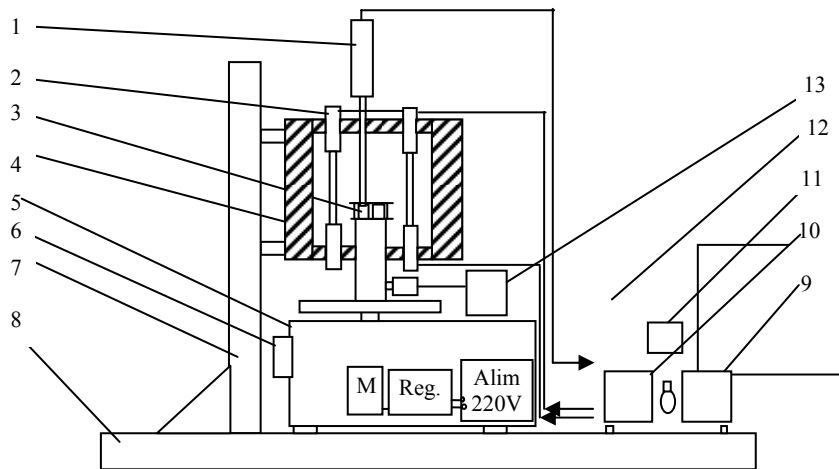


Fig. 3. Plant components: 1 – temperature measurement system (thermocouple); 2 – heating elements; 3 – crucible steel; 4 – electric furnace; 5 – vibrating equipment; 6 – mechanical system for adjustment of amplitude and frequency; 7 – support column; 8 – motherboard; 9 – ampere indicator; 10 – voltage indicator; 11 – temperature regulator; 12 – power source provided with temperature; 13 – vibration measuring device (amplitude and frequency) X – Viber.

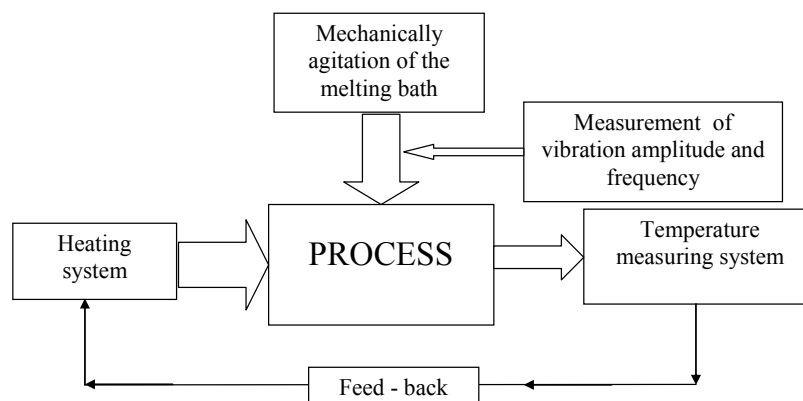


Fig.4. Block diagram of experimental stand function, mechanical stirring, through vibration type during solidification.

Characterization:

Charge:-weight, max. 40 [g]

Electric heating:

-forced bar heating elements:

-R = 4 [Ω]

-Power = 0 ... 3.6 [kW]

Temperature Control System:

-PID - 1RT96

-temperature sensor - K (chromel-alumel)

-range - 0 ... 900 [$^{\circ}$ C]

System for measuring amplitude and frequency:

-X-Viber.

Samples used:

We considered several options for obtaining the Al/FeTi32 deoxidant varying the reinforcing phase size - FeTi32 particles.

We performed their rank using set of sites with the following dimensions: 0.8 mm 0.63 mm 0.40 mm 0.32 mm 0.20 mm 0.16 mm 0.10 mm; 0.056 mm, 0.04 mm <0.04 mm as standard determination.

Working mode:

The working procedure has been established and followed consisted of:

- the composition of the load: it was dispensed by weighing the amount of aluminum and ferroalloy FeTi32 size sorting.

- unloading was made on the top of crucible steel.

- programming of temperature was done in accordance with established experimental procedure.

- melting: phase transition is from solid aluminum liquid temperature monitoring work with fixed by experiment.

- shaking vibrating bath of aluminum metal.
- cooling and removal of the cast from the crucible.

Experimental procedures:

Designing and making the experiment aimed to highlight the inclusion of different ferro-alloy

granulometric classes in aluminum metal matrix. So, we varied the ferroalloy particle sizes (FeTi32) maintaining constant the other parameters: temperature, mixing duration, frequency, magnitude and composition of the load. We chose a 1:1 ratio Al/FeTi32.

Table 2. Experimental data

Nr. crt.	Load composition			Ratio Al/FeTi32	Temperature	Mixing time	Frequency	Amplitude
	Al	FeTi32						
		Mass	Granulation					
u.m	[g]	[mm]	[%]	[°C]	[min.]	[Hz]	[mm]	
1	20	20	0.800	1:1	750	10	46	1
2	20	20	0.400	1:1	750	10	46	1
3	20	20	0.056	1:1	750	10	46	1

On the evidence obtained, we made the following determinations:

a. Chemical analysis

We use X-ray fluorescence spectrometer mark Innov-X System.

Table 3. Chemical analysis

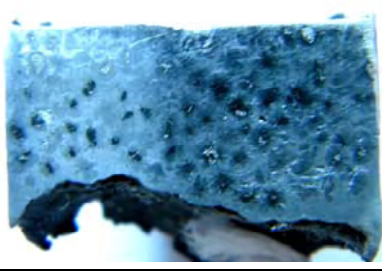
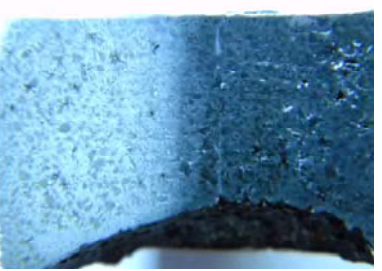
Nr. crt.	Granulation	Chemical analysis		
		Al	Fe	Ti
u.m.	[mm]	[%]	[%]	[%]
P1	0.800	65.36	8.73	12.94
P2	0.400	76.51	13.82	7.48
P3	0.056	58.73	24.55	12.91

b. Metallographic analysis

For this purpose, we collected samples from the Al/FeTi32 composite and we prepared them by grinding and polishing the samples.

When we obtained a high polish, we analyzed in a micro-structural way the prepared surfaces but without metallographic attack for the following increases (x64) in order to highlight the dispersion, shape and size of ferro-alloy particles embedded in aluminum metal matrix.

The same samples were analyzed after the metallographic attack with specific reagent (10% HF in H₂O). It can be seen the dispersion of FeTi32 particles into the aluminium matrix.

Nr. crt.	Ferroalloy particle diameter, FeTi32, mm	Macrostructures
1	0.800	
2	0.400	

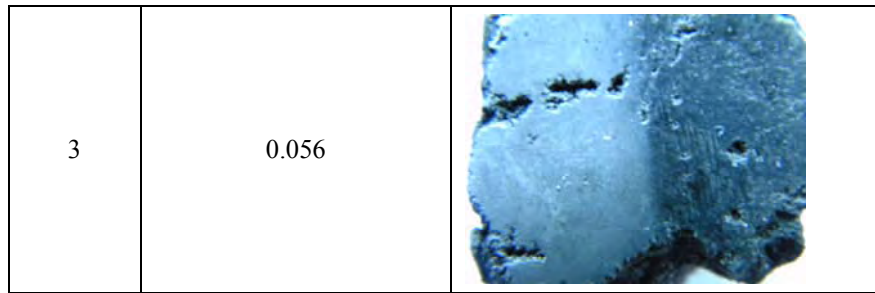


Fig.5. Macrostructures of the FeTi32 ferroalloy samples.

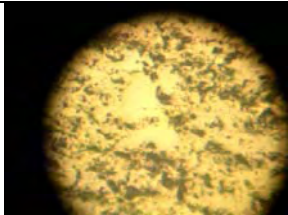
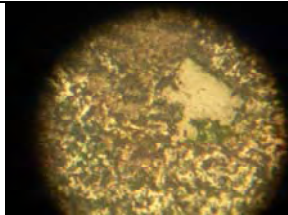
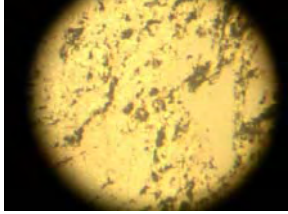
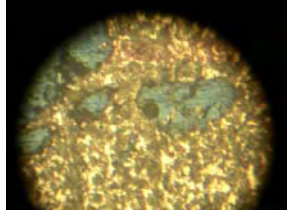
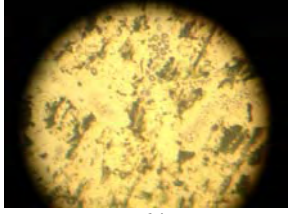
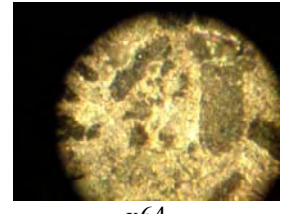
No.	Ferroalloy particle diameter, FeTi32, mm	Microstructures	
		un-attacked	attacked
1	0.800	 x64	 x64
2	0.400	 x64	 x64
3	0.056	 x64	 x64

Fig.6. Microstructures of the FeTi32 ferroalloy samples.

3. Conclusion

The research was completed with the achievement of a laboratory stand, elucidation some phases in homogenization and dispersion of the reinforcing phase in the metal matrix highlighted by microscopic analysis.

References

- [1]. Florin Stefanescu, Gigel Neagu, Alexandrina Mihai – *Materialele viitorului se fabrica azi*. Materiale compozite. Editura Didactica si Pedagogica 1996.
- [2]. Ioan Carcea – *Materiale compozite*. Fenomene la interfata. 2008.

MANUSCRISELE, CĂRȚILE ȘI REVISTELE PENTRU SCHIMB, PRECUM ȘI ORICE
CORRESPONDENȚE SE VOR TRIMITE PE ADRESA:

MANUSCRIPTS, REVIEWS AND BOOKS FOR EXCHANGE COOPERATION, AS WELL
AS ANY CORRESPONDANCE WILL BE MAILED TO:

LES MANUSCRIPTS, LES REVUES ET LES LIVRES POUR L'ECHANGE, TOUT AUSSI
QUE LA CORRESPONDANCE SERONT ENVOYES A L'ADRESSE:

MANUSKRIPTEN, ZIETSCHRIFTEN UND BUCHER FUR AUSTAUCH SOWIE DIE
KORRESPONDENZ SIND AN FOLGENDE ANSCHRIFT ZU SEDEN:

UNIVERSITATEA "DUNĂREA DE JOS" DIN GALAȚI
REDAȚIA ANALELOR
Str. Domnească nr. 47 – 800036 Galați,
ROMÂNIA
email: mbordei@ugal.ro

After the latest evaluation of the journals achieved by National Center for the Science and Scientometry Politics (CENAPOSS), as recognition of its quality and impact at national level, the journal is included in B category, 215 code (http://www.cncsis.ro/2006_evaluare_rev.php).

The journal is indexed in Cambridge Scientific Abstract
(http://www.csa.com/ids70/serials_source_list.php?db=materials-set-c).

The papers published in this journal can be visualized on the "Dunarea de Jos" University of Galati site, the Faculty of Metallurgy, Material Science and Environment, page: www.fmsm.ugal.ro.

AFFILIATED WITH:

- ***ROMANIAN SOCIETY FOR METALLURGY***
- ***ROMANIAN SOCIETY FOR CHEMISTRY***
- ***ROMANIAN SOCIETY FOR BIOMATERIALS***
- ***ROMANIAN TECHNICAL FOUNDRY SOCIETY***
- ***THE MATERIALS INFORMATION SOCIETY***
(ASM INTERNATIONAL)

Annual subscription (4 issues per year)

**Edited under the care of
Faculty of
METALLURGY, MATERIALS SCIENCE AND
ENVIRONMENT
and Research Center
QUALITY OF MATERIALS AND ENVIRONMENT**

Edited date: 30.03.2010

Issues number: 200

Printed by

Galati University Press

accredited CNCSIS

47 Domneasca Street, 800036 Galati,
Romania